universität wien

DISSERTATION

Titel der Dissertation

The effect of the lathyrogens beta-aminopropionitril and homocysteine on osteoblastic differentiation in regard to collagen matrix formation and epigenetic regulation of gene expression

Verfasser

Mag. rer. nat. Roman Thaler

angestrebter akademischer Grad
Doktor der Naturwissenschaften (Dr. rer. nat.)

Wien, June 2011

Studienkennzahl lt.Studienblatt:	A 091 474
Matrikelnummer:	a0004154
Dissertationsgebiet lt. Studienblatt:	Ernährungswissenschaften
Betreuer:	Univ.-Prof. Dr. Klaus Klaushofer

Erklärung:

Ich erkläre an Eides statt, dass ich die hier vorliegende Arbeit selbst verfasst und nur die angegebene Literatur verwendet habe. Ich habe mich bemüht, sämtliche Inhaber der Bildrechte ausfindig zu machen und ihre Zustimmung zur Verwendung der Bilder in dieser Arbeit eingeholt. Sollte dennoch eine Urheberrechtsverletzung bekannt werden, ersuche ich um Meldung bei mir.

Wien, Juni 2011

Danksagung

Besonderen Dank gilt meinem Abteilungsleiter und wissenschaftlichen Mentor **Dr. Mag. Franz Varga** für die essentielle Unterstützung, seine wissenschaftliche Kompetenz und den vielen wissenschaftlichen Diskussionen die ich mit Ihm teilen durfte. Die Erreichung der in dieser Dissertation vorgestellten wissenschaftlichen Erkenntnissen währe ohne sein Mitwirken nur schwer möglich gewesen.

Mein Dank gilt **Herrn Univ. Prof. Dr. Klaus Klaushofer** für die Aufnahme am Ludwig Boltzmann Institut für Osteologie, für die Bereitstellung der Arbeitsmittel und der guten Arbeitsbedingungen sowie für das Interesse an der durchgeführten Arbeit.

Weiters möchte ich mich bei all meinen Mitarbeitern, insbesondere bei **Frau Dr. Monika Rumpler** und **Frau PMA Silvia Spitzer** für die tatkräftige Unterstützung über diese 3 Jahre bedanken.

Nicht zum Schluss möchte ich mich bei meiner Freundin Kathrin Liszt für die große Geduld die Sie während meiner Dissertationszeit aufgebracht hat, bedanken.

Abstract

Collagen, the main component of bone extracellular matrix (ECM) represents a protein with a defined super-molecular organization. For stable fibril formation, the basic element of collagen, the fiber undergoes several intra- and extracellular modifications. One major process of collagen / matrix maturation is collagen cross-link formation. This process is tissue-specific, and involves a variety of cellular and matrix derived signals. Inhibition of lysyl oxidase (*Lox*), an enzymatic key player in cross-link formation, leads to improper collagen cross-linking and altered fibrillogenesis. In vitro and in vivo experiments confirmed that these aberrations in matrix formation are accompanied by loss of bone mineral, reduced bone strength and altered mineralization.

A further factor involved in tissue development is regulation of gene expressions by epigenetic DNA methylation. To date, sparse research has been performed regarding the significance of this mechanism for bone development and pathogenesis. Therefore, in this thesis the role of epigenetic mechanisms in osteoblastic development was examined.

By treatment of the murine pre-osteoblastic MC3T3-E1 cell line with two lysyl oxidase inhibitors, namely beta aminopropionitrile (bAPN) and homocysteine (hcys), we monitored and compared the effects of these two lathyrogens on the osteoblastic cells. The expression levels of osteoblastic genes were analyzed employing quantitative real time PCR (qPCR) and gene expression microarrays. Markers for osteoblastic activity and cell proliferation were analyzed by viability tests and alkaline phosphatase activity tests and effects on collagen cross-link formation were measured by FTIR. First results indicated that bAPN as well as hcys, besides the enzymatic inhibition down regulate the mRNA expression of *Lox*. Due to the greater clinical relevance of hcys, using ELISA, immuno blotting and chromatin immuno precipitation techniques we identified the cellular pathway responsible for the effect of hcys on the expression of *Lox*. This involves IL-6, the transcription factor FLI1 and the DNA methyltransferase DNMT1. DNA methylation analysis of the *Lox* promoter revealed that hcys suppresses *Lox* expression by DNA methylation.

Finally, a new mechanism controlling ECM mediated proliferation and differentiation of osteoblasts was elucidated. By seeding MC3T3-E1 cells on collagen type I we observed an up-regulation of osteoblastic genes and a down regulation of

the pro-apoptotic gene Fas when compared to control. Using several inhibitors, qPCR and DNA methylation analysis we found that extra-cellular collagen type I via FAK, MAPK and the transcription factor AP1 directly up-regulates *Dnmt1* which in turn maintains promoter methylation of the gene *Fas* thus repressing its expression.

Zusammenfassung

Kollagen Typ I, der Hauptbestandteil der extrazellulären Matrix des Knochens, weist eine super-molekulare Organisation auf. Die einzelnen Kollagenmoleküle werden einer Reihe von intra- und extrazellulären Modifikationen unterzogen, die es ihnen ermöglicht extrazellulär Kollagenfibrillen auszubilden. Ein wesentlicher Schritt dabei ist die Ausbildung von Kollagenquervernetzungen. Dieser Prozess ist gewebespezifisch und wird von vielen zellulären und matrix-abhängigen Signalen gesteuert. Hemmung der Lysyloxidase (Lox), ein Schlüsselenzym der Kollagenvernetzung, führt zu veränderten Quervernetzungen und gestörter Fibrillogenese. Ergebnisse aus in-vitro als auch in-vivo durchgeführten Experimenten bestätigten, dass solche Veränderungen zu Knochenmineralverlust, reduzierter Knochenfestigkeit und einer veränderten Mineralisation führen.

Ein weiterer Faktor der eine wesentliche Rolle in der Organ und Gewebsentwicklung spielt ist die Regulierung der Expression von Genen durch epigenetische DNA-Methylierung. Bis zum jetzigen Zeitpunkt ist die Bedeutung von diesem Mechanismus in der Knochenentwicklung und Pathogenese nur wenig erforscht worden. In dieser Dissertation wurde daher auf die Rolle epigenetischer Genregulationen im Osteoblasten intensiv eingegangen.

Nach Behandlung der pre-osteoblastären MC3T3-E1 Maus Zelllinie mit den zwei Inhibitoren der *Lox*, beta aminopropionitrile (bAPN) und Homocysteine (hcys), haben wir den Effekt von diesen zwei Lathyrogenen auf die Zelllinie analysiert und verglichen. Die Expression von osteoblastären Genen wurde mittels „real time polymerase chain reaction“ (qPCR) und „gene expression microarrays“ untersucht. Marker der osteoblastischen Aktivität und Zellproliferation wurden durch Messung der Aktivität der Alkalischen Phosphatase sowie Viabilitätstest bestimmt. Die Effekte der Substanzen auf die Kollagenquervernetzung wurden durch „Fourier-Transform-Infrarot-Spektrometrie“ (FTIR) gemessen.

Die ersten Ergebnisse zeigten dass sowohl bAPN als auch hcys *Lox* nicht nur enzymatisch hemmen sondern auch dessen mRNA Expression vermindern. Unter Berücksichtigung der klinischen Bedeutung von hcys, haben wir den zellulären Signalweg für die hcys-abhängige Verminderung der *Lox* Expression erforscht. Dabei nutzten wir Techniken wie „Enzyme-linked immunosorbent assay“ (ELISA), Immuno Blotting und Chromatin-Immunopräzipitation (ChIP). Auswertungen ergaben das

Interleukin 6 (IL-6), der Transkriptionsfaktor „Friend leukemia integration 1“ (FLI1) und die DNA-Methyltransferse 1 (DNMT1) in der Repression von *Lox* durch hcys involviert sind. Untersuchungen an der Promotorregion des *Lox*-Gens ergaben eine DNA-methylierungsabhängige Regulation der *Lox* Expression durch hcys.

Im letzten Teil der Arbeit wurde ein neuer Signal –Transduktionsweg aufgeklärt, durch den die extrazelluläre Matrix (ECM) die Proliferation und Differenzierung von Osteoblasten fördern kann. Beim Aussähen von MC3T3-E1 Zellen auf mit Kollagen Typ I beschichtete Platten haben wir eine erhöhte Expression an osteoblastären Genen und eine verminderte Expression des pro-apoptotischen Gens Fas beobachtet. Durch die Verwendung verschiedener Inhibitoren, qPCR und DNA-Methylierungsanalysen konnten wir zeigen, dass das extrazelluläre Kollagen Typ I via FAK, MAPK und den Transkriptionsfaktor AP1 direkt die Expression des Gens *Dnmt1* stimuliert was in weiterer Folge für die Stilllegung des Gens *Fas* durch epigenetischer DNA-Methylierung verantwortlich ist.

Contents

Abbreviations:

ALP	alkaline phosphatase activity
bAPN	β-aminopropionitrile
ChIP	chromatin immuno precipitation
CpG	cytosine-guanine di-nucleotide
DMSO	dimethly sulfoxid
ECM	extra cellular matrix
ELISA	enzyme-linked immunosorbent assay
ERK	extracellular-signal regulated kinase
FTIR	fourier transform infrared spectroscopy
hcys	homocysteine
JAK2	janus kinase 2
MAPK	mitogen-activated protein kinase
OI	osteogensis imperfecta
PBS	phosphate buffered saline
qPCR	quantitative real-time polymerase chain reaction
s.d.	standard deviation

Abbreviations of directly analyzed genes

Bglap2	bone gamma-carboxyglutamate protein 2 (osteocalcin)
Ccna2	cyclin A2
c-Fos	FBJ osteosarcoma oncogene
c-Jun	jun oncogene
Col1a1	collagen, type I, alpha 1
Dnmt1	DNA methyltransferase (cytosine-5) 1
Dnmt3b	DNA methyltransferase (cytosine-5) 3
Fas	Fas - TNF receptor superfamily member 6
Fli1	friend leukemia integration 1
Hells	helicase, lymphoid specific
IL-6	interleukine 6
Lox	lysyl oxidase
Plod2	procollagen lysine, 2-oxoglutarate 5-dioxygenase 2
Runx2	runt related transcription factor 2

1. Introduction

1.1 Lathyrism, clinical manifestations, causes and mechanisms

Lathyrism is one of the oldest neurotoxic diseases known in Man but the causes leading to this pathology were only recognized by the early twentieth century (1). Once prevalent throughout Europe, North Africa, Middle East and parts of the Far East, the disease is presently restricted to India, Bangladesh and Ethiopia (2). Lathyrism is a form of irreversible, non-progressive spastic paraparesis associated with pathological degenerations of connective tissues like bone or blood vessels (3, 4).

Initially, the disease appeared distinct between humans and animals and was diagnosed by degeneration of the nervous system associated with spastic paraplegia, pain and hypesthesias in Man (neurolathyrism) and by skeletal lesions like kyphoscoliosis, exostoses and lameness in animals (osteolathyrism, Fig. 1 and 2). Later, a variety of skeletal lesions were also identified in Man: slipping of the upper femoral epiphysis and kyphoscoliosis as well as weakness and fragility of bone (1, 3, 4).

Lathyrism results from excessive consumption of food compounds containing a chemical class carrying a nucleophilic amino-group as for example β-aminopropionitrile (bAPN, for molecular structure see Fig. 3) (4). These compounds, known as lathyrogens, are mainly found in legumes such as chick peas and vetch, are derivatives of amino acids and act as metabolic antagonists of glutamic acid, a neurotransmitter in the brain (2, 4). Furthermore, lathyrogens were described to inhibit the enzymatic activity of the enzyme lysyl oxidase (LOX), a gene involved in the formation of cross-links between the collagen chains (5-7). The mechanism by which bAPN inhibits LOX activity is still unknown, other LOX inhibitors like ureides, semicarbazides and thiosemicarbazides are believed to

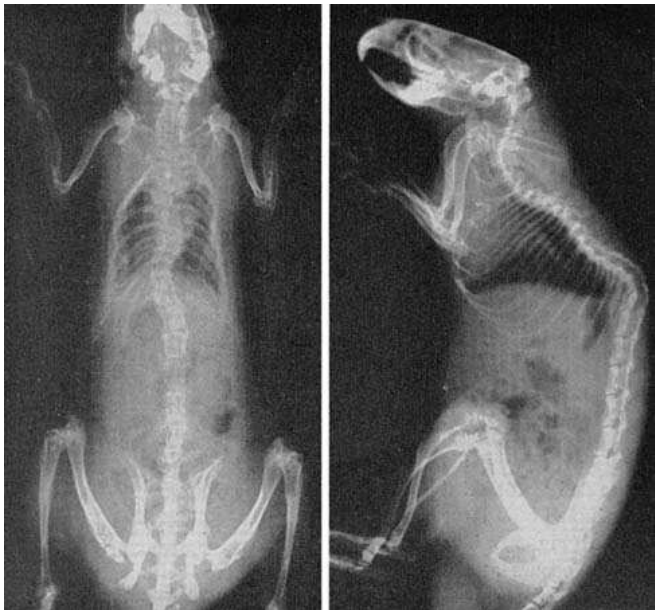

Figure 1 Radiogram of a 13-week-old rat fed with a diet containing 50 per cent Lathyrus odoratus peas from 4 weeks of age. Scoliosis, subluxation of the shoulders, thoracic deformity and bowing of the long bones are clearly observalble (1).

chelate the prosthetic Cu(II)-bipyridine cofactor complex in the enzyme (8). A recent work showed that bAPN clearly inhibited the formation of the two major bone collagen type I cross-links, pyr and dehydrodihydroxylysinonorleucine (deH-DHLNL) (6). The work showed also that bAPN not only inhibits collagen cross-link formation but also influences the expressions of genes important for osteoblastic proliferation and differentiation. Thus, the mRNA expression of collagen type I alpha 1 (*Col1a1*) was increased and the mRNA expressions of osteocalcin (*Bglap2*) and of *Lox* was significantly decreased after bAPN treatment in murine pre-osteoblastic MC3T3-E1 cells (6). Thus, beside the enzymatic inhibition of LOX by bAPN, the decreased collagen-cross-links after bAPN treatment may also be attributed to the suppressive effect of the lathyrogen on the mRNA expression of *Lox* showing a dual effect of the compound on osteoblasts development and bone strength. Furthermore, it was shown that culturing of MC3T3-E1 cells for 1 week on bAPN-marred ECM, still significantly increased *Col1a1* mRNA levels and significantly reduced *Bglap2* mRNA levels when compared to cells seeded on untreated ECM (6). This indicates that even in absence of the lathyrogen, bAPN marred ECM still influences osteoblastic gene expressions suggesting the existence of feedback mechanisms between ECM and interacting osteoblast like cells regulating osteoblastic function and differentiation.

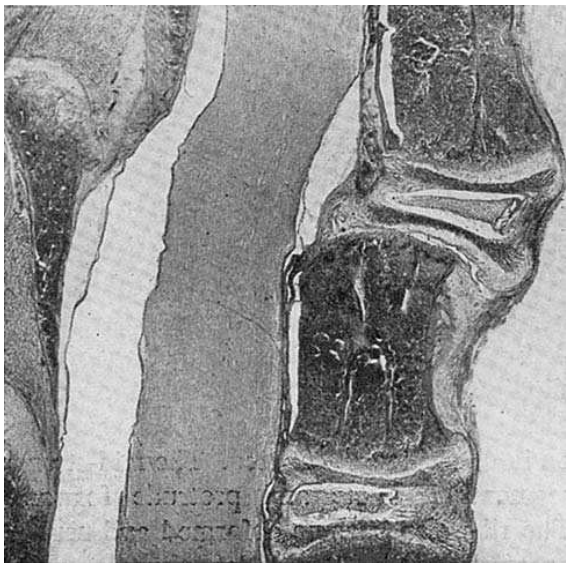

Figure 2. Sagittal section of the mid-thoracic vertebrae in a 56-day old rat fed a diet containing 0.2 per cent bAPN from 23 days of age. Slipping of one vertebra and loosening of the interspinous ligaments at the level of the slipping can be seen (1).

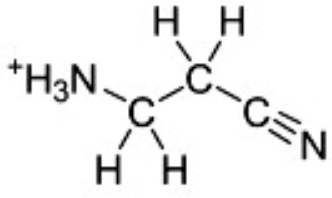

Figure 3. Molecular structure of beta aminopropionitrile (Molecular weight: 256 g/mol)

1.2 Collagen cross-linking and folding in relevance to bone development

Correct collagen folding and cross-linking is essential for the formation of an adequate extra cellular matrix (ECM) which guarantees stability, elasticity and maturation of various connective tissues of mesodermal and mesenchymal origin (9-14). The organic part of bone's ECM consists mainly of collagen type I triple helices

which are composed by two alpha 1 (COL1A1) polypeptide chains and one alpha 2 (COL1A2) polypeptide chain. Each triple helix is firstly synthesized as pro-collagen and undergoes a variety of processing and modification steps, intra- as well as extracellularly (15). For post-translational collagen modifications at least 10 different enzymes are needed, whereby most of them being specific to collagens or proteins with collagenous sequences (16). During intracellular steps, specific lysyl and prolyl residues are hydroxylated as well as some hydroxylysines are glycosylated, collagen polypeptide chains are then assembled to pro-collagen triple-helix domains which are packed into saccules and secreted extracellularly via the Golgi complex (16, 17). Intracellular hydroxylation of prolines is necessary for the generation of stable triple-helical domains. Lysyl-hydroxylations mediate specific cross-linking sources and constitute furthermore glycosylation sites which hinder staggering and lateral packing of collagen fibers within the cell (16). Extracellularly, the pro-collagen molecule is converted to collagen and incorporated into stable, cross-linked collagen fibrils (18, 19). To assure this process, firstly C- and N-terminal pro-collagen peptides are removed from the collagen triple helix by procollagen C-proteinase (BMP1) and procollagen N-proteinase, respectively (15). The resulting tropocollagen molecules are incorporated into collagen fibrils which become stabilized by covalent cross-linking between the individual collagen molecules. For extracellular collagen cross-linking, oxidative deamination of ε-amino groups of lysine and hydroxylysine residues on the collagen triple helix by the enzyme LOX is necessary. This forms highly reactive aldehyde moieties which lead to the formation of covalent intra- and intermolecular cross-links among the helices by spontaneous condensation reactions (16). Six different collagen cross-links have been identified yet: histidinohydroxylysino-norleucine (HHL) dehydrohistidinohydroxy-merodesmosine (deH-HHMD), pyridinoline (pyr), deoxypyridinoline (d-pyr), pyrrole (prl), and deoxypyrrole (d-prl). Depending from tissue type, the cross-linking patterns and molecular distributions vary from tissue to tissue (20).

1.3 ECM and osteoblastic differentiation

Beside this physical attribute played in connective tissues, correct cross-linking and folding of fibrillar ECM components strongly influence cell differentiation of precursor cells by feedback mechanisms (9-11, 21). A functional collagenous bone matrix is critical for cell-cell and cell-matrix interactions; recently it was demonstrated that un-

correct folding of collagen type I protein exposes cryptic binding sites regulating osteoblastic behavior during cell differentiation, tissue repair, and regeneration (11). Furthermore, studies suggested that beside the already known differentiation stimuli, the structural conformation of extracellular collagen I plays a crucial role in the differentiation of specific cell lineages (21-23). Pluripotent mesenchymal bone marrow stromal cells are an important source for tissue homeostasis and repair and have the potential to differentiate into diverse lineages like osteoblasts or adipocytes (24). Several works proposed that dependent on the structural state of the matrix, cell differentiation into specific lineages is specifically regulated through distinct signaling pathways. Thus, on native (triple-helix folded) collagen I matrices inefficient adipogenesis is observed, whereas on denatured (partially unfolded) collagen I matrices an efficient p38 kinase dependent adipogenesis is observed. To the contrary, on native collagen I matrix osteogenic differentiation occurs efficiently but not on the denatured counterpart. The osteogenic differentiation process was demonstrated to be mitogen-activated protein kinase 1 (*MAPK1*) and heat shock protein 90 (*HSP90*) dependent (25). The matrix conformation-mediated regulation of cell differentiation appears to be caused by differential cellular stress responses after exposure of the cells to the native or to the denatured collagen I matrices. The matrix mediated cellular stress responses are proposed to originate from the different matrix properties between native and denatured collagen-ECM to which the cells are exposed, namely matrix contractions and matrix tenseness. Integrin α2β1, a dimer of integrin alpha 2 (ITGA2) and beta 1 (ITGB1) was identified as stress-signal mediator between the by native collagen composed ECM and the *MAPK1*-dependent osteoblastic differentiation pathway (25). Thus, increases of HSP90 levels induce the expression and activation of integrin α2β1 which in turn activates the *MAPK1*-signaling pathway hence facilitating osteogenesis and suppressing adipogenesis. The authors suggested that ECM mediated cellular stress responses might be frequently implicated in differentiation of several specific cell lineages as diverse factors involved in cellular stress response seem to activate differentiation of diverse cell lineages (21, 22, 25). Thus, it was shown that myogenesis of satellite stem cells is promoted by ECM mediated activation and nuclear translocation of Beta-catenin (CTNNB1), a stress response component which was shown to be essential for skeletal myogenesis (21, 26, 27). Further, activation of HSP70 may induce

chondrogenesis as HSP70 was demonstrated to stimulate of the chondrogenic transcription factor SOX9 (21).

Clinically, beside lathyrism further pathological manifestations caused by disrupted collagen-folding or by inappropriate ECM formation affecting bone homeostasis are known. Osteogenesis imperfecta (OI) is a dominant genetic bone disorder resulting from defective connective tissue formation mostly caused by functional mutations of type I collagen genes (*COL1A1* and *COL1A2*). These point mutations often substitute glycines with other residues (28, 29). For collagen triple-helix formation, the protein primary structure requires glycine residues at every third position as for assembly of the triple helix this residue at the interior of the helix-axis is indispensable because there is no space for a larger side group than glycine's single hydrogen atom (15, 18). Therefore, polymorphisms substituting this amino acid hinder a correct triple-helix formation of the collagen fibril creating a bulge in the collagen complex, which in turn influences both, the formation of an adequate ECM as well as appropriate interactions between ECM and cellular networks. Depending on the type of OI, the severity of the symptoms varies from patient to patient and includes bone fragility, skeletal deformities, scoliosis, hearing loss and others (29). Genes that concern post-translational modifications of type I collagen molecules such as cartilage-associated protein (*CRTAP*), leucine proline-enriched proteoglycan (*LEPRE1*), peptidylprolyl isomerase B (*PPIB*), serpin peptidase inhibitor, clade H (heat shock protein 47, *SERPINH1*) and FK506 binding protein 10 (*FKBP10*) were also found to be the causative candidates for OI (30).

1.4 Molecular basics of osteoblastic differentiation

Osteoblasts, the bone forming cells, derive from undifferentiated mesenchymal stem cells (31). The differentiation stages of osteoblasts were defined as osteoprogenitor cells, pre-osteoblasts, mature osteoblasts, osteocytes, and lining cells (32). Osteoprogenitor cells are committed cells which are induced to differentiate into preosteoblasts or osteoblasts by growth factors like the bone morphogenetic proteins (BMPs). Pre-osteoblasts are characterized by a high cell proliferation rate in concomitance with the expression of matrix forming collagens, Osteopontin (*SPP1*) and other genes (33-35). Mature osteoblasts express high levels of osteocalcin (*OCN*, *BGLAP2*) and mineralize the extra cellular matrix (33, 36). Osteocytes are housed in lacunae, they stabilize bone mineral and play a key role in homeostatic,

morphogenetic, and restructuring processes that regulate the mineral content and architecture of bone mass (37). Bone lining cells are inactive osteoblasts which cover the surface of most bones in an adult. Bone lining cells are suggested to regulate the transport of calcium and phosphate into and out of the bone (38). Although, the proposed schema suggests that an osteoblast moves through all differentiation stages, the co-existence of diverse functional sub-groups of osteoblasts is discussed (39, 40).

Cell fate determination of bone marrow deriving mesenchymal stem cells (MSC) depends mainly on extra-cellular stimuli like growth factors, extra-cellular matrix and other microenvironmental factors (21, 22, 41, 42). These multi-potent cells are predisposed to differentiate into various tissue lineages including chondrocytes, adipocytes, muscle cells and osteoblasts. BMPs play thereby an important role (43, 44). *BMP2* for example, induces MSC to osteoblastic differentiation and inhibits myogenic cells to differentiate into myotubes (45). The runt-related transcription factor 2 (*RUNX2*), which is induced by bone morphogenetic proteins, play an essential role in osteoblastic commitment and differentiation (12) as well as in the formation of the mineralized skeleton during embryogenesis and regulates maturation of the osteoblastic phenotype (46); as a central factor it implements extra-cellular signals from BMPs and Wnt-pathways thus promoting cellular phenotypic commitment and osteogenesis (47). Knock out of *Runx2* in mice results in the inability to form a mineralized skeleton and in perinatal lethality (48, 49). *Runx2* over expression represses the differentiation of other cellular phenotypes of mesenchymal origin, as for example the development of myoblasts or chondrocytes, by *Runx2* dependent suppression of the gene for myogenic differentiation (*Myod1*) and *Sox9*, respectively (47, 48). Generally, cell differentiation is accompanied by down regulation of cell proliferation. Thus, it was shown that forced expression of *Runx2* in pre-osteoblasts suppresses their proliferation (44, 49). Furthermore, the cyclin dependent kinase inhibitors p21 (*Cdkn1a*) and p27 *(Cdkn1b)* were shown to be *Runx2* target genes (50, 51) and inhibition of p53 *(Trp53)* was demonstrated to be a prerequisite for *Runx2* activation and bone formation (52).

At the early stages of osteoblastic differentiation RUNX2 controls the expression of many extracellular matrix proteins like COL1A1 (53), fibronectin (FN1) (53), bone sialoprotein-2 (IBSP), osteopontin (SPP1) (54) or osteocalcin (BGLAP2) (48, 54). As very recently shown, during the late phase of osteoblastic differentiation, *Runx2*

expression is down regulated by the zink finger protein 521 (*Zfp521*) which is suggested to permit complete osteoblastic differentiation as *Runx2* over expression during this differentiation phase was shown to inhibit complete osteoblast maturation, thus provoking diverse bone pathologies in mice (55-58). *Runx2* expression itself is regulated by diverse factors in osteoblasts. BMP4 and BMP7 induce its transcription, SATB2 directly interacts with it and enhances its activity whereby RUNX2 auto regulates its own expression by a negative feedback mechanism (47). The homeodomain proteins msh homeobox 2 (*Msx2*), distal-less homeobox (*Dlx3*) and *Dlx5* represent a regulatory network for commitment of the bone cell phenotype. They are important regulators of osteoblastic differentiation in the adult skeleton whereby acting upstream, *Msx2* repress *Runx2*, while *Dlx3* and *Dlx5* are potent activators of *Runx2* and other bone related genes in osteoblastic lineage cells (47). *Msx2* promotes commitment and early differentiation of osteoprogenitor cells and inhibits adipocyte differentiation. However, *Msx2* hinders ossification of non-osseous cells and expression of genes of the mature osteoblastic phenotype (59-62). A further bone tissue specific transcription factor regulated by *Runx2* which is also significantly involved in osteoblastic differentiation is osterix (*Sp7*). Similar to *Runx2*, *Sp7* depleted mice also lack bone tissue formation, although *Runx2* is normally expressed. This suggests that both transcription factors are essential for normal bone development and cover distinct fields of action: *Sp7* promotes proliferation of progenitor cells, while *Runx2* regulates genes of the pre-osteoblastic/osteoblastic phenotype having an anti-proliferative effect (63, 64).

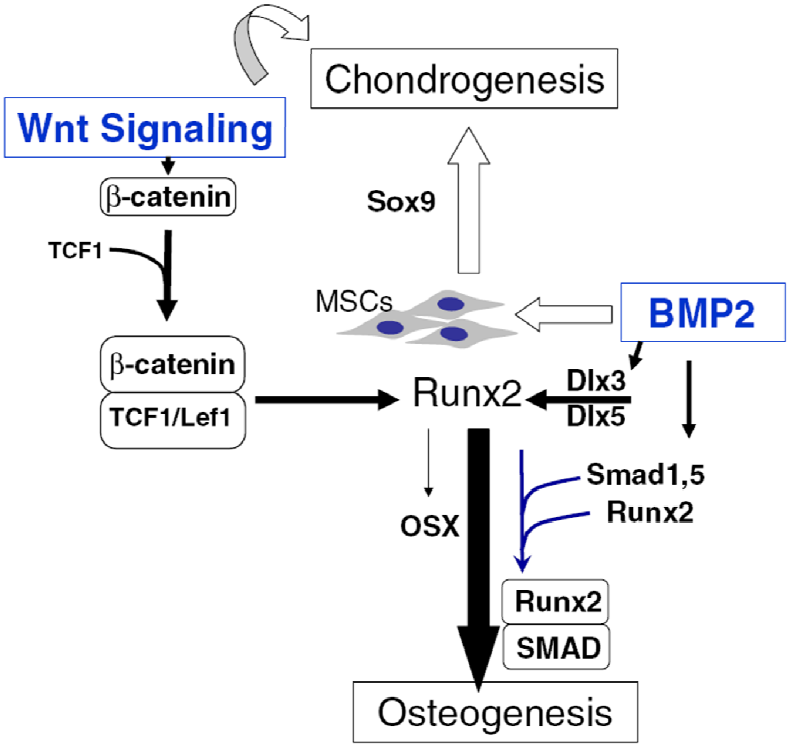

Figure 4. Signal pathways involved in mesenchymal stem cell differentiation. The role of Wnt signaling and BMP2 for osteoblastogenesis and chondrogenesis are shown. The central role played by Runx2 in osteoblastic differentiation is demonstrated (Figure adapted from 47).

As summarized in figure 4, *Runx2* plays a central role in bone development. Wnt pathways and BMP signaling regulate chondrogenesis as well as osteogenesis. The Wnt/ß-catenin pathway as well as *Bmp2* activates *Runx2* in MSCs. *Bmp2* induces *Dlx3* and *Dlx5* which increase *Bmp2* induced *Runx2* expression. Furthermore, *Bmp2* induces *Sp7* which is up regulated by *Runx2*. *Dlx3*, *Dlx5* and *Sp7* can also directly stimulate the expression of bone genes independently of *Runx2*. Further, *Runx2* in concomitance with *Smad1* and *Smad5* functions as a hub for differentiation of a progenitor cell into the osteogenic lineage via integration of the *Bmp2* signal (47).

The biological functions of the dimeric transcription factor complex activator protein - 1 (AP-1) in skeletal development was clearly shown by several genetically modified mice and cells models. AP-1-components like *Fos* were demonstrated to be key players in osteoblastic and osteoclastic cell differentiation (65). Knock out of *Fos* in mice were shown to provoke osteopetrosis whereby the *Fos* trans-gene mice developed osteosarcomas (66) . The AP-1 complex can be formed by a great variety of proteins of the *Fos*, *Jun*, and activating transcription factor (ATF)-families and it is differentially composed during osteoblast differentiation (65). Thus, *Fos* and *Jun* proteins are highly expressed in precursor and pre-osteoblasts. However, during extracellular matrix production and mineralization their levels decline. In fully

differentiated osteoblasts FOSL2 and JUND represent the major components of the AP-1 complex (67). Several osteoblastic genes are known to be regulated by the AP-1 transcription factor complex as for example *Col1a1* (65). In summary, the AP-1 complex was shown to regulate proliferation, differentiation, and apoptosis of osteoblasts and osteoclasts (62, 64).

1.5 Homocysteine and bone homeostasis

1.5.1 The role of homocysteine as cell metabolite

In the last years, the non proteinogenic α-amino acid L-homocysteine (hcys, formula: $HSCH_2CH_2CH(NH_2)CO_2H$) is with increasing interest discussed to affect bone homeostasis as proposed to act as lathyrogen (6, 69). Hcys is a natural eukaryotic metabolite known to be involved in the one carbon metabolic cycle (Fig. 5). Here it co-regulates several physiological and pathological pathways. In the first step of this cycle, hcys becomes methylated by the vitamin B12 dependent enzyme methionine synthetase (MS) which results in the generation of methionine. Activation of methionine to S-adenosylmethionine (SAM) by the enzyme methionine adenosyltransferase leads to methylation of DNA, proteins, membrane phospholipids or neurotransmitters. After transfer of the methyl group, SAM converts to S-adenosyl-homocysteine (SAH) which via reversible hydrolysis by the enzyme SAH hydrolase re-generates hcys completing the cycle (68).

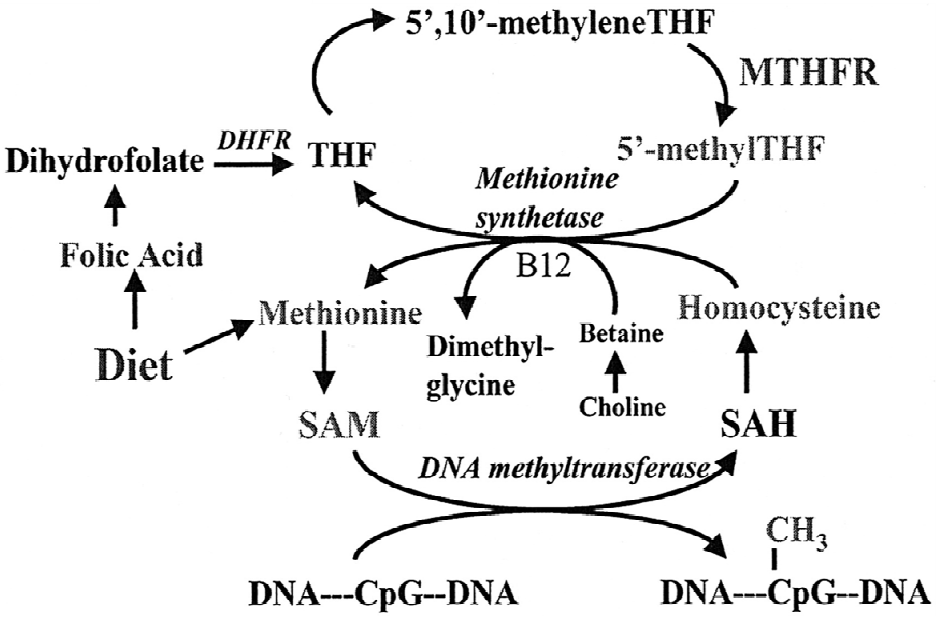

Figure 5. One carbon metabolic cycle showing Homocystein metabolism (Figure adapted from 68).

However, hcys has also been shown to interfere with the activity of the collagen cross-linker LOX (69), altering post-translational modifications and cross-linking of collagen.

1.5.2 Homocysteine as metabolic risk factor

Epidemiological studies have shown that elevated hcys serum levels (>10 µmol/L) represent a risk factor for several chronic disorders such as cardiovascular disease, atherosclerosis, chronic renal failure, diabetes or the metabolic syndrome (70, 71). Moreover, hyperhomocysteinemia is known to affect bone development and homeostasis (68-70). In this context, a correlation between plasma hcys levels and collagen cross-link ratio in forming trabecular surfaces in human bone was recently reported (72). Furthermore, recent clinical and epidemiological data reported a correlation between elevated blood hcys levels and bone fracture risk (73-76).

Several factors can lead to hyperhomocysteinemia. Risk factors include chronic kidney diseases, cigarette smoking, hypothyroidism, specific malignant tumors as well as the intake of definite drugs (73-76). Genetic causes include polymorphisms in the genetic code of mediator enzymes involved in homocysteine metabolism (81, 82). Among these, the most investigated single nucleotide polymorphism (SNP) affects the enzyme methylenetetrahydrofolate-reductase (MTHFR) which catalyzes the conversion of 5,10-methylenetetrahydrofolate to 5-methyltetrahydrofolate thus providing methyl-groups to the enzyme MS for methionine generation from hcys. This mutation substitutes a cytosine with a thymine at base pair 677 on MTHFR's mRNA, thus replacing an alanine with a valine at the protein level. The SNP is present in the homozygous state in 5-10% of the general Caucasian population and causes a thermolabile form of the enzyme with an approximately 70% reduced activity thus provoking an hcys accumulation (77) . Elevated hcys levels can also be caused by nutritional deficiencies in folate, vitamin B12 or vitamin B6 (78). As mentioned before, vitamin B12 and folate are directly involved in hcys's methylation cycle; the vitamin B6 dependent enzyme cystathionine-beta-synthase (CBS) metabolizes in further metabolic steps hcys firstly to cystathionine and subsequently to the amino acid cysteine. As shown by Papandreu et al. (79), folate supplementation (5 mg oral folate, twice a week) for two months to hyperhomocysteinemic children significantly decreased total hcys serum levels. In a large polish study, an inverse association between vitamins B6, B12 as well as folate consumption and hcys concentration and

prevalence of hyperhomocysteinemia was observed (80). Another study correlated folic acid supplemented food intake with higher serum and red blood folate and vitamin B12 concentrations and lower hcys serum levels (81). Moreover, an association between vegetarian diet, plasma hcys levels and bone mineral density was found in Slovak women (82). In this study, several bone development markers, serum folate and vitamin B12 levels, plasma levels of total hcys as well as bone mineral density of the femoral neck, trochanter, total femur and lumbar spine were compared between 141 long-term ovo-lacto-vegetarian women and a control group of 131 women consuming a standard western diet. The results show that vegetarians have significantly higher hcys plasma levels while vitamin B12 levels are significantly lower in this group. However, no differences were observed in folate levels between the two groups. Furthermore, vegetarians show significantly lower bone mineral densities (BMD) at the trochanter and on the total femur. A strong correlation between homocysteine levels and the BMD of the femoral neck, of the trochanter and of the total femur was found in all subjects (87). Thus, low vitamin B12, folate or vitamin B6 serum levels in concomitance with high hcys serum levels may function as predictors for negative bone development and homeostasis.

1.6 Regulation of gene expression by epigenetic DNA methylation and the role of homocysteine

1.6.1 DNA methylation and homocysteine, the principles

A new, interesting issue raised in the last years concerns the role of hcys in the modulation of epigenetic DNA methylation. As a metabolite hcys is directly involved in DNA methylation as it acts as methyl-group “carrier”. Therefore, numerous efforts have been done during the last years to understand the impact of supplementations or depletions of this compound as well as of folate, vitamin B12 and vitamin B6 on epigenetic regulation of gene expressions. In mammals, DNA methylation is mediated by DNA (cytosine-5-)-methyltransferases (Dnmts) (83). By now three active Dnmts are known. *Dnmt1* is discussed to be responsible for maintaining of global DNA methylation, whereas specific methylation by this enzyme was recently demonstrated as well (84). *Dnmt3a* and *Dnmt3b* are related to specific de-novo DNA methylation and Dnmt3l was shown to support Dnmt3a and Dnmt3b methylation, but lacks itself methyl-transferase activity (83). The biological role of Dnmt2 is still

unknown in mammals. *Hells* (PASG, LSH), a gene involved in chromatin remodeling, was recently shown to associate with *Dnmt1* and *Dnmt3b* enhancing DNA methylation (85). Dnmts' mediated epigenetic DNA methylation is characterized by deoxycytidine methylation at position 5' of the base, whereas neighboring deoxyguanosines are essential resulting in specific methylation at CG sites, also called CpG sites; thereby "p" represents the base-linking phosphodiester bond in DNA backbone (83). Dnmts are part of the transcriptional machinery protein complex thus methylating the CpG sites during DNA replication (86). Generally, DNA is highly methylated at CpG sites, especially in non-coding regions. To the contrary, CpG islands are normally largely un-methylated at CpG sites (83, 87). CpG islands are regions of ~ 300 to 3000 base pairs (bp) in length with CpG content greater than 50%, and ratio of observed CpG's by expected CpG's of 0.6. CpG methylation mostly suppresses gene expression of specific genes inhibiting transcription factor binding on the affected promoters (82, 86). Several transcription factor binding sites contain CpG dinucleotides as for example the binding sites for the transcription factors activating protein 2 (AP-2, *TFAP2A*) or for the specificity protein 1 (*Sp1*). Thus, after cytosine methylation of such sites, binding of a specific transcription factor is reduced by the methyl-group itself or by block of the transcription factor binding site through binding of methyl-binding proteins (MeCP2, MBD1, MBD2 and MBD4) or with this proteins bound repressors at the methylated CpG site (88); the gene becomes epigenetically silenced. However, it was also shown that in some cases hindrance of repressor binding at methylated CpG sites induces the opposite effect (89). Methylation of a single or of a few CpG's in a gene promoter were shown to be sufficient for gene silencing (90), in other cases a correlation between promoter CpG methylation and gene expression were described (91, 92). Binding of methyl binding proteins generally recruit histone deacetylases to the affected sites provoking a condensed chromatin structure. Thus, changes in DNA methylation pattern lead furthermore to changes of chromatin status and stability determining differentiation, pathogenesis and senescence of a cell (88, 93-95). Aberrant CpG methylation of gene promoters are related to several pathologies and several factors are known to influence methylation of DNA. Thus epigenetic research focuses on cancer development, cardiovascular diseases, mental health, stem cell research, cell and tissue development and differentiation, gene imprinting and the interactions between environment and epigenetic regulation of gene expression. Furthermore epigenetic

research investigates silencing of transposons, retroviruses and imprinting of genes as CpG methylation is strongly involved in these mechanisms.

1.6.2 Disruptions of the homocysteine metabolism affect DNA methylation patterns

Studies in several cell cultures, animal models and humans show that high hcys levels affect DNA methylation patterns (101-103). However, despite intense research, due to apparently contradictory results, the impact of aberrant hcys, folate, vitamin B6 and vitamin B12 levels on global and specific DNA methylation remains still unclear. For example, it was demonstrated that during the earliest stages of bovine embryonic development, high hcys concentrations induce hypermethylation of genomic DNA and developmental retardation in bovine embryos (96). Further, genome-wide analysis of CpG dinucleotides methylation identified gene-specific CpG methylation patterns associated with cord blood plasma homocysteine concentration and birth weight centile in humans (97). Moreover, it was shown that dietary methyl supplementation of pregnant agouti mice with extra folic acid, vitamin B12, choline, and betaine alters the phenotype of their offspring via increased CpG methylation at the agouti gene locus (98). However, it was also shown that long-term administration of folate/methyl-deficient diet in Fisher 344 rats causes global DNA hypermethylation in brain tissue but at the same time these epigenetic changes are opposite in the liver of the same folate/methyl-deficient rats (99, 100). Therefore, it seems that aberrant levels of hcys, folate, vitamin B6 and vitamin B12 alter DNA methylation dependent by cell type, phenotype, tissue and developmental stage of the organism. Furthermore, in vivo DNA methylation may also be influenced by various other factors as for example by rate of cell growth or inflammation (101-104). Consequently, the effect of aberrant hcys levels on epigenetic alteration of gene expressions relevant to pathogenesis of diseases has to be evaluated cell, tissue, and developmental stage specifically.

2. Aims and focuses of this PhD thesis

In regard to the above illustrated research state and to the effects of bAPN and hcys in bone development and homeostasis, the following aims were set in this PhD thesis.

First, to investigate and compare the effects of the lathyrogens bAPN and hcys on

osteoblastic collagen matrix formation by using the pre-osteoblastic MC3T3-E1 cell line. Thereby collagen cross-linking and expression of genes involved in osteoblastic differentiation, matrix formation and collagen cross-linking (lysyl oxidase, lysyl hydroxylase, collagen type I, and others) were assessed by FTIR and quantitative real time polymerase chain reaction (qPCR) as well as by genome wide expression (GeneChip) analysis, respectively. Moreover, feedback signals from the matrix to the matrix producing cells should be analyzed and characterized.

According to the first results, which showed that additionally to hcys dependent LOX enzymatic inhibition, hcys represses *Lox* mRNA expression as well, as second goal the mechanism behind this observation was defined. To gain an overview of the effects of hcys on MC3T3-E1 cells, genome wide expression analysis of hcys treated osteoblasts were performed. A special focus was set on the investigation of putative intra-cellular pathways involved in the hcys dependent down regulation of *Lox* mRNA expression. To accomplish this aim, selected molecular methods including qPCR, immuno-blotting, molecular cloning, DNA methylation analysis, ELISA and chromatin immuno precipitation (ChIP) were used.

Finally, interactions between collagen type I containing ECM and osteoblasts are known to significantly influence osteoblastic adhesion, proliferation and differentiation. Thus, using several inhibitors, qPCR, global and specific DNA methylation analysis, mechanisms involved in collagen type I mediated prevention of anoikis and induction of differentiation were analyzed in MC3T3-E1 cells.

Summarizing, this PhD thesis aimed to analyze and compare the effects of hcys and bAPN on osteoblastic proliferation and differentiation with a special focus on collagen cross-link formation. Further, feedback mechanisms between ECM and osteoblasts were examined. Generally, possible epigenetic mechanisms involved in these processes were investigated.

3. Results

3.1. Differential effects of homocysteine and beta aminopropionitrile on pre-osteoblastic MC3T3-E1 cells (105)

Hcys, a metabolite of the methionine-folate metabolism, and bAPN, a model component of natural occurring lathyrogens, were compared in regard to their effect on collagen cross-linking and on their impact on the mRNA expression of several

osteoblastic genes. As mentioned before, osteoblast-synthesized collagen matrix regulates the differentiation of precursor cells into mature osteoblasts. The aim of this study was to investigate the effects of bAPN and hcys on collagen cross-links and gene expression at the mRNA level by FTIR and quantitative qPCR, respectively. We found that bAPN and hcys down-regulated cell multiplication. While bAPN also down-regulated the metabolic activity of MC3T3-E1 cells, hcys down-regulated it by lower concentrations but up-regulated it by higher; both substances up-regulated alkaline phosphatase activity. The substances increased the ratio of pyr/divalent cross-links of collagen, and down-regulated mRNA expression of lysyl hydroxylase *Plod2* and *Lox*, genes which play an important role in the formation of a stable matrix. Furthermore, we demonstrated that both substances stimulated the expression of the indispensable regulator of osteoblastic differentiation *Runx2*. However, analysis of genome wide mRNA expression suggests that hcys and bAPN have differential effects on genes involved in osteoblastic differentiation and phenotype regulation. The results indicate that although both bAPN and hcys affect collagen cross-link post-translational modifications in a similar manner as far as pyr and divalent cross-links are concerned, they have differential effects on the monitored gene expression at the mRNA level, with hcys exerting a broader effect on the genome wide mRNA expression.

3.2 Homocysteine suppresses the expression of the collagen cross-linker lysyl oxidase involving IL-6, Fli1 and epigenetic DNA-methylation (106)

As recently shown, hcys influences the formation of a stable bone matrix not only directly through the inhibition of the collagen cross-linking enzyme LOX but also by repressing its mRNA expression (105). The aim of this study was to elucidate the mechanisms underlying the hcys dependent down regulation of Lox expression. By means of genome wide expression analysis, qPCR, immuno-blots, chromatin immuno precipitation, molecular cloning and ELISA we identified a hcys-dependent stimulation of Interleukin 6 (IL-6) and genes involved in IL-6/JAK2 (Janus kinase 2) dependent signal transduction pathways in pre-osteoblastic MC3T3-E1 cells. Moreover, up-regulation of genes essential for epigenetic DNA methylation (DNA (cytosine-5-)-methyltransferases (Dnmts) and lymphoid-specific Helicase (LSC,

Hells) was observed. Further investigations demonstrated that hcys increased via IL-6/JAK2 the expression of *Fli1* (Friend leukemia virus integration 1), a transcription factor, which we found essential for IL-6 dependent Dnmt1 transcription. Analysis of CpG rich *Lox* proximal promoter revealed an increased CpG methylation status after treatment of the cells with hcys indicating an epigenetic cause for hcys dependent *Lox* repression. Inhibition of the IL-6/JAK2 pathway or of CpG-methylation reversed the repressive effect of hcys on *Lox* expression. In conclusion we demonstrated that hcys stimulates IL-6 synthesis in osteoblasts, which is known to affect bone metabolism via osteoclasts. Further, IL-6 stimulation results via JAK2, FLI1 and DNMT1 in down-regulation of LOX expression by epigenetic CpG methylation revealing a new mechanism negatively affecting bone matrix formation.

3.3 Extra-cellular matrix suppresses expression of the apoptosis mediator Fas by epigenetic DNA methylation (107)

The extracellular matrix (ECM) of bone consists mainly of collagen type I, which induces osteoblastic differentiation and prevents apoptosis. Fas induces apoptosis in cells improperly adhering to ECM. Recently, it was described that Fas expression is modulated by epigenetic DNA methylation. Mouse MC3T3-E1 pre-osteoblastic cells were cultured either on collagen coated or on uncoated culture dishes for control. mRNA was isolated and gene expression was analyzed by quantitative qPCR. Furthermore, we measured global and specific DNA methylation. Compared to controls, cells cultured on collagen-coated dishes increased the expression of *Runx2* and OCN indicating differentiation of pre-osteoblastic cells. Additionally, collagen up-regulated cyclin-A2 and down-regulated *Fas* expression suggesting increased cell multiplication. Furthermore, the expression of *Dnmt1* and *Hells*, key mediators of the DNA-methylation process, was increased. As a consequence, we demonstrate that global DNA methylation and specific methylation of the *Fas* promoter was higher in MC3T3-E1 cells cultured on collagen when compared to controls. Investigation of signal transduction pathways by mean of inhibitors suggests that focal adhesion kinase, MAP- and *Jun*-kinases and AP-1 are involved in this process. In summary, we demonstrate that ECM prevents activation of *Fas* by epigenetic DNA methylation.

4. Materials and Methods

4.1 Cell line used and culture conditions

In the here presented published articles, the clonal murine calvarial pre-osteoblastic MC3T3-E1 cell line was used (Fig 6). This cell line has been established from C57BL/6 mouse calvaria and was selected because of the high ALP activity in the differentiated state. MC3T3-E1 cells differentiate form a pre-osteoblastic phenotype into mature osteoblasts which form mineral deposits extra-cellularly (108). During this differentiation process expression of *Bglap2* (osteocalcin) and its regulator *Runx2*, two well-known markers of osteoblastic differentiation, increases (35). MC3T3-E1 cells secrete also high amounts of collagen type I which significantly influence their proliferation and differentiation.

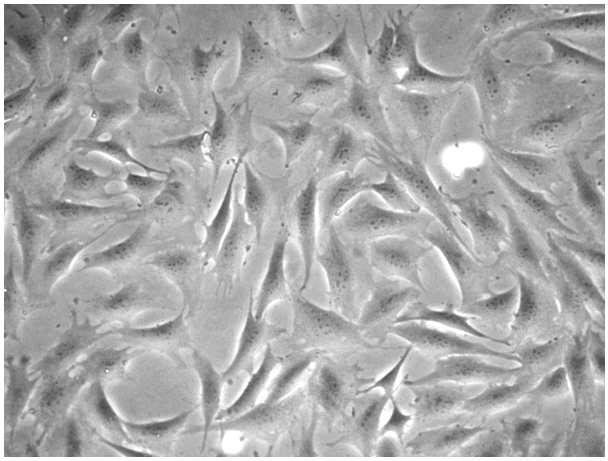

Figure 6. MC3T3-E1 Cells 48h after seeding at 10.000 cells/cm²

MC3T3-E1 cells were cultured in humidified air under 5% CO_2 at 37℃ in alpha-minimum essential medium (a-MEM; Biochrom, Berlin, Germany) supplemented with 5% fetal calf serum (Biochrom), 50 µg/ml ascorbic acid (Sigma), and 10 µg/ml gentamycin (Sigma). For propagation, cells were sub-cultured twice a week using 0.001% pronase E (Roche) and 0.02% EDTA in Ca^{2+}- and Mg^{2+}-free phosphate-buffered saline (PBS) before achieving confluence. To prevent a potential phenotypic drift during repeated sub-cultures the cells were not used more than 4 weeks after thawing. For experiments the cells were seeded in culture dishes at the indicated densities with or without the indicated inhibitors or additives and cultured for the specified culture times with medium changes twice a week.

4.2 MC3T3-E1 treatment with diverse compounds and inhibitors, culture plate and ECM preparation

To study influence of the lathyrogens, MC3T3-E1 cells were seeded in culture dishes at a density of 20,000/cm² and cultured overnight. On the next day, the medium was changed and the cells were treated with or without bAPN (Sigma) or hcys (Sigma) for 1 week to gain two to three cell layers (109). Medium was changed once during the

treatment time. Based on previous publications (6, 69), the concentrations of the substances were 0.1 mM, 0.4 mM, 1 mM, and 4 mM. For hcys an additional concentration of 10 mM was studied. Culture time for matrix production was 7 days because previous results demonstrate that during this period MC3T3-E1 cells produces about 2 to 3 cells layers embedded in collagen (109). Moreover, this makes the results of the present study directly comparable with our previous report concerning bAPN (6).

To demonstrate effects of hcys on the JAK2-pathway and on DNA methylation, cells were seeded at 20,000 cells/cm^2 and cultured overnight. On the next day medium was changed and cell treated with 0.108, 3.6 or 10.8 mM mM hcys for 3, 6 or 14 days. To demonstrate the effect of hcys on the JAK2 pathway or on DNA-methylation, cells were seeded and cultured with 3.6 mM hcys for 3 days; thereafter 30 µM of the specific JAK2 inhibitor AG490 (Calbiochem) solved in DMSO (Sigma) or 50 µM of the DNA methylation inhibitor zebularine (Sigma) solved in H_2O were added to the medium for further 3 days. To test effects of recombinant mouse IL-6 protein (PeproTech,Great Britain) on the cells, they where cultured with increasing concentrations (3 to 30 ng/ml) for 36 and 48 hours. To demonstrate the IL-6 dependent activation of the JAK2 pathway by hcys, cells were treated with 3.6 mM hcys for 3 days, thereafter 4 µg/ml IL-6 antibody (AB) (PeproTech, Great Britain) were added to the medium for further 3 days.

To study epigenetic effects of collagen-I matrix on expression and promoter methylation of *Fas* (110), MC3T3-E1 cells were seeded in culture dishes coated with or without rat-tail collagen at a density of 2,000/cm² and cultured for 2, 4, 6 hours, 1, 2, 4 and 8 days with medium changes twice a week. For collagen coating, culture dishes were incubated for 1 hour with a collagen solution of 5 µg/cm² rat tail collagen (BD Biosciences) in 0.02 N CH_3COOH as suggested by the supplier. Cells cultured on collagen-coated dishes were confluent after 4–5 days while control cells needed 6–7 days culture time for confluence. For ECM production, living cells were removed by treatment with 0.5 % sodium deoxycholate (DOC) in PBS leaving the ECM after being cultured for a total of 7 days (Fig 7). Therefore cells were firstly washed twice with PBS and then incubated with the DOC solution for 20 minutes at 4℃. After dissolving of the cells, ECM was carefully washed 4 times with PBS to remove traces of DOC. For reseeding experiments, fresh MC3T3-E1 cells were seeded on the prepared ECM at a density of 20,000/cm² and cultured for 1 week. Treatment with

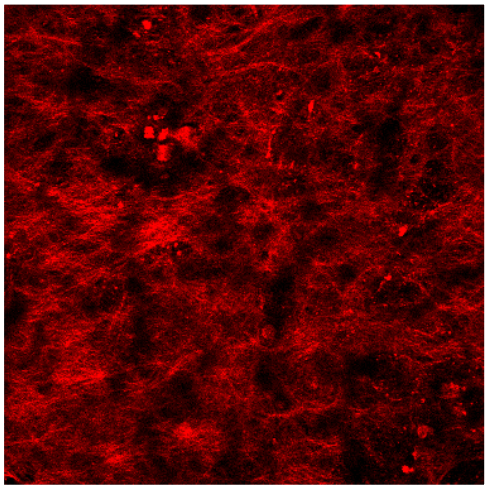

Figure 7. Extra cellular matrix of MC3T3-E1 cells after 1 week of culture. After cell culture cells were dissolved with 0.5% sodium deoxycholate and the

inhibitors of signal transduction was performed with the focal adhesion kinase inhibitor (FAK) genistein (111) (10 µM, Sigma), the selective MAP-/ER-kinase inhibitor PD98059 (112) (10 µM, Promega) and the AP-1 inhibitor resveratrol (113) (40 µM, Sigma). In these experiments, inhibitors were added to the cell suspensions 30 minutes before seeding of the cells. Genistein and PD98059 were solved in DMSO as 1,000-fold stock-solution to prevent influence on gene expression (Thaler, R et al. in preparation) and resveratrol was dissolved in ethanol.

4.3 Cell multiplication, viability and alkaline phosphatase activity (ALP)

To estimate effects of the lathyrogens on cell multiplication, cell viability and ALP-activity, a major indicator for osteoblastic differentiation (114, 115), MC3T3-E1 cells were seeded at a density of 20,000/cm² and cultured overnight.

On the next day, the medium was changed and the cells were treated with or without bAPN or hcys at various concentrations for 1 week. For determination of cell number (DNA amount employed as surrogate), cell layers were washed with PBS and frozen with 1 mM Tris–HCl buffer (pH 8.0) containing 0.1 mM EDTA. During thawing, Hoechst 33258 dye (Polysciences, Warrington, PA) was added (1 µg/ml) and, after an incubation of 15 minutes at room temperature, the fluorescence was measured (excitation 360, emission 465 nm). The amount of DNA was estimated using a standard curve prepared from calf thymus DNA (Roche). Thereafter, alkaline phosphatase (ALP) activity was measured with p-nitrophenylphosphate (2.5 mg/ml in 0.1 M diethanolamine buffer [pH 10.5], 150 mM NaCl, 2 mM $MgCl_2$) by incubation of the cell layers for 15 minutes at room temperature. Absorption was measured in a microplate reader at 405/490 nm. ALP activity (units per milligram DNA) was estimated using a standard curve prepared from calf intestinal ALP (Roche). To assess cell viability, a commercially available assay (EZ4U; Biomedica, Vienna, Austria) was used, according to the protocol of the supplier.

4.4 Nucleic acid isolation

RNA isolation

RNA isolation was performed with the spin column format “SV Total RNA Isolation System Kit” (Promega) or similar RNA extraction Kits from other suppliers following manufactures instructions. In brief, firstly up to 1 x 10^6 cells were lysed in 175 µl of RNA lysis buffer and lysate was expelled into a 1.5 ml tube. Then, 350 µl of RNA dilution buffer was added to the lysate and heated on in a thermo block at 70℃ for 3 minutes. Afterwards, the solution was centrifuged at 13,000 × *g* for 10 minutes at room temperature and the cleared lysate solution was transferred to a fresh microcentrifuge tube by pipetting avoiding disturbing the pelleted debris. 200µl 95% ethanol were added to the cleared lysate, and mixed by pipetting. The mixture was then transferred to a spin column assembly and centrifuged at 13,000 × *g* for one minute. After centrifugation, nucleic acids were bound to the silica matrix of the spin basket; the liquid in the collection tube was discarded. For first purification, 600 µl of RNA wash solution was added to the spin column assembly and centrifuged at 13,000 × *g* for 1 minute. Subsequently 50 µl of freshly prepared DNase solution was directly added to the membrane inside the spin basket and incubated for 15 min for DNA digestion. After this incubation, 200 µl of DNase stop solution was added to the spin basket, and centrifuged at 13,000 × *g* for 1 minute. Next, the spin column was washed with 600 µl RNA wash solution and centrifuged at 13,000 × *g* for 1 minute. Finally, the spin basket was transferred to a 1.5 ml elution tube and RNA was eluted with 100 µl of nuclease-free water by centrifugation at 13,000 × *g* for 1 minute. Purified RNA was stored at –80℃ or subjected to cDNA synthesis.

DNA isolation

For specific CpG methylation analyses, DNA was isolated with the DNeasy Blood & Tissue Kit (Qiagen) or with comparable DNA extraction kits following manufacturer’s instructions. In brief, a maximum of 5 x 10^6 cells were collected in 200 µl PBS in a 1.5 ml tube and 20 µl proteinase K were added. Next 200 µl Buffer AL were added and solution was mixed thoroughly by vortexing and incubated at 56℃ for 10 minutes. Afterwards, 200 µl ethanol (96%) were pipetted to the sample, mixture was transferred to a DNeasy mini spin column assembly and centrifuged at 6000 x g for 1 min. DNA was bound to the collection basket and flow-through was discarded. Subsequently, 500 µl buffer AW1 was added to the spin column and centrifuged for 1

minute at 6000 x g. Then, 500 µl buffer AW2 was added spin column assembly was centrifuged for 3 min at 20,000 x g. Finally collection basket was placed into a 1.5 ml tube and DNA was eluted with 200 µl buffer AE by incubation at room temperature for 1 minute followed by centrifugation for 1 min at 6000 x g. RNA concentrations were measured spectroscopically at 260/280 nm.

4.5 cDNA synthesis

cDNA was synthesized from about 0.5 µg RNA using the Transcriptor 1st Strand cDNA Synthesis Kit (Roche) as described by the supplier (Roche). Thus, following components were mixed in a 1.5 ml tube (table 1):

Component	Volume	Final conc.
Total RNA	X	0.5 µg
Random hexamer primer, 600 pmol/µl	2 µl	60 µM
Water, PCR-grade	X	
Total volume	13 µl	

Afterward, the template-primer mix was denatured by heating the tube for 10 min at 65℃ in a thermal block. Then tube was immediately cooled on ice. Subsequently the following components were added to the reaction mixture (table 2):

Component	Volume	Final conc.
Transcriptor Reverse Transcriptase Reaction Buffer, 5× conc.	4 µl	1×(8 mM MgCl2)
Protector RNase Inhibitor, 40 U/µl	0.5 µl	20 U
Deoxynucleotide Mix, 10 mM each	2 µl	1 mM each
Transcriptor Reverse Transcriptase, 20 U/µl	0.5 µl	10 U
Final volume	20 µl	

Reaction vial was incubated for 10 minutes at 25℃ followed by 60 min at 50℃. Reverse transcriptase reaction was stopped by heating the vial to 85° for 5 min followed by placing the tube on ice. cDNA was stored at -20℃.

4.6 Measurement of gene expressions

Changes in gene expressions were measured with two techniques. Genome wide effects on gene expressions were measured with Affymetrix GeneChip. Quality

control of the RNA's as well as labeling, hybridization, and scanning of the hybridized arrays was performed by the Kompetenzzentrum fuer Fluoreszente Bioanalytik (KFB) (Regensburg, Germany) using the “mouse 430 2.0 chip” (Affymetrix). Changes in gene expression levels were shown as fold change in expression level in relation to the untreated cultures.

To confirm the effects on the expressions of the principal genes analyzed, gene expression measurements by quantitative real-time polymerase chain reaction (qRT-PCR) were performed. Thereby, real-time quantization was measured by TaqMan as well as by Sybr-Green technique. In brief, real time gene expression quantization by Sybr-Green technique measures the increasing fluorescence generated by the intercalation of the asymmetrical cyanine dye Sybr-Green into the amplifying target gene as shown in fig 8. The DNA-dye-complex absorbs blue light (λ_{max} = 494 nm) and emits green light (λ_{max} = 522 nm). For quantification of gene expression by TaqMan technique, additional to the sense and anti-sense primer, a third probe dual labeled with a fluorescent dye and a suitable quencher is used. This probe is usually designed to bind 3’ next to the sense primer. As long as this labeled probe remains un-cleaved, no fluorescent signal will be generated because prevented by the quencher on the probe. After binding of primers and labeled probe on the target sequence, during synthesis of the DNA, the 5´–3´ exonuclease activity of the Taq polymerase digests the dual-labeled probe disclosing the fluorescent signal as shown in fig 9. This permits quantitative measurements of the accumulation of the product during the exponential stages of the qPCR. The Sybr-

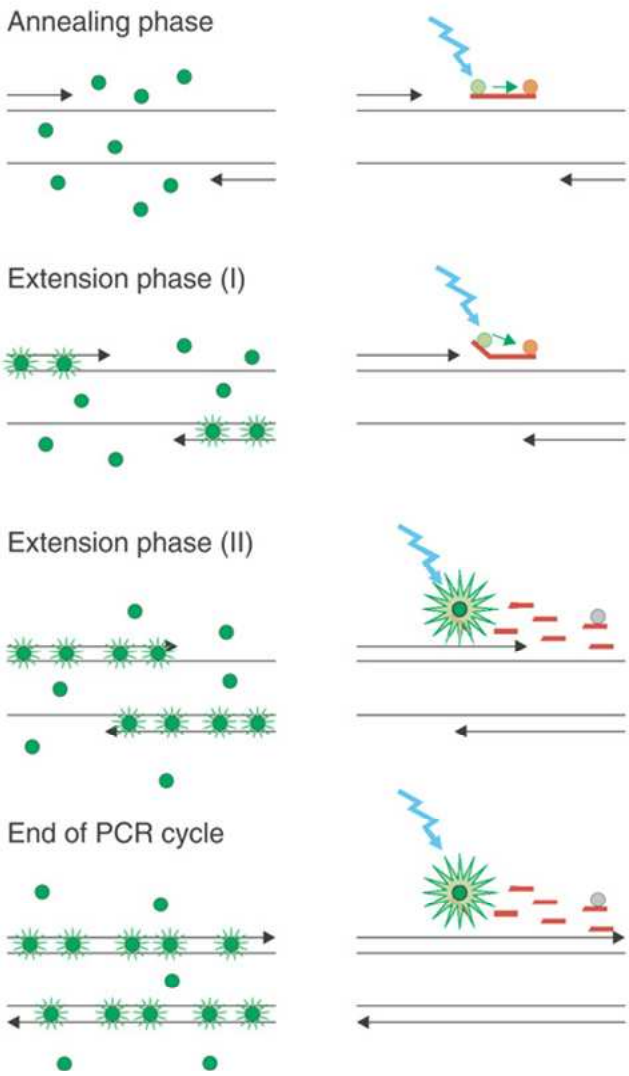

Figure 8. Principles of Sybr Green and TaqMan qPCR

Green primers and reference numbers for the FAM-fluorescent dye (emission λ_{max} 520 nm) labeled TaqMan primers (all predesigned by Applied Biosystems) used for gene expression analysis in the here presented publications are summarized in table 3. For Sybr-Green qPCR, cDNA was amplified with FastStart Sybr-Green Master Mix (Roche) using the following cycling conditions: 10 minutes of initial denaturation at 95℃ followed by 45 cycles consisting of 30 seconds denaturation at 95℃, 30 seconds annealing at primer specific temperatures and extension at 72℃. For TaqMan qPCR, cDNA was amplified with the TaqMan Gene expression Master Mix (Applied Biosystems) with an initial denaturation step at 95℃ for 10 minutes followed by 45 cycles alternating 60℃ and 90℃. For gene ex pression normalization, we usually used an *18 S* RNA TaqMan probe or alternatively a *Gapdh* TaqMan Probe (both Applied Biosystems, VIC-fluorescent dye labeled, emission λ_{max} 550 nm) as indicated in the publications, all in combination with TaqMan Gene expression Master Mix (Applied Biosystems) at the indicated TaqMan cycling conditions. All qPCRs were performed in triplicate using the Corbett Rotor Gene 6000 real-time PCR cycler and expression was evaluated using the comparative quantitation method (116). For each experiment, the triplicate results of the qPCR were averaged and this mean value was treated as a single statistical unit. The data of the experimental results were presented as means ± standard deviation (s.d.).

Sybr Green primers

Gene	Forward primer (5'–3')	Reverse primer (5'–3')	Tm (℃)
Dnmt1	ACCGCTTCTACTTCCTCGAGGCCTA	GTTGCAGTCCTCTGTGAACACTGTGG	62
Dnmt3b	GGAGAAAGCCAGGGT	AAGAGGGGGTGGAAGGA	63
Hells	TGAGGATGAAAGCTCTTCCACT	ACATTTCCGAACTGGGTCAAAA	62
Fas	TATCAAGGAGGCCCATTTTGC	TGTTTCCACTTCTAAACCATGCT	64
Ccna2	ACATTCACACGTACCTTAGGGA	CATAGCAGCCGTGCCTACA	62
c-Fos	CGGGTTTCAACGCCGACTA	TTGGCACTAGAGACGGACAGA	63
c-Jun	CCTTCTACGACGATGCCCTC	GGTTCAAGGTCATGCTCTGTTT	63
Fli1	ATGGACGGGACTATTAAGGAGG	GAAGCAGTCATATCTGCCTTGG	62

TaqMan probe sets (Applied Biosystems)			
Gene	**Reference number**	**Dye**	**Tm (℃)**
Plod2	Mm00478767_m1	FAM	60
Bglap2	X04142-EX2	FAM	60
Lox	Mm00495386_m1	FAM	60
Runx2	Mm00501578_m1	FAM	60
18sRNA	Hs4319413E	VIC	60
Gapdh	Mm4352339E	VIC	60

Table 3. Primers and reference numbers of primers used for qPCR

4.7 Measurement of protein expression by immunoblot technique

Protein expression of genes regulated by hcys (106) was analyzed by immuno-bloting. For protein extraction, after cell culture, MC3T3-E1 cell layers were washed 2 times with cold (+4℃) PBS and scraped in SDS-sample b uffer (2% SDS, 100 mM ß-mercaptoethanol, 125 mM Tris-HCl, pH 6.8) and heated at 95° for 5 minutes. 30 µg protein-extracts were fractionated on 8% or 10% SDS-PAGE depending on molecular weight of the proteins analyzed. Following SDS-gel electrophoresis, the proteins were transferred to nitrocellulose filters (Millipore) and blocked overnight with 10% blocking reagent (Roche) in TN Buffer (50 mM Tris, 125 mM NaCl, pH 8). Subsequently, the filters were incubated for 1 hour at room temperature with specific antibodies against the proteins to analyze (FLI1 (ref# C19), HELLS, (Lsh, ref# H-240), LOX (ref# H-140), DNMT1 (ref# K-18), all purchased from Santa Cruz Biotechnologies, CA)) diluted 1:200 in blocking buffer. Afterwards, all filters were washed three times with immuno-blot wash buffer (TN buffer containing 0.01% Tween) and the FLI1-, HELLS- and LOX-blots were incubated for one further hour with an anti-mouse IgG/ anti-rabbit IgG horseradish peroxidase (HRP) labeled secondary antibody (Roche) diluted 1:20,000 in blocking buffer. The DNMT1-blot was incubated for one hour with an anti-goat IgG HRP labeled secondary antibody (Sigma) diluted 1:160,000 in blocking buffer. Finally, the blots were washed again three times with immuno-blot washing buffer before detection of light emission with the BM Chemiluminescence Western Blotting Kit (Roche) as described by the supplier. Chemiluminescence was measured with an image acquisition system (Vilber Lourmat, France).

4.8 Measurement of protein expression by enzyme-linked immunosorbent assay (ELISA)

As gene expression measurements by qPCR indicated an hcys dependent up-regulation of interleukin-6 (IL-6) mRNA expression in MC3T3-E1 cells, IL-6 protein expressions were measured by ELISA assay. For this purpose, MC3T3-E1 cells were seeded in triplicate and treated with or without increasing hcys concentrations (0.108 mM, 1,08 mM, 3.6 mM) for 3, 6 and 14 days; culture medium was changed twice a week. After the corresponding hcys treatment, 1 ml of culture supernatant was saved and stored at -80℃. For IL-6 quantification, 96 well ELISA plates (Iwaki) were prepared by using the Murine IL-6 ELISA Development Kit as described by the supplier (PeproTech). In brief, Capture antibody was diluted in PBS to a concentration of 2 µg/ml and 100 µl were added to an ELSIA plate well (IWAKI) and incubated at room temperature overnight. Next day, liquid was removed and plate was washed three times with wash buffer (0.05% Tween-20 in PBS). Subsequently the wells were blocked with 300 µl blocking buffer (1%BSA in PBS) for 2 hours followed by plate wash. For IL-6 protein quantization, IL-6 standard was diluted from 6 ng/ml to zero in diluent (0.05% Tween-20, 0.1% BSA in PBS) and 100 µl of each concentration or of sample were added in triplicate to the ELISA plate. The plate was incubated 2 hours at room temperature. Afterwards liquid was removed and plate was washed four times with wash buffer. Next, avidin-HRP conjugate was diluted 1:2,000 in diluent, 100 µl were added per well and incubated at room temperature for 30 minutes. Finally, IL-6 concentration was monitored by color development of ABTS liquid substrate (Sigma, 100 µl/well) with an ELISA plate reader (Glomax, Promega) at 405 nm with wavelength correction set at 650 nm. Every cultured well was measured in triplicate, these triplicate results were averaged and the mean value was treated as a single statistical unit. The complete experiment was performed twice.

4.9 Analysis of specific DNA methylation

To determine specific promoter methylation of *Lox* and *Fas* (106, 107) in MC3T3-E1 cells, appropriate promoter fragments were generated by digestion of 1 µg of genomic DNA with 40 U of the CpG-methylation insensitive restriction enzyme MboII (New England Biolabs) for 20 minutes. Subsequently, the enzyme was heat inactivated at 65℃ for 20 minutes. The promoter regions were selected according to

literature (110) or/and depending by CpG content. After MboII digestion, DNA was purified using a commercially available PCR clean-up Kit (Promega) following the supplier's instructions. In the next step methylated DNA fragments were captured with the ''MetylMiner Methylated DNA Enrichment Kit'' (Invitrogen) following the supplier's instructions. In brief, methylated DNA was captured by methyl blinding protein 2 (MBD2) coupled to magnetic beads and subsequently separated from the unmethylated DNA fraction. Methylated DNA was eluted from the MBD2-beads with 200 µl of 2 M NaCl solution as single fraction independent from the CpG methylation density and concentrated by ethanol precipitation. Finally, the mean methylation status of the fragments was determined by amplifying the fragments by qPCR. Amplification ratios of the bound (methylated) DNA fraction to unbound (unmethylated) DNA fraction were calculated (for primer design see Table 4). Specific promoter configurations and CpG allocations are accurately described in the publications presented.

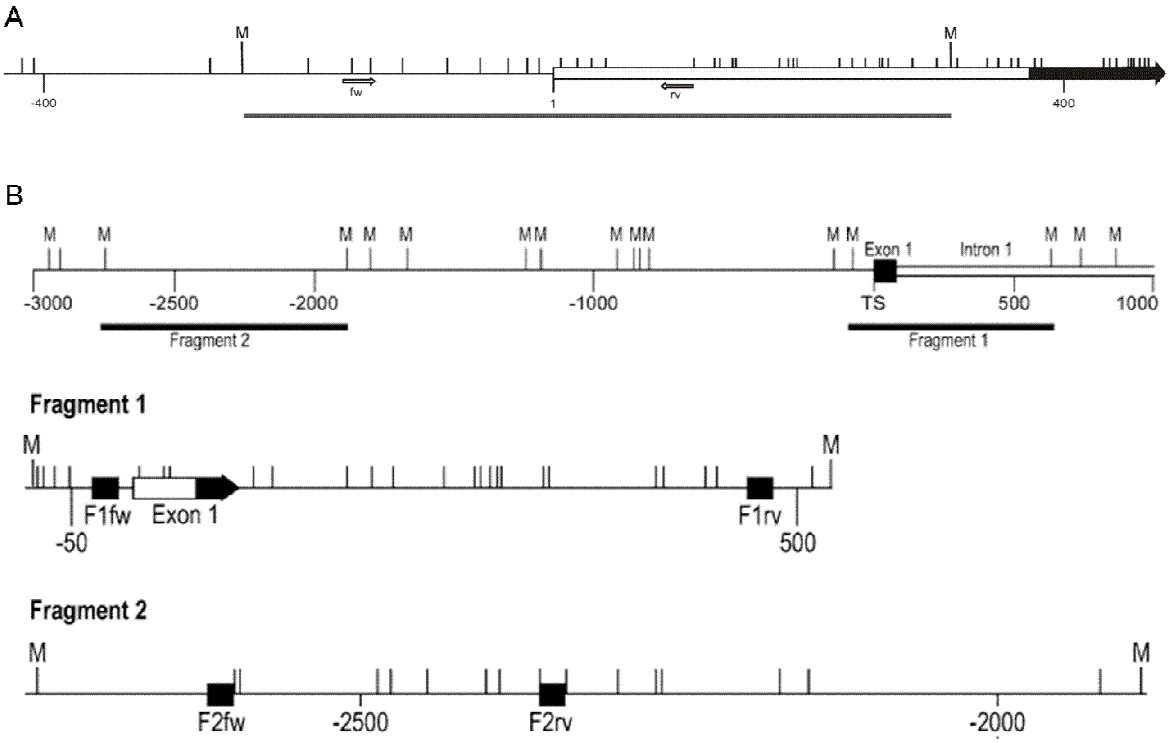

Figure 9. Schematic representation of Lox (A) and Fas (B) promoters and first exons. Untranslated regions are represented as open boxes and coding regions as black arrows. The vertical bars above the horizontal line of the genes indicate the CpGs in the region. The Mbo II restriction sites are indicated with M and the numbers below the geneline denote the distance to the transcription start (TS)

Gene	Forward primer (5'–3')	Reverse primer (5'–3')	Tm (℃)
Fas fragment 1	CATACCCACAGGCAGTCTAGA	CAGCCCAGAGTAACTCACTTC	62
Fas fragment 2	GAAGTAGAAACAGAAGCTGAG	TTGCTACATCCCAACTGTAAC	62
Lox promo-ter/first exon	GCATGTTCGGCCCAGATTAAGTCG	CAGAGTCTGGAGTAGAAGGAGGAGG	65

Table 4. Primers used for assessment of Fas and Lox promoter methylation status

4.10 Analysis of global DNA methylation

For determination of global methylation of DNA in dependence of collagen type I (107), a recently published assay was used, which bases upon sensitivity of the HpaII restriction enzyme to methylated CpGs compared to the insensitivity of MspI to cut such restriction sites. To this end, 100 ng DNA was digested in multi core buffer (Promega) with 5 U MspI or HpaII or incubated without restriction enzyme (background) for 3 hours at 37℃ in a total volume of 30 µl. The restriction of the DNA was followed by an end-fill reaction where to the restriction digest 20 µl of a mixture containing 0.1 µM Biotin-11-dCTP and 0.1 µM Biotin-11-dGTP (Perkin Elmer, Boston, MA) and 0.5 U Klenow-fragment of DNA-polymerase III (Promega) in 500 mM Tris–HCl, pH 7.2, 100 mM $MgSO_4$ and 1 mM dithiothreitol were added and incubated at room temperature for half an hour. Thereafter, the reaction was transferred into multi-well plates (Optiplate, Beckman) and 100 µl of Reacti-Bind^{TM} DNA Coating Solution (Pierce, Rockford, IL) was added to each well and incubated overnight at room temperature. On the next day, the wells were washed once with TBS (10 mM Tris–HCl pH 8.0, 150 mM NaCl). After a blocking step with 1% blocking solution (Roche) in TBS for 1 hour, a solution of 50 ng/µl streptavidin HRP-conjugate (Promega) in TBS was added and incubated for one further hour at room temperature. Thereafter, the wells were washed three times with TBS containing 0.5% Tween 20 and two times with water. 100 µl of the chemo-luminescence substrate was added to each well and the light emission was measured in a top-counter (Packard Instruments). Evaluation of DNA global methylation level of each biological sample was performed by forming the ratio between the signals given by the HpaII restriction (un-methylated CpGs) to the MspI restrictions (total CpGs).

4.11 Determination of specific transcription factor binding by chromatin immuno-precipitation (ChIP)

ChIP assays are used to evaluate the association of proteins (mostly transcription factors) with specific DNA regions. The technique involves cross-linking of proteins with DNA, fragmentation and preparation of soluble chromatin followed by immuno-precipitation with an antibody recognizing the protein of interest. The segment of the genome associated with the protein is then identified by qPCR amplification of the DNA in the immuno-precipitates. To demonstrate binding of FLI1 transcription factor to *Dnmt1* promoter (106), this technique was chosen by using the ChampionChip One-Day Kit (SABiosciences, MD) following manufacturer's instructions. In brief, for this purpose, after MC3T3-E1 cell culture, medium was aspirated from the dish and 10 ml of fresh fixing Buffer (1% formaldehyde in PBS) was added to the dish and cells were incubated at 37℃ for 10 minutes. After fixation cells were washed twice with ice cold PBS, harvested in 1.5 ml PBS and pelleted by centrifugation (800 x *g* for 10 minutes at 4℃). Afterwards, cells were lysed with a lysis buffer and chromatin was sonicated with 3 rounds at 0.5 W for 8 s on, 10 s off, 5 times per round. Subsequently, the debris was pelleted by centrifugation (14,000 x *g* for 10 min at 4 ℃) and supernatant (shared chromatin) was transferred to a 2 ml tube. Chromatin was incubated overnight on a rotor at 4℃ with 4 µg anti-FLI1 antibody (ref# C-19, Santa Cruz, CA) or with 4 µg non-immune serum as negative control. Before immunoprecipitation 1% (10 µl) of the chromatin was saved and stored at 4℃ for further use as reference. After immuno-precipitation of chromatin, antibody-bound DNA was extracted by protein beads, next protein was digested with proteinase K, DNA was washed and isolated. For quantization, enriched *Dnmt1* promoter fragments which included 3 FLI1 binding sites (Fig. 10) were quantified by qPCR with the primers: forward (5' - 3') CTTCCCCCACTCTCTTGC, reverse (5' – 3') GAACAGCTCTGAACGAGAC. DNA signal of the FLI1 precipitated chromatin was normalized to the un-precipitated chromatin.

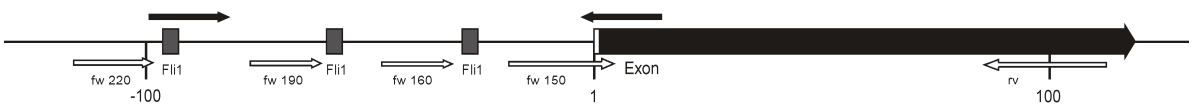

Figure 10. Schematic representation of Dnmt1 promoter with first exon. Untranslated regions are represented as open boxes and coding regions as black arrows. Primers used for ChIP assay are represented as thin black arrows and Fli1 binding sites as grey boxes.

4.12 Fourier transform infrared spectroscopy (FTIR) imaging

Spectroscopic analysis by FTIR Imaging Analysis was used for determination of pyr/divalent collagen cross-link ratio in MC3T3-E1 cell cultures after 7 days hcys treatment in the first work here presented. Therefore, after cell culture, medium was removed and cells/ECM were fixed in alcohol, scraped off the culture dishes, and transferred onto barium fluoride windows, where they were air dried. Following this, spectra were obtained in transmission with a Bruker (Germany) Equinox 55 spectrometer coupled to a Bruker Hyperion 3000 FTIR microscope equipped with a motorized stage (±1 μm) and a 15× objective. The spectra were baseline-corrected in the amide I and II spectral area (~1500–1700 cm−1); water vapor was subtracted and then subjected to second derivative spectroscopy and curve fitting routines as described elsewhere (117). The collagen cross-link ratio was determined as previously described (117).

4.13 Measurement of *Dnmt1* promoter activity

For localization of hcys's/IL-6's reactive sites on *Dnmt1* promoter (106), several lengths and mutant forms of the promoter were cloned into the secreted alkaline phosphatase 2 (SEAP2) reporter vector (Clontech). More precisely, four fragments of the mouse *Dnmt1* promoter were firstly cloned from MC3T3-E1 genomic DNA into the pGEM T-easy Vector (Promega) by using the following 5'-primers elongated to contain a BglII restriction site (underlined): TCGAGATCTGCCTTCGGGC-ATAGCATGGTC for a 220 bp fragment carrying three putative FLI1 binding sites (as suggested in (118), at -30 bp, at -60 bp and at -96 bp from the somatic transcriptional start site (103), TCGAGATCTGCCTGTGTGGTACATGCTGC for the 190 bp fragment carrying two putative FLI1 binding sites (at -30 bp and at -60 bp), TCGAGATCTGGCCGCCCCCTCCCAATTGG for the 160 bp fragment carrying one putative FLI1 binding site (at -30 bp), TCGAGATCTGCGAAAAAGCCGGGGTCTCGTTC for the 150 bp fragment carrying no FLI1 binding sites. As 3'-primer we used GCCTGCGGACATGGTCCGGGAGCGAGCCTG. These fragments were subsequently cloned into the SEAP2 reporter vector by using BglII and EcoRI restriction enzymes. To generate mutated *Dnmt1*-SEAP2 fragments, the following primers with modified, putative FLI1 binding sites were designed (mutation sites form 5´-*TTCC* to *TTAA* are in italics and underlined): 5´ CGGGCATAGCATGGTC*TT AA*CCCACTCTCTTGCCCTG and complementary 3` CAGGGCAAGAGAGTGGG*TT-*

*AA*GACCATGCTATGCCCG for the putative Fli1 binding site at -96 bp from the somatic transcriptional start site, 5` GTGGTACATGCTGC*TTAA*GCTTGCGCCG-CCCC and complementary 3´ GGGGCGGCGCAAGC*TTAA*GCAGCATGTACCAC for the putative FLI1 binding site at -60 bp from the somatic transcriptional start site and 5´ CTCCAAATTGGT*TTAA*GCGCGCGCGAA AAAGCCG and 3` CGGCTTTTTCG-CGCGCGC*TTAA*ACCAATTGGGAG for the putative FLI1 binding site at -30 bp from the somatic transcriptional start site. For transfection experiments with the various *Dnmt1*-SEAP2 vectors, SEAP2-control vector and the SEAP2-basic vector, MC3T3-E1 cells were seeded at 20.000 cells/cm² in 48 multiwell plates. Six hours after seeding, cells were transfected with 0.15 µg/cm² vector construct using 1 µg/cm² DOSPER transfection reagent (Roche) following the suppliers protocol. After two days, cells were treated for further 3 days with 30 ng/ml of murine IL-6 (PeproTech) and finally, SEAP2-activity was measured in 50 µl culture supernatant using the SEAP2 bio-luminescence Kit (Roche) following suppliers instructions. Each experiment was run in biological quadruplicates and was repeated at least twice.

4.14 Reference numbers of the used gene sequences

Ref-number	Organism	Gene
NM_010234	Mus musculus	cFos
NM_010591	Mus musculus	cJun
CH466522	Mus musculus	Dnmt1
CH466623	Mus musculus	Dnmt3a
NT_039207	Mus musculus	Dnmt3b
CH466534	Mus musculus	Fas
CH466522	Mus musculus	Fli1
CH466534	Mus musculus	Hells
CH466528	Mus musculus	Lox

Table 5. Sequence references

4.15 Statistical analysis

Statistical analyses were performed using either ANOVA or Student's t-test using Prism 4.03 software (GraphPad Software, San Diego, CA). $P \leq 0.05$ was considered as significant. All experiments were performed at least in three independent

biological replicates and results are presented as mean ± standard deviation (s.d.) of the three biological replicates.

Bone 46 (2010) 703–709

Contents lists available at ScienceDirect

Bone

journal homepage: www.elsevier.com/locate/bone

Differential effects of homocysteine and beta aminopropionitrile on preosteoblastic MC3T3-E1 cells

Roman Thaler [a], Silvia Spitzer [a], Monika Rumpler [a], Nadja Fratzl-Zelman [a], Klaus Klaushofer [a], Eleftherios P. Paschalis [a,b], Franz Varga [a,*]

[a] Ludwig Boltzmann Institute of Osteology at the Hanusch Hospital of WGKK and AUVA Trauma Center Meidling, 4th Medical Department, Hanusch Hospital, Vienna, Austria
[b] University General Hospital "Attikon", National Kapodistrian University of Athens, School of Medicine, 1st Department of Orthopaedic Surgery, Greece

ARTICLE INFO

Article history:
Received 22 September 2009
Revised 26 October 2009
Accepted 27 October 2009
Available online 4 November 2009

Edited by: R. Baron

Keywords:
Osteoblast
Collagen cross-links
Gene expression
Beta aminopropionitrile
Homocysteine

ABSTRACT

Compounds, like beta-aminopropionitrile (bAPN) and homocysteine (hcys), are known to inhibit a stable matrix formation. Osteoblast-synthesized collagen matrix regulates the differentiation of precursor cells into mature osteoblasts. They express lysyl oxidase, an enzyme involved in the collagen cross-linking process. Lately, plasma hcys levels have recently been strongly correlated with fracture in humans. We have previously shown that bAPN not only disturbs collagen cross-links but also affects osteoblastic differentiation in a cell culture system.

The aim of the present study was to investigate the effects of bAPN and hcys on collagen cross-links and gene expression at the mRNA level by FTIR and quantitative RT-PCR, respectively. We found that bAPN and hcys down-regulated cell multiplication. While bAPN also down-regulated the metabolic activity of MC3T3-E1 cells, hcys down-regulated it by lower concentrations but up-regulated it by higher; both substances up-regulated alkaline phosphatase activity. The substances increased the ratio of pyr/divalent cross-links of collagen, and down-regulated mRNA expression of lysyl hydroxylase (Plod2) and lysyl oxidase (Lox), genes which play an important role in the formation of a stable matrix. Furthermore, we demonstrate that both substances stimulated the expression of Runx2, an indispensable regulator of osteoblastic differentiation. However, analysis of genome wide mRNA expression suggests that hcys and bAPN have differential effects on genes involved in osteoblastic differentiation and phenotype regulation.

The results indicate that although both bAPN and hcys affect collagen cross-link post-translational modifications in a similar manner as far as pyr and divalent cross-links are concerned, they have differential effects on the monitored genes expression at the mRNA level, with hcys exerting a broader effect on the genome wide mRNA expression.

Introduction

We have previously reported that beta-aminopropionitrile (bAPN), a known lathyrogen, not only disrupts collagen cross-linking but also affects osteoblastic activity and gene expression [1]. Homocysteine (hcys), a natural eukaryotic metabolite related to several chronic pathologies such as cardio-vascular diseases has also been shown to interfere with lysyl oxidase (Lox) action [2], altering collagen post-translational modifications and cross-links. However, an ambivalent classification of hcys as lathyrogen is found in literature. We have recently reported that there is a correlation between plasma hcys levels and collagen cross-link ratio in forming trabecular surfaces in humans [3]. Furthermore, recent clinical and epidemiological data [4–7] report a correlation between blood hcys levels and fracture risk. Clinical reports to the contrary also exist, as well as ones casting doubt as to whether hcys affects collagen cross-linking [8–10]. The situation does not become clearer when animal models are considered [11–15].

In the present study, using the preosteoblastic MC3T3-E1 cell line, the effects of hcys and bAPN on cell viability, cross-link formation and mRNA expression were compared as a function of concentration. Using quantitative reserve transcription polymerase chain reaction (qRT-PCR) and gene chip analysis, we investigated on the effects of both substances on the expression of genes involved in extracellular matrix formation, on general mRNA expression and on differentiation factors. Concerning cell viability and multiplication as well as expression of genes involved in post-translational collagen cross-linking, both interventions affected collagen in a similar manner. However, gene expression of selected gene groups responsible for the osteoblastic phenotype and development was mostly differentially regulated by the used interventions. Furthermore, a general gene array analysis revealed that hcys regulated at all concentrations more genes than bAPN and that the effects of hcys were generally stronger.

* Corresponding author. Fax: +43 1 91021 86929.
E-mail address: franz.varga@osteologie.at (F. Varga).

8756-3282/$ – see front matter © 2009 Elsevier Inc. All rights reserved.
doi:10.1016/j.bone.2009.10.038

When considered together, the results of the present study show, in addition to collagen cross-linking inhibition, the breadth by which bAPN and hcys affect osteoblastic function.

Materials and methods

Cell culture and matrix production

MC3T3-E1 cells (kindly donated by Dr. Kumegawa, Meikai University, Department of Oral Anatomy, Sakado, Japan), a clonal preosteoblastic cell line derived from newborn mouse calvaria, were cultured in humidified air under 5% CO_2 at 37 °C. Alpha-minimum essential medium (α-MEM; Biochrom, Berlin, Germany) supplemented with 5% fetal calf serum (Biochrom), 50 μg/mL ascorbic acid (Sigma), and 10 μg/mL gentamycin (Sigma) was used as culture medium. For propagation, cells were subcultured twice a week using 0.001% pronase E (Roche) and 0.02% EDTA in Ca^{2+}- and Mg^{2+}-free phosphate-buffered saline (PBS) before achieving confluence. MC3T3-E1 cells were seeded in culture dishes at a density of 20,000/cm^2 and cultured overnight. On the next day, the medium was changed and the cells were treated with or without bAPN (Sigma) or hcys (Sigma) for 1 week to gain two to three cell layers [16]. The various concentrations for the substances, the range of whose was chosen based on previous publications, were 0.1 mM, 0.4 mM, 1 mM, and 4 mM. Given the breadth of the outcomes of the gene array analysis, we decided for these specific experiments to investigate an extra concentration for hcys (10 mM), given its potential clinical significance in relation to fracture. In vitro formed extra-cellular matrix was subjected to Fourier-transform infrared (FTIR) analysis for determination of collagen cross-link ratio.

The 7 day time point was chosen based on previously published results that show that, in a cell culture system, collagen mRNA expression and synthesis are at their respective highest at day 7, whereas protein accumulation is at its lowest. When accumulation is at its highest (at day 30), both mRNA expression and protein synthesis are at their respective minima [17]. Moreover, this makes the results of the present study directly comparable with our previous report concerning bAPN [1].

Cell multiplication, alkaline phosphatase activity (ALP), and viability

MC3T3-E1 cells were seeded in culture dishes at a density of 20,000/cm^2 and cultured overnight. On the next day, the medium was changed and the cells were treated with or without the chemicals at the various concentrations for 1 week. Cell number and ALP-activity were analyzed. For determination of cell number (DNA amount employed as surrogate), cell layers were washed with PBS and frozen with 1 mM Tris–HCl buffer (pH 8.0) containing 0.1 mM EDTA. During thawing, Hoechst 33258 dye (Polysciences, Warrington, PA) was added (1 μg/mL) and, after an incubation of 15 min at room temperature, the fluorescence was measured (excitation 360, emission 465 nm). The amount of DNA was estimated using a standard curve prepared from calf thymus DNA (Roche). Thereafter, alkaline phosphatase (ALP) activity was measured with p-nitrophenylphosphate (2.5 mg/mL in 0.1 M diethanolamine buffer [pH 10.5], 150 mM NaCl, 2 mM $MgCl_2$) by incubation of the cell layers for 15 min at room temperature. Absorption was measured in a microplate reader at 405/490 nm. ALP activity (units per milligram DNA) was estimated using a standard curve prepared from calf intestinal ALP (Roche). To assess cell metabolic activity, a commercially available assay (EZ4U; Biomedica, Vienna, Austria) was used, according to the protocol of the supplier.

FTIR imaging

After 7 days in culture, one well per experiment was processed for spectroscopic analysis by FTIR Imaging for the determination of pyr/divalent collagen cross-link ratio. The cells (7 day old cultures) and ECM were fixed in alcohol, scraped off the culture dishes, and transferred onto barium fluoride windows, where they were air-dried. Following this, spectra were obtained in transmission with a Bruker (Germany) Equinox 55 spectrometer coupled to a Bruker Hyperion 3000 FTIR microscope equipped with a motorized stage (±1 μm) and a 15× objective. The spectra were baseline-corrected in the amide I and II spectral area (~1500–1700 cm^{-1}); water vapor was subtracted and then subjected to second derivative spectroscopy and curve fitting routines as described elsewhere [18]. The collagen cross-link ratio was determined as previously described [18].

Expression analysis by qRT-PCR

RNA was extracted using a RNA Isolation Kit (Qiagen), and cDNA was synthesized from the mRNA using the 1st Strand cDNA Synthesis Kit (Roche). The obtained cDNA was subjected to PCR amplification with a real-time cycler using TaqMan Gene Expression Master Mix (Applied Biosystems) and TaqMan probes (Applied Biosystems) for all genes monitored. 18S RNA was used as a housekeeping gene for normalization, amplified in the same tube. All PCRs were performed in triplicate. After 10 min of initial denaturation at 95 °C, PCR was performed with 60 cycles: 10 s denaturation at 95 °C, 30 s annealing, and extension at 60 °C. Expression was quantified using the comparative quantification method [19].

Affymetrix GeneChip analysis

Total RNA was isolated using a RNA Isolation Kit (Qiagen). Quality control of the RNA's as well as labeling, hybridization, and scanning of the hybridized arrays was performed by the Kompetenzzentrum fuer Fluoreszente Bioanalytik (KFB) (Regensburg, Germany) using the mouse 430 2.0 chip (Affymetrix).

Statistical analysis

Each experiment was performed four times. Analysis by qRT-PCR was performed as triplicate for each sample. Each measurement was used for statistical analysis by ANOVA (Prism 4.0, GraphPad Software, San Diego, CA). The data are represented as means ± standard deviation (SD).

Results

The effect of hcys and bAPN on cell multiplication and ALP activity

Cell metabolic activity, as well as cell number results are summarized in Fig. 1. bAPN induced a dose-dependent reduction in both outcomes (Figs. 1a, b). On the other hand, although hcys exhibited a similar effect as far as cell number (DNA amount employed as a surrogate) is concerned (Fig. 1d), a decrease in cell metabolic activity was evident only for the lowest concentration employed, while the higher ones had either no or even an increasing effect (Fig. 1c). Both bAPN and hcys had a dose-dependent increasing effect on the ALP activity of MC3T3-E1 cells (Fig. 2).

Hcys and bAPN inhibited cross-linking of collagen

Fig. 3 summarizes the effects of bAPN and hcys on the collagen cross-link ratio (pyr/divalent). Both had an increasing effect on this ratio (due to a disproportionate decrease in both cross-links) as a function of concentration, with the exception of the lowest concentration at which bAPN was similar to the untreated control cultures.

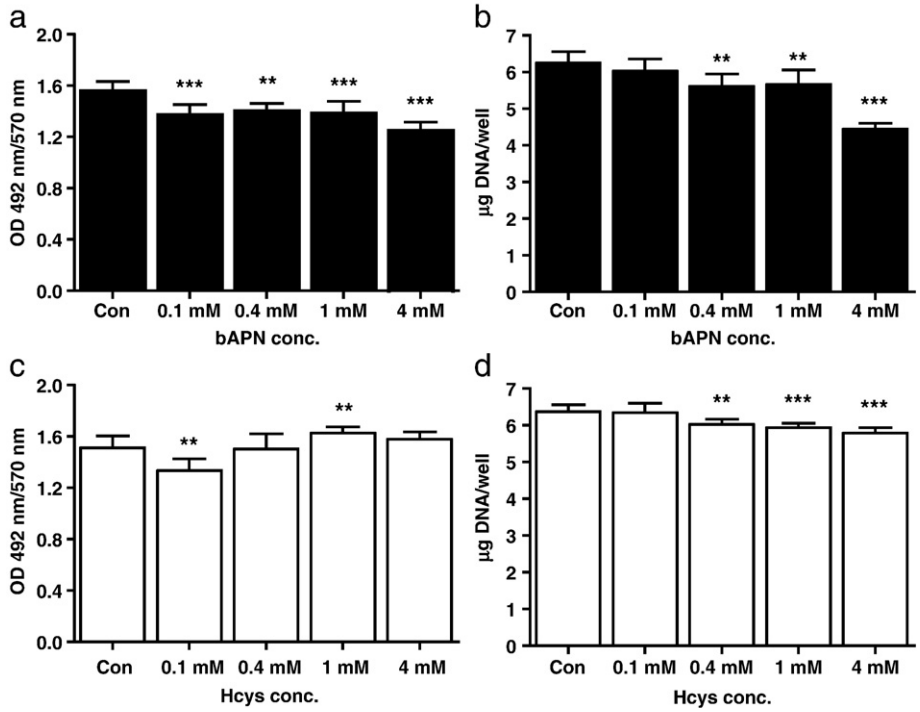

Fig. 1. Results for cell viability expressed as optical density (OD) (a, c) and cell multiplication expressed as µgDNA/well (b, d) for hcys (white bars) and bAPN (black bars). bAPN induced a dose-dependent reduction in both cell viability and cell multiplication (a, b), while hcys exhibited a similar effect as far as cell multiplication is concerned (d), and a decrease in cell viability at the lowest concentration employed (c). The bars represent mean ± SD. $^{**}P<0.01$; $n=8$; $^{***}P<0.001$; $n=8$.

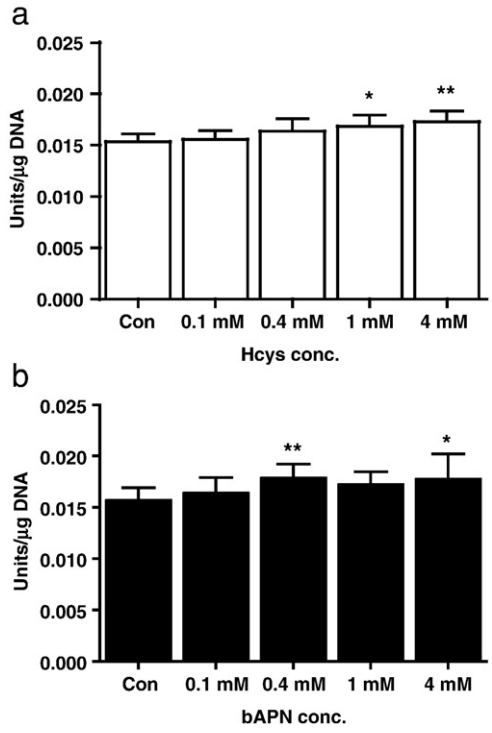

Fig. 2. Alkaline phosphatase activity results. After measuring the DNA content as a surrogate of the cell number (Fig. 1), ALP activity was measured in the same well and normalized to the amount of DNA. Both hcys (a) and bAPN (b) exhibited a dose-dependent increasing effect in MC3T3-E1 cells. The bars represent mean ± SD. $^{**}P<0.01$; $n=8$; $^{*}P<0.05$; $n=8$.

Hcys and bAPN regulated the expression of genes involved in collagen cross-linking

First investigation focused on whether inhibition of cross-linking by both substances also influenced the mRNA expression of the genes involved in this process. Fig. 4 shows a significant down-regulation of Plod2 by both compounds at the higher concentrations. Similar observations were made when expression of Lox, another important enzyme for collagen post-translation modifications, was monitored at the mRNA level: both bAPN and hcys had down-regulating effects on the Lox expression when they were present at higher concentrations in the culture media (Figs. 5a, b). The results of the qRT-PCR were confirmed by the results of the gene array, where a down-regulation of Lox and Plod2 is shown as well (Table 1). Moreover, gene chip data demonstrated that Plod1 and the Proline 4-hydroxylase alpha polypeptide I and II (P4ha1 and P4ha2)

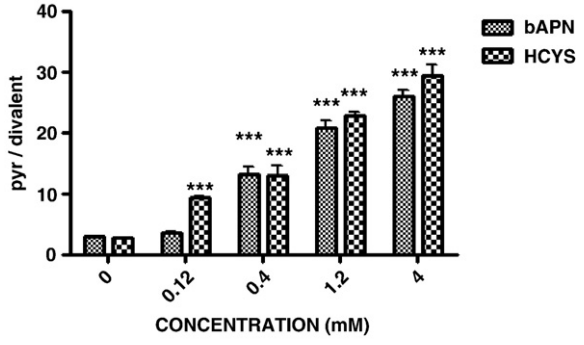

Fig. 3. Summary of the effects of bAPN and hcys on the collagen cross-link ratio (pyr/divalent). Both had an increasing effect on this ratio as a function of concentration, with the exception of the lowest concentration at which bAPN was similar to the control cultures (no lathyrogen in the culture media). Provided *P* values indicate significantly different values vs. control cultures. The bars represent mean ± SD. $^{***}P<0.01$.

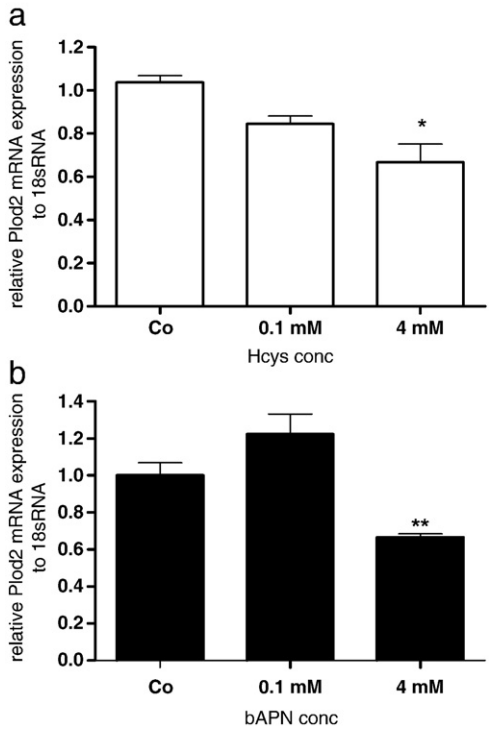

Fig. 4. Plod2 mRNA expression in hcys (a) and bAPN (b) treated MC3T3-E1 cells. MC3T3-E1 cells were treated for 1 week with the listed concentration of lathyrogens. Thereafter, mRNA was isolated, reverse transcribed, and subjected to qRT-PCR. The specific gene expression was normalized to 18S RNA expression. At higher concentrations, both substances decreased Plod2 mRNA levels significantly. The bars represent mean ± SD. *$P<0.05$; $n=12$; **$P<0.01$; $n=12$.

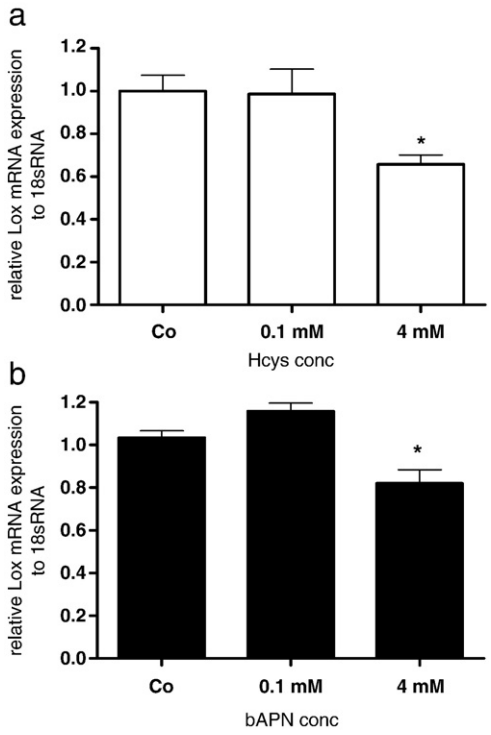

Fig. 5. Lox mRNA expression in hcys (a) and bAPN (b) treated MC3T3-E1 cells. MC3T3-E1 cells were treated for 1 week with the listed concentration of lathyrogens. Thereafter, mRNA was isolated, reverse transcribed, and subjected to qRT-PCR. At higher concentrations, both substances decreased Lox mRNA levels significantly. The specific gene expression was normalized to 18S RNA expression. The bars represent mean ± SD. *$P<0.05$; $n=12$.

Table 1
Gene array analysis of genes involved in the post-translational cross-linking of collagen.

Gene (NCBI gene symbol)	Co	bAPN 0.1 mM	bAPN 4 mM	Hcys 0.1 mM	Hcys 4 mM	Hcys 10 mM
Lox	1.00	1.01	0.59	0.93	0.60	0.61
Plod1	1.00	0.90	0.62	0.97	0.43	0.32
Plod2	1.00	1.18	0.56	0.61	0.35	0.28
Plod3	1.00	0.91	0.89	1.26	0.98	1.04
P4ha1	1.00	1.04	0.72	0.68	0.41	0.25
P4ha2	1.00	0.97	0.47	1.11	0.32	0.27
P4ha3	1.00	0.89	1.01	0.74	0.92	0.91

Fold increase in mRNA expression of the genes compared to untreated control culture cells. Genes down-regulated beyond 1.3-fold are marked green.

were down-regulated (Table 1) showing a more pronounced effect in the case of hcys treatment. Summarizing, the two compounds influence in a similar manner the enzymatic activity as well as the mRNA expression of genes involved in collagen post-translational modifications. Furthermore, mRNA expression data obtained from qRT-PCR were comparable to gene array data.

Impact of hcys and bAPN on the expression of genes of the osteoblastic phenotype and bone development

Having demonstrated that both compounds disrupted collagen cross-linking and down-regulated the expression of genes important for this process, the effect of the two compounds on the mRNA expression of genes characteristic for the osteoblastic phenotype was studied. Following recently published osteoblast differentiation schemas, at the beginning of the differentiation (at the mesenchymal stem cell level), three transcription factors Msx2, Dlx3, and Dlx5 are expressed in temporal sequence [20,21]. Of these factors, only Dlx5 had a signal strong enough to suggest mRNA expression and showed a trend to be down-regulated by hcys (Table 2). Components of the transcription complex AP-1 that are cFos, cJun, Fosl1, and FosB, are linked to skeletal distortions. In our experiments, cJun was not regulated while cFos and Fosl1 were down-regulated by hcys (Table 2).

During osteoblastic differentiation, the expression of the transcription factors Runx2 and Osterix (Sp7) is known to be essential [20,21]. Both factors were expressed in MC3T3-E1 cells, and as shown in Table 2, Runx2 and Sp7 were up-regulated at least by about 140% by both compounds, respectively. The gene array expression analysis for Runx2 was confirmed by qRT-PCR as shown in Fig. 6. Again the extent of the regulation was consistent between both techniques.

Impact of hcys and bAPN on genes modulating Runx2 activity

The function of Runx2 is not only regulated by transcription but interacting proteins modulate its activity as well. Co-activators of the

Table 2
Gene array analysis of transcription factors involved in osteoblastic differentiation.

Gene (NCBI gene symbol)	Co	bAPN 0.1 mM	bAPN 4 mM	Hcys 0.1 mM	Hcys 4 mM	Hcys 10 mM
Dlx5	1.00	1.10	1.14	0.83	0.94	0.92
Runx2	1.00	1.14	1.42	1.11	1.40	1.16
Cbfb	1.00	0.98	1.13	1.53	1.29	1.22
Sp7	1.00	1.06	1.78	1.28	1.16	1.42
Fos	1.00	0.87	1.64	0.49	0.41	0.53
Fosl1	1.00	1.10	0.52	0.97	0.43	0.37
Jun	1.00	1.13	0.99	0.94	1.16	1.27
Fosb	1.00	0.88	0.80	0.84	0.79	0.61

Fold increase of mRNA expression of the genes compared to untreated control culture cells. Genes up- or down-regulated beyond 1.3-fold are marked in red or green, respectively.

Runx2 activity whose expression was suggested by gene array analysis are Aes, Myst3 and 4, as well as Wwtr1 [22]. These genes were all up-regulated by hcys but not affected by bAPN. A recently described activator of Runx2 and with it of the osteoblastic differentiation is Satb2 [22]. It works as a modular node in the transcriptional network of osteoblastic differentiation [23] and was clearly up-regulated by hcys. Also the co-repressors Tle2 and Stat1 were expressed, however, only regulated by hcys as shown in Table 3.

Table 3
Gene array analysis of genes modulating Runx2 activity.

Gene (NCBI gene symbol)	Co	bAPN 0.1 mM	bAPN 4 mM	Hcys 0.1 mM	Hcys 4 mM	Hcys 10 mM
Aes	1.00	0.78	1.10	1.24	1.39	1.83
Myst3	1.00	1.28	1.20	1.25	1.86	1.84
Myst4	1.00	1.18	1.07	1.03	1.36	1.28
Wwtr1	1.00	0.94	1.03	1.31	1.16	1.15
Satb2	1.00	1.18	1.07	1.33	1.91	1.78
Tle2	1.00	1.03	1.18	1.46	1.75	2.15
Stat1	1.00	0.98	1.23	1.59	3.05	3.44

Fold increase of the mRNA expression of the genes compared to untreated control culture cells. Genes up-regulated over 1.3-fold are marked in red.

Discussion

Recent clinical reports have debated whether plasma homocysteine levels are associated with fracture risk in humans [4–9,24–45]. Hcys has been reported to interfere with collagen post-translational modifications [2] by inhibition of lysyl oxidase, an important enzyme for collagen cross-link formation. We have reported that plasma hcys levels are correlated with altered collagen cross-link ratio (pyr/divalent) in humans [3], in a manner consistent with the action of a lathyrogen. We have also reported that another "lathyrogen," bAPN, changes not only collagen cross-links but also osteoblastic proliferation and differentiation in a cell culture system [1]. The purpose of the present study was to expand on our previous studies and compare the effect of bAPN and hcys on collagen cross-links and on the gene expression at the mRNA level of genes involved in post-translational modification of collagen cross-linking by qRT-PCR as a function of the concentration of the substances. Moreover, gene array analysis was performed to explore differences and potential mechanisms by which these substances may regulate osteoblastic gene expression.

The results indicated that cell metabolic activity measured by the EZ4U assay was decreased in the case of bAPN in a dose-dependent fashion, while hcys decreased it at the lowest concentration (which is within normal range in humans) and increased it at the higher one.

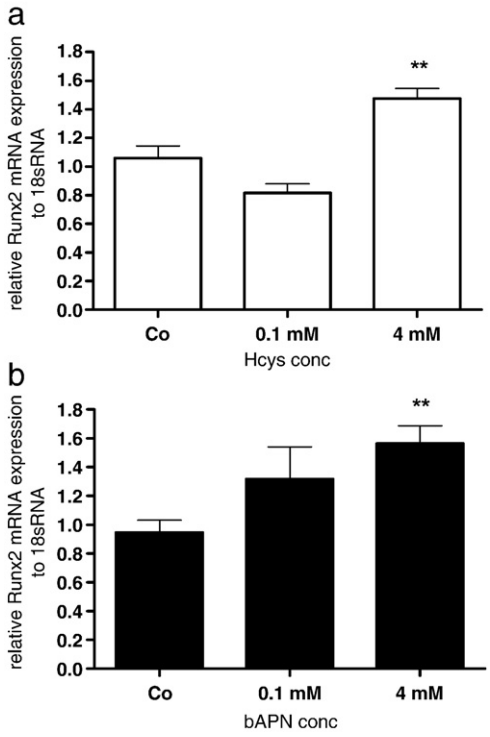

Fig. 6. Runx2 mRNA expression in hcys (a) and bAPN (b) treated MC3T3-E1 cells. MC3T3-E1 cells were treated for 1 week with the listed concentration of lathyrogens. Thereafter, mRNA was isolated, reverse transcribed, and subjected to qRT-PCR. At higher concentrations, both substances increased Runx2 mRNA levels significantly. The specific gene expression was normalized to 18S RNA expression. The bars represent mean ± SD. $^{**}P<0.01$; $n=12$.

Interestingly, when the amount of DNA was measured as a surrogate for cell number, both bAPN and hcys decreased the number in accordance with the concentration. The hcys effect may be attributed to the fact that it is known to arrest the cell cycle at the G1/S transition via cyclin A2 transcriptional inhibition, dependent on cell type and concentration [46]. Furthermore, both bAPN and hcys showed a similar effect on the ALP activity; this result is in agreement with previously published results [1,13].

FTIR spectroscopic analysis indicated that both bAPN and hcys resulted in a dose-dependent increase of the pyr/divalent cross-link ratio, due to a disproportionate reduction in both pyr and divalent cross-links (data not shown), consistent with observations in our study in humans investigating the relationship between plasma hcys levels and collagen cross-link ratio [3].

Moreover, both compounds had not only a similar effect on the collagen cross-link ratio monitored, but also down-regulated the expression of Plod2 mRNA, an important enzyme for collagen post-translation modifications, and one whose action precedes that of Lox in collagen post-translational modification cascade that was down-regulated as well. The results of the qRT-PCR analyses were in excellent agreement with the gene array data, confirming the down-regulation of Plod2 and Lox by both interventions.

Analysis of the data regarding the cross-linking process demonstrated that bAPN and hcys had comparable effects. This is reflected by the fact that both inhibited cross-linking and affected mRNA expression of genes involved in post-translational modifications in a similar manner: they down-regulated these genes.

These results suggest that both interventions act on two levels. The disruption of cross-linking on the enzymatic level seems to be amplified by the common down-regulation of the mRNA of the genes involved in this process. The change in the ratio of the cross-links, however, could be explained by differential inhibitory effects of the interventions on responsible enzymes and/or influence on regulation of expression of the genes coding for these enzymes. A common regulation of these genes was found recently, where vitamin D [47] as well as thyroid hormones (Varga et al., unpublished results) up-regulated genes involved in collagen cross-linking, thus influencing collagen quality. Common regulation of genes in osteoblasts could be achieved by an upstream expressed transcription factor like the osteoblast-specific Runx2 and Osterix. According to the schema of Lian and Stein, during differentiation, osteoblasts express time dependently a series of transcription factors and structure genes [21]. Both compounds up-regulated the mRNA levels of Runx2 and Osterix, which could regulate inversely the mRNA expression of Lox and Plod2. Another possible explanation could be the common regulation of those by Fosl1, which was down-regulated by both compounds.

Up-regulation of Runx2 and Osterix mRNA expression suggests that bAPN and hcys accelerate osteoblastic differentiation in MC3T3-E1 cells, which is further confirmed by the increase of the ALP activity. This is also supported by the down-regulation of Dlx5 mRNA expression, a gene that precedes Runx2 during osteoblastic differentiation. However,

Runx2 is not only regulated at its mRNA expression level, but interacting proteins modulate its enzymatic activity as well. Interestingly, the mRNA expression of many of these Runx2 interacting proteins is up-regulated by hcys but not by bAPN. These results suggest that, although bAPN and hcys affect Runx2 mRNA expression in a similar manner, at this stage, the activity of Runx2 and with it the osteoblastic differentiation depends on the expression of Runx2 interacting proteins, which may be affected by both compounds differentially.

A general evaluation of genome wide gene expression revealed that only a small part of genes is co-regulated by both compounds. 5.5-fold more genes are down- and 3.8-fold more genes are up-regulated by hcys compared to bAPN (not shown). This finding could be due to the fact that hcys being a physiological metabolite is involved and affects many intracellular metabolic pathways. The common regulated genes, however, could be exposed to the "lathyritic" effect of the agents.

For this study, we used 0.1 and 4 mM for bAPN and hcys, and for the latter we used an additional concentration of 10 mM. The lower concentration used resembles the "pathological" one, while the higher one was used to accentuate significant effects on gene expression.

As previously stated, hcys stimulated expression of genes involved in the regulation of Runx2 function, while bAPN did not. Runx2 function, essential for the development of the osteoblastic phenotype, can be activated or inactivated at the protein level. Our results demonstrate that hcys has the capacity to up-regulate both co-activators and in-activators. This may imply that through their receptors, the local environment (growth- and differentiation factors, ECM) of the cells, and the hormonal status of an individual influence the expression and activity of co-activators and in-activators. This suggests that the physiological and hormonal status of an individual regulates the expression of these in/co-activators, which have different impact on Runx2 function and consequently on the osteoblast activity. As an example, one may consider Stat1, a co-repressor, and Satb2, an activator of Runx2, both of which were up-regulated by hcys; the local environment or the hormonal status, however, will dictate whether Runx2 is either activated or repressed. This suggests that each individual may be differentially influenced by hcys. This could explain some contradictory results found in the literature with hcys concerning bone quality [4–6,8–10,48].

In summary, the results of the present study demonstrated that concerning collagen cross-linking both compounds not only act as lathyrogens influencing the enzymatic activity of genes involved in collagen cross-linking but they also influence on a similar manner the mRNA expression of these genes. Furthermore, induction of differentiation is suggested for both compounds by their up-regulating effect on Runx2 mRNA expression. However, in the case of hcys which simultaneously up-regulates co-activators and repressors of the Runx2 activity, the net effect on differentiation may depend on the local environment (individual). Finally, gene array analysis revealed that hcys regulated considerably more genes in MC3T3-E1 cells compared to bAPN. All these data emphasize that bAPN and hcys not only have comparable, but also have differing effects on osteoblasts.

Acknowledgments

This study was supported by the Fonds zur Foederung der wissenschaftlichen Forschung (FWF; The Austrian Science Fund) Project P20646-B11, the WGKK (Social Health Insurance Vienna), and the AUVA (Austrian Social Insurance for Occupational Risks).

References

[1] Turecek C, Fratzl-Zelman N, Rumpler M, Buchinger B, Spitzer S, Zoehrer R, et al. Collagen cross-linking influences osteoblastic differentiation. Calcif Tissue Int 2008;82:392–400.
[2] Liu G, Nellaiappan K, Kagan HM. Irreversible inhibition of lysyl oxidase by homocysteine thiolactone and its selenium and oxygen analogues. Implications for homocystinuria. J Biol Chem 1997;272:32370–7.
[3] Blouin S, Thaler H, Korninger C, Schmid R, Hofstaetter J, Zoehrer R, et al. Bone matrix quality and plasma homocysteine levels. Bone 2009.
[4] Raisz LG. Homocysteine and osteoporotic fractures—culprit or bystander? N Engl J Med 2004;350:2089–90.
[5] McLean RR, Jacques PF, Selhub J, Tucker KL, Samelson EJ, Broe KE, et al. Homocysteine as a predictive factor for hip fracture in older persons. N Engl J Med 2004;350:2042–9.
[6] van Meurs JB, Dhonukshe-Rutten RA, Pluijm SM, van der Klift M, de Jonge R, Lindemans J, et al. Homocysteine levels and the risk of osteoporotic fracture. N Engl J Med 2004;350:2033–41.
[7] Gjesdal CG, Vollset SE, Ueland PM, Refsum H, Meyer HE, Tell GS. Plasma homocysteine, folate and vitamin B12 and the risk of hip fracture. The Hordaland Homocysteine Study. J Bone Miner Res 2007;22:747–56.
[8] Perier MA, Gineyts E, Munoz F, Sornay-Rendu E, Delmas PD. Homocysteine and fracture risk in postmenopausal women: the OFELY study. Osteoporos Int 2007;18:1329–36.
[9] Herrmann M, Widmann T, Herrmann W. Re: "Elevated serum homocysteine and McKusick's hypothesis of a disturbed collagen cross-linking: What do we really know?". Bone 2006;39:1385–6 author reply 1386-7.
[10] Toohey JI. Homocysteine toxicity in connective tissue: theories, old and new. Connect Tissue Res 2008;49:57–61.
[11] Masse PG, Boskey AL, Ziv I, Hauschka P, Donovan SM, Howell DS, et al. Chemical and biomechanical characterization of hyperhomocysteinemic bone disease in an animal model. BMC Musculoskelet Disord 2003;4:2.
[12] Herrmann M, Wildemann B, Wagner A, Wolny M, Schorr H, Taban-Shomal O, et al. Experimental folate and vitamin B12 deficiency does not alter bone quality in rats. J Bone Miner Res 2009;24:589–96.
[13] Herrmann M, Umanskaya N, Wildemann B, Colaianni G, Widmann T, Zallone A, et al. Stimulation of osteoblast activity by homocysteine. J Cell Mol Med 2008;12:1205–10.
[14] Ozdem S, Samanci S, Tasatargil A, Yildiz A, Sadan G, Donmez L, et al. Experimental hyperhomocysteinemia disturbs bone metabolism in rats. Scand J Clin Lab Invest 2007;67:748–56.
[15] Herrmann M, Schmidt J, Umanskaya N, Colaianni G, Al Marrawi F, Widmann T, et al. Stimulation of osteoclast activity by low B-vitamin concentrations. Bone 2007;41:584–91.
[16] Luegmayr E, Varga F, Frank T, Roschger P, Klaushofer K. Effects of triiodothyronine on morphology, growth behavior, and the actin cytoskeleton in mouse osteoblastic cells (MC3T3-E1). Bone 1996;18:591–9.
[17] Gerstenfeld LC, Chipman SD, Kelly CM, Hodgens KJ, Lee DD, Landis WJ. Collagen expression, ultrastructural assembly, and mineralization in cultures of chicken embryo osteoblasts. J Cell Biol 1988;106:979–89.
[18] Paschalis EP, Verdelis K, Doty SB, Boskey AL, Mendelsohn R, Yamauchi M. Spectroscopic characterization of collagen cross-links in bone. J Bone Miner Res 2001;16:1821–8.
[19] Pfaffl MW. A new mathematical model for relative quantification in real-time RT-PCR. Nucleic Acids Res 2001;e45:29.
[20] Komori T. Regulation of osteoblast differentiation by transcription factors. J Cell Biochem 2006;99:1233–9.
[21] Lian JB, Stein GS, Javed A, van Wijnen AJ, Stein JL, Montecino M, et al. Networks and hubs for the transcriptional control of osteoblastogenesis. Rev Endocr Metab Disord 2006;7:1–16.
[22] Huang W, Yang S, Shao J, Li YP. Signaling and transcriptional regulation in osteoblast commitment and differentiation. Front Biosci 2007;12:3068–92.
[23] Dobreva G, Chahrour M, Dautzenberg M, Chirivella L, Kanzler B, Fariñas I, et al. SATB2 is a multifunctional determinant of craniofacial patterning and osteoblast differentiation. Cell 2006;125:971–86.
[24] Roblin X, Phelip JM, Genevois M, Ducros V, Bonaz B. Hyperhomocysteinaemia is associated with osteoporosis in patients with Crohn's disease. Aliment Pharmacol Ther 2007;25:797–804.
[25] Herrmann W, Herrmann M, Obeid R. Hyperhomocysteinaemia: a critical review of old and new aspects. Curr Drug Metab 2007;8:17–31.
[26] Gerdhem P, Ivaska KK, Isaksson A, Pettersson K, Vaananen HK, Obrant KJ, et al. Associations between homocysteine, bone turnover, BMD, mortality, and fracture risk in elderly women. J Bone Miner Res 2007;22:127–34.
[27] Baines M, Kredan MB, Usher J, Davison A, Higgins G, Taylor W, et al. The association of homocysteine and its determinants MTHFR genotype, folate, vitamin B(12) and vitamin B(6) with bone mineral density in postmenopausal British women. Bone 2007;40:730–6.
[28] Selhub J. The many facets of hyperhomocysteinemia: studies from the Framingham cohorts. J Nutr 2006;136:1726S–30S.
[29] Saito M, Fujii K, Marumo K. Degree of mineralization-related collagen crosslinking in the femoral neck cancellous bone in cases of hip fracture and controls. Calcif Tissue Int 2006;79:160–8.
[30] Saito M. Elevated plasma concentration of homocysteine, low level of vitamin B6, pyridoxal, and vitamin D insufficiency in patients with hip fracture: a possible explanation for detrimental cross-link pattern in bone collagen. Clin Calcium 2006;16:1974–84.
[31] Koh JM, Lee YS, Kim YS, Kim DJ, Kim HH, Park JY, et al. Homocysteine enhances bone resorption by stimulation of osteoclast formation and activity through increased intracellular ROS generation. J Bone Miner Res 2006;21:1003–11.
[32] Herrmann W. Significance of hyperhomocysteinemia. Clin Lab 2006;52:367–74.
[33] Gjesdal CG, Vollset SE, Ueland PM, Refsum H, Drevon CA, Gjessing HK, et al. Plasma total homocysteine level and bone mineral density: the Hordaland Homocysteine Study. Arch Intern Med 2006;166:88–94.

[34] van Meurs JB, Uitterlinden AG. Homocysteine and fracture prevention. JAMA 2005;293:1121–2.
[35] Sato Y, Iwamoto J, Kanoko T, Satoh K. Homocysteine as a predictive factor for hip fracture in elderly women with Parkinson's disease. Am J Med 2005;118:1250–5.
[36] Sato Y, Honda Y, Iwamoto J, Kanoko T, Satoh K. Effect of folate and mecobalamin on hip fractures in patients with stroke: a randomized controlled trial. JAMA 2005;293:1082–8.
[37] Sato Y, Honda Y, Iwamoto J, Kanoko T, Satoh K. Homocysteine as a predictive factor for hip fracture in stroke patients. Bone 2005;36:721–6.
[38] Ravaglia G, Forti P, Maioli F, Servadei L, Martelli M, Brunetti N, et al. Folate, but not homocysteine, predicts the risk of fracture in elderly persons. J Gerontol A Biol Sci Med Sci 2005;60:1458–62.
[39] Morris MS, Jacques PF, Selhub J. Relation between homocysteine and B-vitamin status indicators and bone mineral density in older Americans. Bone 2005;37: 234–42.
[40] Herrmann M, Widmann T, Herrmann W. Homocysteine—a newly recognised risk factor for osteoporosis. Clin Chem Lab Med 2005;43:1111–7.
[41] Cashman KD. Homocysteine and osteoporotic fracture risk: a potential role for B vitamins. Nutr Rev 2005;63:29–36.
[42] Perez-Castrillon JL, Arranz-Pena ML, Luis DD. Homocysteine as a predictive factor for hip fracture in older persons. N Engl J Med 2004;351:1027–30 author reply 1027-30.
[43] Ellenberg SS, Orloff DG, Temple RJ. Homocysteine as a predictive factor for hip fracture in older persons. N Engl J Med 2004;351:1027–30 author reply 1027-30.
[44] Bursztyn M. Homocysteine as a predictive factor for hip fracture in older persons. N Engl J Med 2004;351:1027–30 author reply 1027-30.
[45] Auer J, Lamm G, Eber B. Homocysteine as a predictive factor for hip fracture in older persons. N Engl J Med 2004;351:1027–30 author reply 1027-30.
[46] Jamaluddin MD, Chen I, Yang F, Jiang X, Jan M, Liu X, et al. Homocysteine inhibits endothelial cell growth via DNA hypomethylation of the cyclin A gene. Blood 2007;110:3648–55.
[47] Nagaoka H, Mochida Y, Atsawasuwan P, Kaku M, Kondoh T, Yamauchi M. 1,25(OH) 2D3 regulates collagen quality in an osteoblastic cell culture system. Biochem Biophys Res Commun 2008;377:674–8.
[48] Gjesdal CG, Vollset SE, Ueland PM, Refsum H, Meyer HE, Tell GS. Plasma homocysteine, folate, and vitamin B 12 and the risk of hip fracture: the hordaland homocysteine study. J Bone Miner Res 2007;22:747–56.

THE JOURNAL OF BIOLOGICAL CHEMISTRY VOL. 286, NO. 7, pp. 5578–5588, February 18, 2011

Homocysteine Suppresses the Expression of the Collagen Cross-linker Lysyl Oxidase Involving IL-6, *Fli1*, and Epigenetic DNA Methylation*

Received for publication, July 20, 2010, and in revised form, November 14, 2010 Published, JBC Papers in Press, December 9, 2010, DOI 10.1074/jbc.M110.166181

Roman Thaler[‡], Marlies Agsten[‡], Silvia Spitzer[‡], Eleftherios P. Paschalis[‡], Heidrun Karlic[§], Klaus Klaushofer[‡], and Franz Varga[‡1]

From the [‡]Ludwig Boltzmann Institute of Osteology, Hanusch Hospital, Wiener Gebietskrankenkasse and AUVA Trauma Center Meidling, 1st Medical Department, Hanusch Hospital, 1140 Vienna, Austria and the [§]Ludwig Boltzmann Institute for Leukemia Research and Hematology, Hanusch Hospital and Ludwig Boltzmann Cluster Oncology, 1140 Vienna, Austria

Elevated homocysteine (Hcys) serum levels represent a risk factor for several chronic pathologies, including cardiovascular disease, atherosclerosis, and chronic renal failure, and affect bone development, quality, and homeostasis. Hcys influences the formation of a stable bone matrix directly through the inhibition of the collagen cross-linking enzyme lysyl oxidase (*Lox*) and, as we have shown recently, by repressing its mRNA expression. The aim of this study was to investigate the mechanisms involved in this process. Through evaluation of gene arrays, quantitative RT-PCR, immunoblots, and ELISA, we identified a Hcys-dependent stimulation of interleukin 6 (IL-6) and genes involved in IL-6/Janus kinase 2 (JAK2)-dependent signal transduction pathways in pre-osteoblastic MC3T3-E1 cells. Moreover, up-regulation of genes essential for epigenetic DNA methylation (DNA (cytosine-5)-methyltransferases and helicase lymphoid-specific (*Hells*) was observed. Further investigations demonstrated that Hcys increased via IL-6/JAK2 the expression of *Fli1* (Friend leukemia virus integration 1), a transcription factor, which we found essential for IL-6-dependent *Dnmt1* stimulation. CpG methylation analysis of CpG-rich Lox proximal promoter revealed an increased CpG methylation status after treatment of the cells with Hcys indicating an epigenetic origin for Hcys-dependent Lox repression. Inhibition of the IL-6/JAK2 pathway or of CpG methylation reversed the repressive effect of Hcys on *Lox* expression. In conclusion, we demonstrate that Hcys stimulates IL-6 synthesis in osteoblasts, which is known to affect bone metabolism via osteoclasts. Furthermore, IL-6 stimulation results via JAK2, *Fli1*, and *Dnmt1* in down-regulation of *Lox* expression by epigenetic CpG methylation revealing a new mechanism negatively affecting bone matrix formation.

Epidemiological studies have shown that high homocysteine (Hcys)[2] serum levels represent a risk factor for several chronic disorders such as cardiovascular disease, atherosclerosis, chronic renal failure, diabetes, or the metabolic syndrome (1, 2). Moreover, hyperhomocysteinemia is known to affect bone development and homeostasis (3–6). Hcys has been shown to interfere with post-translational modifications of collagen directly by inhibiting lysyl oxidase (*Lox*) (7) and indirectly by down-regulation of its mRNA expression and of other genes involved in collagen cross-linking. Enzymatic inhibition or mRNA down-regulation of *Lox* results in changes in collagen cross-linking pattern *in vitro* (8–10) and *in vivo* resulting in decreased bone quality (11–13). In this context, we have recently reported a correlation between plasma Hcys levels and a collagen cross-link ratio in forming trabecular surfaces in human bone (14).

Lysyl oxidase was also identified as a phenotypic suppressor of the ras oncogene in H-ras-transformed NIH3T3 fibroblasts. In this transformed cell line, H-ras participates in an elaborate pathway attenuating the expression of Lox and of many other genes by CpG methylation on DNA. These genes are reactivated by treatment with azacytidine, an inhibitor of DNA (cytosine-5)-methyltransferases. Methylation of cytosine-guanine dinucleotides (CpGs) on DNA is an important epigenetic mechanism involved in the selective regulation of gene expression and in the stabilization of chromatin, thus controlling tissue development and pathogenesis. Aberrant CpG methylation of specific genes is often found in many tumors and tumorigenic cell lines (15).

Besides its role as inhibitor of collagen cross-linking, Hcys is also known to play a role in epigenetic gene regulation being directly involved in the DNA methylation process. Hcys represents a methyl group carrier involved in the *S*-adenosylmethionine-*S*-adenosylhomocysteine methylation cycle. Here, Hcys is remethylated to methionine, which is further activated to *S*-adenosylmethionine, the methyl donor in DNA methylation. *S*-Adenosylmethionine converts to *S*-adenosylhomocysteine after DNA methylation. Hydrolysis of *S*-adenosylhomocysteine to homocysteine completes the cycle (16).

* This work was supported by the Fonds zur Foerderung der Wissenschaftlichen Forschung from the Austrian Science Fund Project P20646-B11, the Social Health Insurance Vienna, and the Austrian Social Insurance for Occupational Risk.

[1] To whom correspondence should be addressed: Ludwig Boltzmann Institute of Osteology, 1st Medical Dept., Hanusch Hospital, Heinrich Collin-Str. 30, A-1140 Vienna, Austria. Tel.: 43-1-91021-86933; Fax: 43-1-91021-86929; E-mail: franz.varga@osteologie.at.

[2] The abbreviations used are: Hcys, homocysteine; Lox, lysyl oxidase; qRT, quantitative RT; Hells, helicase, lymphoid-specific; STAT, signal transducer and activator of transcription.

Nevertheless, in contrast to other cells and tissues, to date sparse research has been performed regarding the significance of epigenetic gene regulation for bone development and pathogenesis. We have recently demonstrated that maintenance of global and specific DNA methylation by collagen type I, the main component of extracellular matrix in the bone, plays an important role in osteoblastic survival (17). Furthermore, we have shown that Hcys affects osteoblastic development and differentiation by altering the expression of osteoblastic genes already at the mRNA level (9).

Assuming an epigenetic cause, in this study we demonstrate the mechanisms involved in suppression of Hcys of *Lox* mRNA expression in pre-osteoblastic MC3T3-E1 cells. Besides the known role of Hcys as a metabolite in the DNA methylation cycle (16), we investigated if Hcys has an impact on the expression of genes involved in DNA methylation such as DNA methyltransferases and helicase, lymphoid-specific (*Hells*). Thereby we found that Hcys regulates the expression of DNA methyltransferase 1 (*Dnmt1*) by inducing a signaling pathway where interleukin 6 (IL-6), Janus kinase 2 (*Jak2*), and Friend leukemia virus integration 1 (*Fli1*) transcription factors were involved. These findings suggest a key role of epigenetic DNA methylation in Hcys-mediated Lox suppression.

MATERIALS AND METHODS

Cell Culture—MC3T3-E1 cells (kindly donated by Dr. Kumegawa, Department of Oral Anatomy, Meikai University, Sakado, Japan), a clonal pre-osteoblastic cell line derived from newborn mouse calvariae, were cultured in humidified air under 5% CO_2 at 37 °C. α-Minimum essential medium (Biochrom, Berlin, Germany) was supplemented with 5% fetal calf serum (Biochrom, Germany), 50 μg/ml ascorbic acid (Sigma), and 10 μg/ml gentamycin (Sigma). For propagation, cells were subcultured twice a week using 0.001% Pronase E (Roche Applied Science) and 0.02% EDTA in Ca^{2+}- and Mg^{2+}-free phosphate-buffered saline (PBS) before achieving confluence. For experiments, MC3T3-E1 cells were seeded in culture dishes at a density of 20,000/cm^2 and cultured overnight. The next day, the medium was changed, and the cells were treated with Hcys (Sigma) at the indicated concentrations for 3, 6, or 14 days.

To demonstrate the effect of Hcys on the JAK2 pathway or on DNA methylation, cells were treated with 3.6 mM Hcys for 3 days; thereafter, 30 μM of the specific JAK2 inhibitor AG490 (Calbiochem) or 50 μM of the DNA methylation inhibitor zebularine (Sigma) was added to the medium for a further 3 days. To test the effects of recombinant mouse IL-6 protein (PeproTech, United Kingdom) on the cells, they where cultured with increasing concentrations (3–30 ng/ml) for 36 and 48 h. To demonstrate the IL-6-dependent activation of the JAK2 pathway by Hcys, cells were treated with 3.6 mM Hcys for 3 days; thereafter, 4 μg/ml IL-6 antibody (Ab) (PeproTech) was added to the medium for a further 3 days.

Isolation of Nucleic Acids and mRNA Expression Analysis by qRT-PCR—DNA and RNA were extracted using a DNA/RNA isolation kit (Qiagen). cDNA was synthesized from about 0.5 μg of RNA using the First Strand cDNA synthesis kit as described by the supplier (Roche Applied Science). The obtained cDNA was subjected to PCR amplification with a real time cycler using FastStart SYBR Green master mix (Roche Applied Science) for the genes *Dnmt1*, *Dnmt3b*, *Hells*, and *Fli1* (for primer design see Table 1). SYBR Green PCR was started with 10 min of an initial denaturation step at 95 °C and then continued with 45 cycles consisting of 30 s of denaturation at 95 °C, 30 s annealing at primer-specific temperatures, and extension at 72 °C. For Lox expression, we used a TaqMan probe (Mm00495386_m1, Applied Biosystems), and for normalization we used the 18 S RNA TaqMan probe (4319413E, Applied Biosystems), both in combination with TaqMan gene expression master mix (Applied Biosystems) with an initial denaturation at 95 °C for 10 min followed by 45 cycles alternating between 60 and 90 °C. All PCRs were performed in triplicate, and expression was evaluated using the comparative quantitation method (18). For each experiment, the triplicate results of the qRT-PCR were averaged, and this mean value was treated as a single statistical unit. The data of the experimental results are presented as means ± S.D.

Affymetrix GeneChip Analysis—Total RNA was isolated using an RNA isolation kit (Qiagen). Quality control of the RNAs as well as labeling, hybridization, and scanning of the hybridized arrays was performed by the Kompetenzzentrum fuer Fluoreszente Bioanalytik (KFB) (Regensburg, Germany) using the mouse 430 2.0 chip (Affymetrix).

IL-6 Quantification by ELISA—For IL-6 ELISA, MC3T3-E1 cells were seeded in triplicate and treated with or without the indicated Hcys concentrations for 14 days as described above. After 3, 6, and 14 days of Hcys treatment, 1 ml of culture supernatant was saved and stored at −80 °C. For IL-6 quantification, 96-well ELISA plates (Iwaki) were prepared by using the murine IL-6 ELISA development kit as described by the supplier (PeproTech). IL-6 concentration was monitored by color development of 2,2′-azino-bis(3-ethylbenzthiazoline-6-sulphonic acid) liquid substrate (Sigma) with an ELISA plate reader (Glomax, Promega) at 405 nm with wavelength correction set at 650 nm. Every cultured well was measured in triplicate; these triplicate results were averaged, and the mean value was treated as a single statistical unit. The complete experiment was performed twice.

Protein Isolation and Immunoblotting—For protein extraction, cell layers were washed two times with PBS and scraped in SDS sample buffer (2% SDS, 100 mM β-mercaptoethanol, 125 mM Tris-HCl, pH 6.8) and heated at 95 °C for 5 min. 30 μg of protein extracts were fractionated on 8 or 10% SDS-PAGE for Dnmt1 or the other proteins, respectively. Following SDS-gel electrophoresis, the proteins were transferred to nitrocellulose filters (Millipore) and blocked overnight with 10% blocking reagent (Roche Applied Science) in TN Buffer (50 mM Tris, 125 mM NaCl, pH 8). Subsequently, the filters were incubated for 1 h at room temperature with antibodies against FLI1 ((C19), HELLS (Lsh, H-240)), LOX (H-140), DNMT1 (K-18, all Santa Cruz Biotechnology) diluted 1:200 in blocking buffer. Afterward, all filters were washed three times with immunoblot wash buffer (TN buffer containing 0.01% Tween) and the FLI1, HELLS, and LOX blots were incubated for an additional hour with an anti-mouse IgG/anti-rabbit IgG horseradish peroxidase (HRP)-labeled secondary antibody

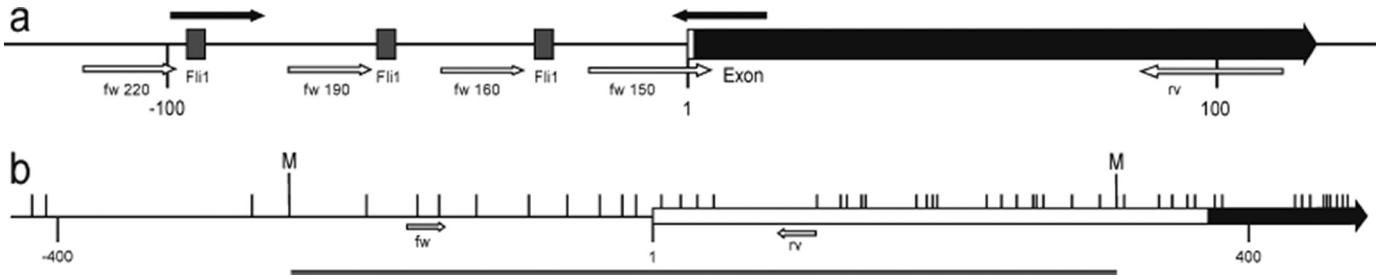

FIGURE 1. **Schematic diagram depicting *Dnmt1* (*a*) and *Lox* (*b*) promoter.** *a,* exon representing the somatic transcription start (marked with *1*) is represented as *small open box* (untranslated region) and *large black arrow* (translated region). The three putative FLI1-binding sites are shown as *gray boxes*. Forward (*fw*) cloning primers annotated with the resulting amplicon size and reverse (*rv*) cloning primer are marked as *white arrows*. Binding sites of amplification primers for *Fli1* ChIP analysis are marked as *black arrows*. The *numbers* below the gene line denote the distance to the transcription start. *b,* representation of *Lox* proximal promoter and the first exon showing the fragment used for methylation analysis (*gray line*). *Lox* genomic structure shows a part of the first exon (475 bp), including 374 bp of the 5′-untranslated region (*open box*) and the first 101 bp of the coding region (*black arrow*). To generate a suitable fragment (*gray line*) for methylation analysis by "Methyl Miner" assay, DNA was restricted by MboII restriction enzyme (*M*). Forward (*fw*) and reverse (*rv*) primers for subsequent amplification by qRT-PCR are marked as *white arrows*. The *vertical bars* indicate the CpGs in the DNA strand, and the *numbers* below the gene line denote the distance to the transcription start.

(Roche Applied Science) diluted 1:20,000 in blocking buffer. The Dnmt1 blot was incubated for 1 h with an anti-goat IgG HRP-labeled secondary antibody (Sigma) diluted 1:160,000 in blocking buffer. Finally, the blots were washed again three times with immunoblot washing buffer before detection of light emission with the BM chemiluminescence Western blotting kit (Roche Applied Science) as described by the supplier. Chemiluminescence was measured with an image acquisition system (Vilber Lourmat, France).

Cloning of Mouse Dnmt1 Promoter—To study the effect of IL-6 on *Dnmt1* promoter activity, four fragments of the mouse Dnmt1 promoter (NC_000075.5) were cloned from MC3T3-E1 genomic DNA into the pGEM T-easy vector (Promega) by using the following 5′-primers elongated to contain a BglII restriction site (underlined): TCG AGA TCT GCC TTC GGG CAT AGC ATG GTC for a 220-bp fragment carrying three putative Fli1-binding sites (as suggested in Ref. 19), at −30, −60, and −96 bp from the somatic transcriptional start site (20); TCG AGA TCT GCC TGT GTG GTA CAT GCT GC for the 190-bp fragment carrying two putative Fli1-binding sites (at −30 and −60 bp); TCG AGA TCT GGC CGC CCC CTC CCA ATT GG for the 160-bp fragment carrying one putative Fli1-binding site (at −30 bp); and TCG AGA TCT GCG AAA AAG CCG GGG TCT CGT TC for the 150-bp fragment carrying no FLI1-binding sites. As 3′-primer we used GCC TGC GGA CAT GGT CCG GGA GCG AGC CTG. These fragments were subsequently cloned into the secreted alkaline phosphatase 2 (SEAP2) reporter vector (Clontech) by using BglII and EcoRI restriction enzymes (Fig. 1*a*).

To generate mutated *Dnmt1*-SEAP2 fragments, as described previously (19), the following primers with modified putative FLI1-binding sites were designed (mutation sites form 5′- TTCC to TTAA are underlined): 5′ CGG GCA TAG CAT GGT CTT AAC CCA CTC TCT TGC CCT G and complementary 3′ CAG GGC AAG AGA GTG GGT TAA GAC CAT GCT ATG CCC G for the putative FLI1-binding site at −96 bp from the somatic transcriptional start site; 5′ GTG GTA CAT GCT GCT TAA GCT TGC GCC GCC CC and complementary 3′ GGG GCG GCG CAA GCT TAA GCA GCA TGT ACC AC for the putative FLI1-binding site at −60 bp from the somatic transcriptional start site; and 5′ CTC CAA ATT GGT TTA AGC GCG CGC GAA AAA GCC G and 3′ CGG CTT TTT CGC GCG CGC TTA AAC CAA TTG GGA G for the putative FLI1-binding site at −30 bp from the somatic transcriptional start site.

For transfection experiments with the various SEAP2-*Dnmt1* vectors, SEAP2-control vector and the SEAP2-basic vector, MC3T3-E1 cells were seeded at 20,000 cells/cm^2 in 48 multiwell plates. Six hours after seeding, cells were transfected with 0.15 μg/cm^2 vector construct using 1 μg/cm^2 DOSPER transfection reagent (Roche Applied Science) following the suppliers' protocol. After 2 days, cells were treated for a further 3 days with 30 ng/ml of murine IL-6 (PeproTech), and finally, SEAP2 activity was measured in 50 μl of culture supernatant using the SEAP2 bioluminescence kit (Roche Applied Science) following the supplier's instructions. Each experiment was run in quadruplicate and was repeated at least twice.

Chromatin Immunoprecipitation of Fli1 Bound on Dnmt1 Promoter—As numerous members of the E-twenty six transcription factor family can bind to GGAA (TTCC) sequence *in vitro*, chromatin immunoprecipitation (ChIP) assay were performed to demonstrate FLI1 TTCC occupancy at the *Dnmt1* locus *in vivo*. For this purpose, MC3T3-E1 cells were treated for 6 days with or without 3.6 mM Hcys. Subsequent chromatin cross-linking, cell lysis, chromatin sharing, FLI1 immunoprecipitation, and DNA clean-up were performed with the ChampionChip one-day kit (SABiosciences, MD) following the manufacturer's instructions. Chromatin from untreated as well as from Hcys-treated cells was incubated overnight on a rotor at 4 °C with 4 μg of anti-FLI1 antibody (C-19, Santa Cruz Biotechnology) or with 4 μg of nonimmune serum as negative control. Before immunoprecipitation, 1% (10 μl) of the chromatin was saved and stored at 4 °C for further use as reference. For quantitation of the qRT-PCR values, for each sample, DNA signal of the FLI1-precipitated chromatin was normalized to the unprecipitated chromatin (for ChIP-*Dnmt1* promoter primer design see Table 1).

Lox Promoter Methylation—To test if down-regulation of Lox by Hcys is due to CpG methylation, CpG content on *Lox* promoter was analyzed. A CpG-rich region starting from ap-

TABLE 1
qRT-PCR primer for mRNA expression and *Lox* CpG methylation analysis (SYBR Green)

Gene	Forward primer (5′–3′)	Reverse primer (5′–3′)	T_m
			℃
Dnmt1	ACCGCTTCTACTTCCTCGAGGCCTA	GTTGCAGTCCTCTGTGAACACTGTGG	62
Dnmt3b	GGAGAAAGCCAGGGT	AAGAGGGGGTGGAAGGA	63
Hells	TGAGGATGAAAGCTCTTCCACT	ACATTTCCGAACTGGGTCAAAA	63
Fli1	ATGGACGGGACTATTAAGGAGG	GAAGCAGTCATATCTGCCTTGG	62
Primer for *Lox* CpG methylation analysis			
Promoter/first exon	GCATGTTCGGCCCAGATTAAGTCG	CAGAGTCTGGAGTAGAAGGAGGAGG	65
Primer for FLI1 ChIP analysis on *Dnmt1* promoter			
Dnmt1 ChIP-FLI1	CTTCCCCCACTCTCTTGC	GAACAGCTCTGAACGAGAC	63

proximately −600 bp 5′ from the transcriptional start site and spanning over the first exon was selected. An appropriate fragment of the targeted *Lox* region was generated by digestion of 1 μg of genomic DNA with 40 units of the CpG methylation-insensitive restriction enzyme MboII (New England Biolabs) for 20 min at 37 °C from cells cultured for 6 and 14 days with or without 3.6 mM Hcys. Subsequently, the enzyme was heat-inactivated at 65 °C for 20 min. As shown in Fig. 1*b*, the generated fragment has 627 bp and contains 30 CpG sites. It includes 243 bp of the proximal promoter region and 312 bp of the untranslated part of the first exon of *Lox*. After MboII digestion, DNA was purified using a commercially available PCR clean-up kit following supplier's instructions. In the next step, methylated DNA fragments were captured with the "Methyl Miner methylated DNA enrichment kit" (Invitrogen) following the supplier's instructions. In brief, methylated DNA was captured by methyl-binding protein 2 (MBD2) coupled to magnetic beads and subsequently separated from the unmethylated DNA fraction. Methylated DNA was eluted from the MBD2 beads with 200 μl of a 2 M NaCl solution as a single fraction and concentrated by ethanol precipitation. Finally, the mean methylation status of the fragments was determined by amplifying the fragments by quantitative real time PCR. Amplification ratios of the bound (methylated) DNA fraction to unbound (unmethylated) DNA fraction were calculated (for primer design see Table 1).

Statistical Analysis—Statistical analyses were performed using either analysis of variance or Student's *t* test using Prism 4.03 (GraphPad Software, San Diego). $p \leq 0.05$ was considered as significant. Results are presented as mean ± S.D.

RESULTS

Homocysteine Stimulates IL-6 Expression thus Affecting JAK2-dependent Signaling Pathways in MC3T3-E1 Cells—As we already have demonstrated by genome-wide expression studies, Hcys affects the expression of genes of the osteoblastic phenotype (9). Further analysis of the data suggested that Hcys regulated the mRNA expression of IL-6 and of genes involved in JAK2 signal transduction pathways (Table 2), which are activated by this cytokine (21, 22).

To understand the temporal dynamics, time and dose dependence of Hcys on MC3T3-E1 cells was studied. Because of variation of basal expression of IL-6 mRNA expression as measured by qRT-PCR, by ELISA, we measured IL-6 protein, which accumulates in the culture medium. Generally, the primary data measured by ELISA showed a decreasing trend for the basal IL-6 expression (from 0.56 ng/ml IL-6 expression after 3 days to 0.33 ng/ml IL-6 expression after 14 days, data not shown). As shown in Fig. 2, after 3 days of Hcys treatment, no significant changes in IL-6 expression could be observed in the pre-osteoblastic cell line. However, after 6 days of Hcys treatment, IL-6 expression strongly increased in a concentration-dependent manner showing a maximal up-

TABLE 2
Regulation of genes involved in the JAK/STAT signal transduction pathway as suggested by genome-wide expression analysis
Fold regulation means change in expression level at a given concentration divided by that of the untreated cultures.

Gene symbol	Fold regulation to untreated control		
	0.108 mM	3.6 mM	10.8 mM
Il6	−1.06	1.51	2.37
Il6ra	−1.01	−1.06	1.09
Il6st	1.04	1.21	1.31
Jak1	−1.22	1.12	1.08
Jak2	−1.74	1.61	1.74
Jak3	−1.30	−1.16	−1.29
Stat1	1.59	3.06	3.44
Stat2	2.52	3.97	3.31
Stat3	−1.21	−1.08	−1.14
Stat4	−1.11	−1.28	−1.10
Stat5a	1.24	1.10	1.03
Stat5b	1.09	1.03	1.07
Stat6	1.20	1.15	1.41
Cbl	1.41	1.96	2.02
Cblb	−1.28	−1.16	−1.35
Cblc	−1.11	−1.39	−1.56

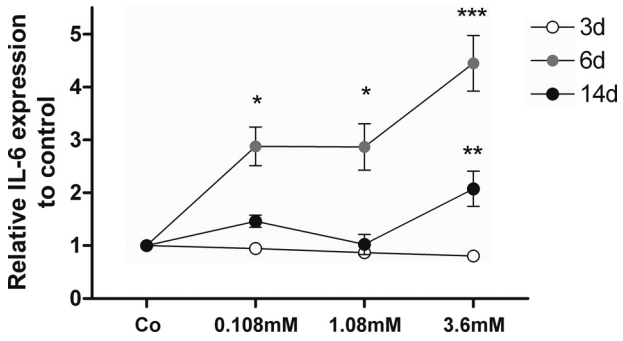

FIGURE 2. **Hcys up-regulates IL-6 in MC3T3-E1 pre-osteoblasts.** After 6 days (*d*) of treatment with 3.6 mM Hcys, expression of the JAK2 activator IL-6 was significantly enhanced in the MC3T3-E1 pre-osteoblastic cell line when compared with untreated cultures (*Co*). After 14 days of treatment, the up-regulative effect of Hcys on IL-6 expression was reduced but remained significant at the highest concentration used. No effects were observed after 3 days of culture with Hcys. To analyze IL-6 expression, cell medium supernatant was saved, and IL-6 expression was measured by ELISA. Values are represented as mean ± S.D.; untreated control is set to 1, and treated probes are referred as fold change to control. *, $p \leq 0.05$; **, $p \leq 0.01$; ***, $p \leq 0.001$; $n = 6$.

regulation of 4.4-fold (corresponding to 1.83 ng/ml IL-6) at 3.6 mM Hcys ($p \leq 0.001$) in the culture medium when compared with untreated cultures. After 14 days of treatment, the Hcys effect on IL-6 expression was attenuated but was still significant at 3.6 mM ($p \leq 0.01$). In Table 3, we present the regulation of those genes that will be described in more detail later to demonstrate the epigenetic influence of Hcys on *Lox* regulation.

Dnmt1 mRNA Expression Is Up-regulated by IL-6 via Putative FLI1-binding Sites on Dnmt1 Promoter in MC3T3-E1 Cells—Recently, it was demonstrated that IL-6 activates the transcription of *DNMT1* via FLI1 in human erythroleukemia cells (19, 23). Fig. 3 demonstrates that a comparable pathway exists in mouse osteoblasts as well. IL-6 significantly increased *Fli1* after 36 h and tended to stimulate expression after 48 h (Fig. 3*a*), although *Dnmt1* mRNA expression did not increase significantly until after 48 h of treatment (Fig. 3*b*). Dose dependence of the expression of both genes at the time when expression was significantly increased demonstrates that a maximum effect was found already at 3 ng/ml IL-6 (Fig. 3, *c* and *d*); this value was in the same order of magnitude as found in the culture medium after Hcys treatment of MC3T3-E1 cells as mentioned above (1.83 ng/ml).

TABLE 3

Regulation of genes involved in the DNA methylation process as suggested by genome-wide expression analysis

Regulation of these genes was verified by qRT-PCR and, except for *Dnmt3b*, by ELISA or immunoblots. Fold regulation means change in expression level at a given concentration divided by that of the untreated cultures.

	Fold regulation to untreated control		
Gene symbol	0.108 mM	3.6 mM	10.8 mM
Il6	−1.06	1.51	2.37
Fli1	1.18	1.15	1.40
Dnmt1	1.09	1.51	1.76
Dnmt3b	1.34	1.09	1.25
Hells	−1.04	2.45	3.60
Lox	−1.07	−1.67	−1.64

Fig. 1*a* depicts three putative FLI1-binding sites (sequence GGAA) in the first 220 bp of the somatic *Dnmt1* promoter (20), which are similarly organized in the human counterpart (19). To test if IL-6 mediated the increase of *Dnmt1* transcription via these binding sites, reporter-vector constructs of the *Dnmt1* gene with different lengths were constructed and transfected into MC3T3-E1 cells. As depicted in Fig. 1*a*, four different truncations were created as follows: a 150-bp fragment without any putative FLI1-binding site and three other fragments with 160, 190, and 220 bps containing one, two, or three putative FLI1-binding sites at −30, −60, or −96 bp, respectively. After 72 h of IL-6 treatment, SEAP2 activity was measured in the culture supernatant. As shown in Fig. 4*a*, when compared with the respective untreated promoter vectors, an IL-6-dependent increase of *Dnmt1* promoter activity correlated with an increasing promoter length and/or an increasing number of GGAA sites in the promoter. The strongest IL-6 effect was observed for the vector containing an insert of 220 bp (3 GGAA sites) of *Dnmt1* promoter with an increase of 2.2-fold ($p \leq 0.05$) when compared with the untreated vector.

To ensure that the IL-6-mediated effect on the activity of the *Dnmt1* promoter was due the predicted sites, in the 220-bp *Dnmt1* promoter-reporter construct these sites were mutated. After transfection into MC3T3-E1 cells and treat-

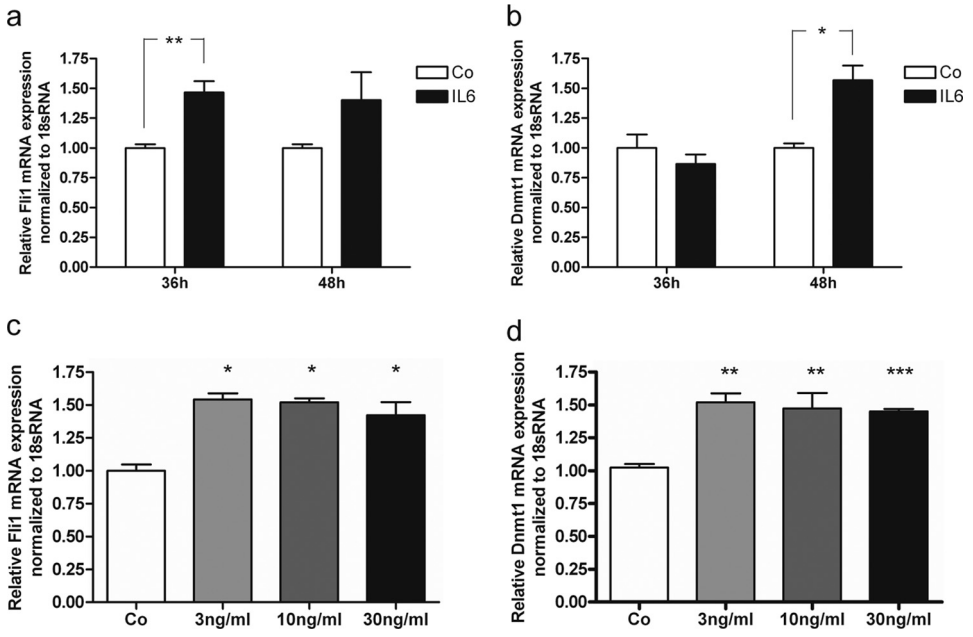

FIGURE 3. ***Fli1* (*a*) and *Dnmt1* (*b*) mRNA expression after treatment of MC3T3-E1 cells with 30 ng/ml recombinant murine IL-6 for 36 and 48 h.** Compared with untreated control (*Co*), *Fli1* mRNA expression is significantly up-regulated after 36 h of IL-6 treatment, whereas Dnmt1 mRNA expression remains unaffected at this time. After 48 h, 12 h after *Fli1* stimulation, *Dnmt1* also shows a significant increase in mRNA expression by IL-6 treatment. At this time, *Fli1* mRNA expression is still increased by IL-6; however, the regulation is not significant. As shown in *c* and *d*, treatment of the cells with increasing concentrations of IL-6 at the times showing significant mRNA stimulation for *Fli1* and *Dnmt1* revealed a significant up-regulation for both genes already at 3 ng/ml IL-6 in culture medium. The up-regulative effect of the cytokine was already reached at this concentration saturation for both genes. To analyze mRNA expression of *Fli1* and *Dnmt1*, RNA was isolated and analyzed by qRT-PCR. Gene expression was normalized to 18 S rRNA. Treated probes are referred as fold change to untreated control; *, $p \leq 0.05$; **, $p \leq 0.01$; ***, $p \leq 0.001$. For all graphs $n = 3$.

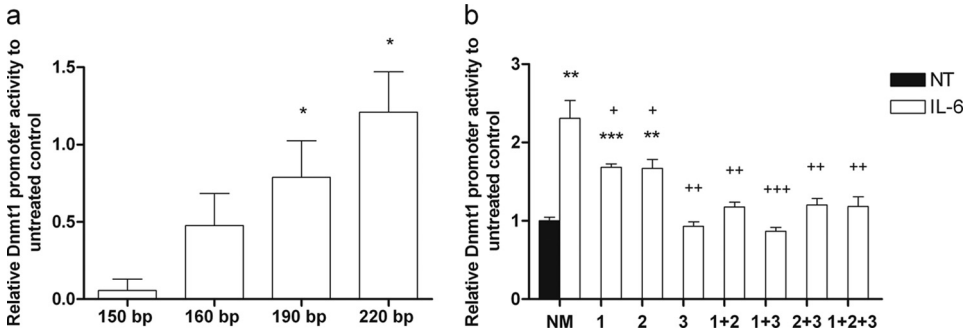

FIGURE 4. *a,* as measured by reporter gene assay, Fli1-binding sites/promoter length correlated with the IL-6-dependent activation of the *Dnmt1* promoter. A significant increase in promoter activity by IL-6 was seen when the putative FLI1-binding sites at −60 bp (190-bp fragment) and at −96 bp (220-bp fragment) from the somatic transcriptional start site were included in the *Dnmt1* promoter. Point mutation at one or more putative FLI1-binding sites in the 220-bp *Dnmt1* promoter fragment reduced IL-6 (30 ng/ml) responsiveness of the *Dnmt1* promoter. Mutation at all putative FLI1 sites decreased significantly IL-6-dependent *Dnmt1* promoter activation (*b*). Promoter activity was measured by SEAP2 reporter gene assay. Values are represented as mean ± S.D., and untreated controls are set to 0 in *a* and to 1 in *b*. *b* depicts one representative result of total three experiments. Treated probes are referred as fold change to nontreated control (*NT*); *, $p \leq 0.05$; **, $p \leq 0.01$; ***, $p \leq 0.001$. *b,* + represents significant differences to IL-6 treated, nonmutated Dnmt1 vector (*NM, white bar*): +, $p \leq 0.05$; ++, $p \leq 0.01$; +++, $p \leq 0.001$. *a,* $n = 3$; *b,* $n = 4$.

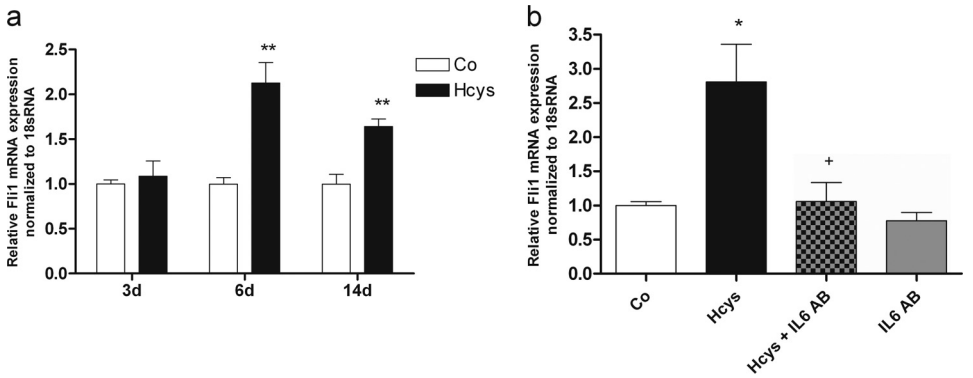

FIGURE 5. **Hcys-stimulated Fli1 expression is inhibited by an IL-6 Ab.** After 6 days (*d*) of treatment, a significant up-regulation of Fli1 mRNA expression was observed at 3.6 mM Hcys in medium when compared with the untreated control (*Co*) (*a*). This effect was slightly decreased after 14 days. No effect on Fli1 mRNA expression was seen after 3 days of Hcys treatment. After 6 days of Hcys treatment, inhibition of IL-6 activity by an IL-6 Ab (4 μg/ml) abrogated the effect of Hcys (3.6 mM) on up-regulation of Fli1 (*b*). To analyze Fli1 mRNA expression, RNA was isolated and analyzed by qRT-PCR. Gene expression was normalized to 18 S rRNA. Values are represented as mean ± S.D.; untreated control (*Co*) is set to 1, and treated probes are referred to as fold change to control. *, $p \leq 0.05$; **, $p \leq 0.01$; +, $p \leq 0.05$ refers to significance to Hcys-treated probes; for all graphs $n = 3$. *Lane M* refers to protein molecular weight standards.

ment with IL-6 for 72 h, SEAP2 activity was measured in culture supernatant again. As shown in Fig. 4*b*, mutation of these binding sites reduced transcription of the *Dnmt1* promoter-reporter construct, where mutation of site 3 (see Fig. 1) showed the strongest effect.

Hcys Up-regulates the Transcription Factor Fli1 via IL-6 and JAK2 in MC3T3-E1 Cells—Hcys regulated *Fli1* mRNA expression similarly to IL-6. After 3 days of Hcys treatment, no effect on mRNA expression of *Fli1* was observed. Subsequently, the highest Hcys-mediated increase of *Fli1* mRNA expression was observed after 6 days of treatment reaching a 2.1-fold ($p \leq 0.01$) up-regulation when compared with control. After 14 days of treatment, the Hcys effect on *Fli1* expression was attenuated but was still significant ($p \leq 0.01$, Fig. 5*a*).

Addition of anti-IL-6 antibody (Fig. 5*b*) or of the JAK2 inhibitor AG490 (Fig. 6) for the last three culture days to 6 days Hcys (3.6 mM)-treated MC3T3-E1 cells abrogated the Hcys effect on *Fli1* mRNA and protein expression (Fig. 6, *a–c*). This indicates that Hcys regulates *Fli1* expression via IL-6/JAK2. No effect of the Ab or of AG490 was found on basal *Fli1* expression.

Hcys Stimulates the Expression of Genes Involved in Epigenetic DNA Methylation—Gene chip analysis indicated an Hcys-dependent mRNA up-regulation of genes involved in DNA methylation (Table 3). The results on the regulation of DNA methylation-related genes obtained by gene chip analysis were confirmed by qRT-PCR. Furthermore, *Dnmt1* and *Hells* expressions were also studied by immunoblot analysis. As shown, when compared with untreated controls, after 3 days of culture 3.6 mM Hcys slightly induced the mRNA expression of *Dnmt1* (Fig. 7*a*) and *Dnmt3b* (Fig. 9) and significantly induced ($p \leq 0.05$) the mRNA expression of *Hells* (Fig. 8*a*). However, after 6 days of treatment, Hcys up-regulated the mRNA expression of all three genes significantly. At this time, Hcys increased the mRNA expression of *Dnmt1* 1.80-fold ($p \leq 0.01$, Fig. 7*a*), the DNMT1 protein expression 3.13-fold ($p \leq 0.05$, Fig. 7, *b* and *c*), the mRNA expression of *Hells* 3.1-fold ($p \leq 0.05$, Fig. 8*a*), the protein expression of HELLS 1.78-fold ($p \leq 0.05$, Fig. 8, *b* and *c*), and the mRNA expression of *Dnmt3b* 1.84-fold ($p \leq 0.001$, Fig. 9) when compared with untreated control. After 14 days of Hcys treatment, the mRNA expression of all three genes was still significantly increased (Figs. 7*a*, 8, and 9).

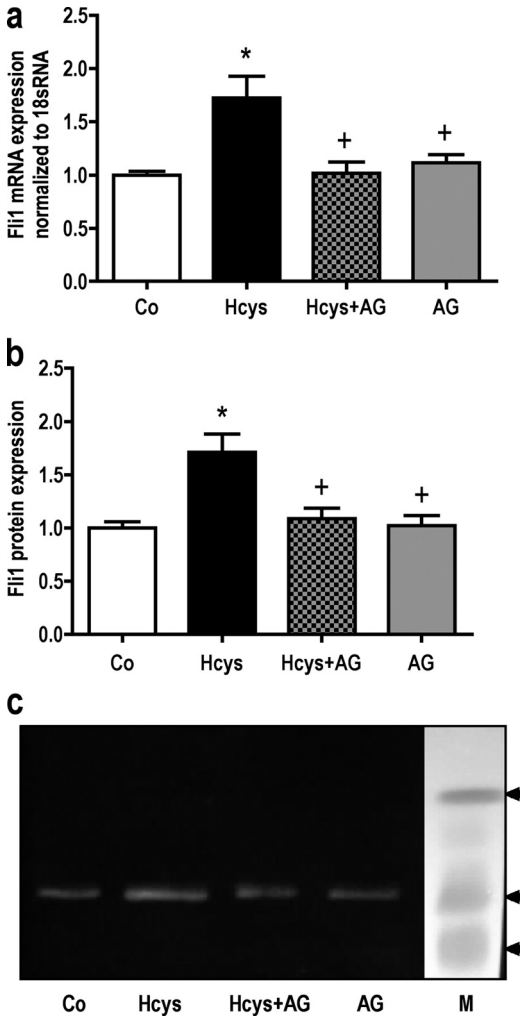

FIGURE 6. **Hcys stimulated Fli1 expression is inhibited by AG490, an inhibitor of JAK2 activity.** After 6 days of Hcys treatment, inhibition of JAK2 by AG490 (*AG*) (30 μM) abrogated the effect of Hcys (3.6 mM) on up-regulation of *Fli1* on the mRNA (*a*) as well as on the protein level (*b* and *c*). To analyze *Fli1* mRNA expression, RNA was isolated and analyzed by qRT-PCR. Gene expression was normalized to 18 S rRNA. 30 μg of protein of each sample were fractionated by SDS-gel electrophoresis and immunoblotted. Values are represented as mean ± S.D.; untreated control (*Co*) is set to 1, and treated probes are referred as fold change to control. *, $p \leq 0.05$; +, $p \leq 0.05$ refers to significance to Hcys-treated probes; for all graphs $n = 3$. One representative immunoblot is shown. *Lane M* refers to protein molecular weight standards.

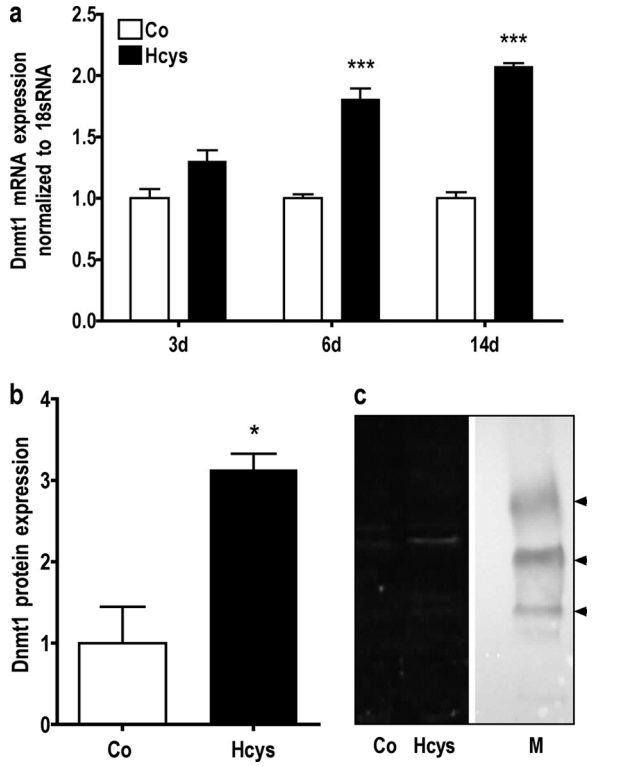

FIGURE 7. **mRNA expression of *Dnmt1*, a gene involved in DNA methylation, is enhanced by Hcys in MC3T3-E1 cells.** As demonstrated in *a*, when compared with untreated control (*Co*), mRNA expression of the DNA methylation-related gene *Dnmt1* was significantly enhanced by 3.6 mM Hcys after 6 and 14 days (*d*) of treatment. Hcys-dependent up-regulation of DNMT1 was confirmed at the protein level after 6 days of treatment (*b* and *c*). To analyze mRNA expressions, RNA was isolated and analyzed by qRT-PCR. Gene expression was normalized to 18 S rRNA. 30 μg of protein of each sample were fractionated by SDS-gel electrophoresis and immunoblotted. Values are represented as mean ± S.D.; untreated control (*Co*) is set to 1, and treated probes are referred as fold change to control. *, $p \leq 0.05$; ***, $p \leq 0.001$; for all graphs $n = 3$. One representative immunoblot is shown. *Lane M* refers to protein molecular weight standards.

Hcys-mediated Up-regulation of Dnmt1 Is IL-6- and FLI1-dependent—To demonstrate that IL-6 is involved in Hcys-dependent up-regulation of *Dnmt1*, as for *Fli1*, we co-treated MC3T3-E1 cells with Hcys and IL-6 antibody. As shown in Fig. 10*a*, Hcys up-regulation of *Dnmt1* was abrogated by co-treatment of the cells with an IL-6 antibody. This demonstrates that the increase of *Dnmt1* expression by Hcys is IL-6-dependent.

Results of our experiments shown in Fig. 3*c* and at 3 days suggest the involvement of a transcription factor belonging to the E-twenty six (ETS) transcription factor family because deletion or mutation of the GGAA sites in the *Dnmt1* promoter abrogated IL-6-dependent promoter activation. After 6 days of Hcys treatment, chromatin immunoprecipitation with an antibody against FLI1 transcription factor was used to demonstrate the interaction of this transcription factor with the *Dnmt1* promoter *in vivo*.

Fig. 10*b* clearly shows that FLI1 bound to the *Dnmt1* promoter sequence exhibiting three GGAA sites. This demonstrates FLI1 occupancy on the *Dnmt1* proximal promoter in MC3T3-E1 cells. Moreover, Hcys treatment of MC3T3-E1 cells increased FLI1 binding to this *Dnmt1* promoter area by 1.97-fold ($p \leq 0.05$) proving involvement of FLI1 in Hcys-mediated Dnmt1 up-regulation. These results demonstrate that in Hcys-dependent stimulation of *Dnmt1* expression in mouse pre-osteoblasts, IL-6 as well as the transcription factor FLI1 play a main role.

Hcys Suppressed Lox Expression by CpG Methylation—As we have already shown before, Hcys suppresses the mRNA expression of *Lox* (9). Fig. 11*a* demonstrates that *Lox* mRNA expression was not affected after 3 days of Hcys treatment but was significantly decreased after 6 days (1.82-fold, $p \leq 0.05$) and after 14 days (1.71-fold, $p \leq 0.05$) at 3.6 mM Hcys. Analysis of the *Lox* promoter showed a CpG-rich region ranging from the proximal *Lox* promoter into the first exon (Fig. 1*b*), which was used to study CpG methylation. As shown in Fig. 11*b*, inversely to *Lox* mRNA expression, *Lox* promoter methylation of the investigated region was significantly increased

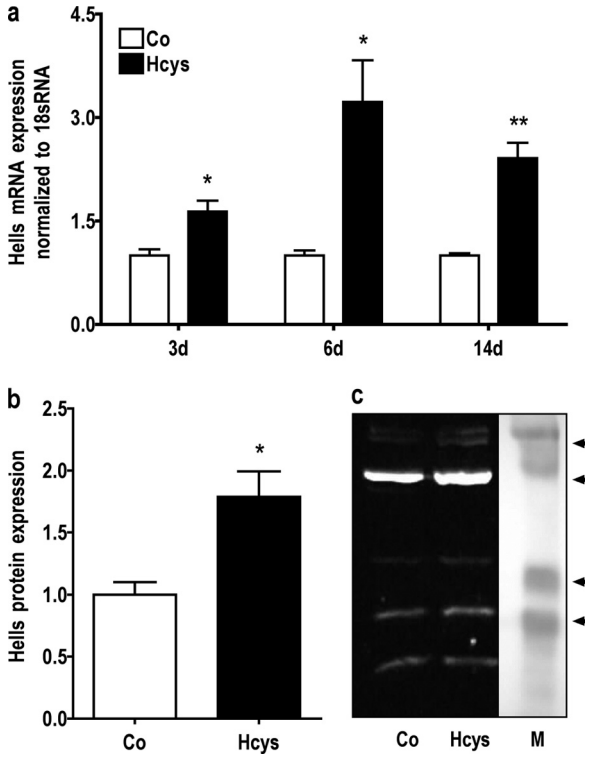

FIGURE 8. **mRNA expression of *Hells*, a co-regulator of DNA methylation, is enhanced by Hcys in MC3T3-E1 cells.** As demonstrated in *a*, when compared with untreated control (*Co*), mRNA expression of the DNA methylation-related gene *Hells* was significantly enhanced at all times measured. Hcys-dependent up-regulation of HELLS was confirmed at the protein level after 6 days (*d*) of treatment (*b* and *c*). To analyze mRNA expressions, RNA was isolated and analyzed by qRT-PCR. Gene expression was normalized to 18 S rRNA. 30 μg of protein of each sample were fractionated by SDS-gel electrophoresis and immunoblotted. Values are represented as mean ± S.D.; untreated control (*Co*) is set to 1, and treated probes are referred as fold change to control. *, $p \leq 0.05$; **, $p \leq 0.01$; for all graphs $n = 3$. One representative immunoblot is shown. *Lane M* refers to protein molecular weight standards.

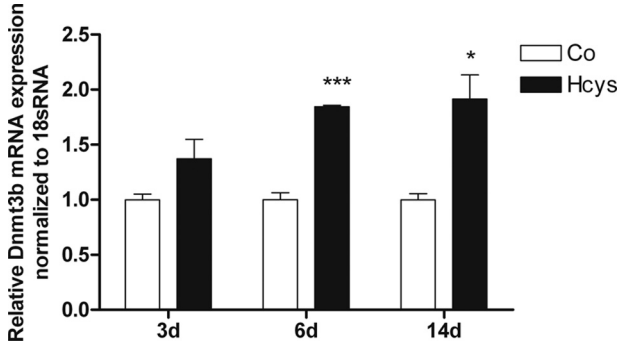

FIGURE 9. **mRNA expression of *Dnmt3b*, a gene involved in DNA methylation, is enhanced by Hcys in MC3T3-E1 cells.** As demonstrated, when compared with untreated control (*Co*), mRNA expression of the DNA methylation-related gene *Dnmt3b* was significantly enhanced by 3.6 mM Hcys after 6 and 14 days (*d*) of treatment. To analyze mRNA expressions, RNA was isolated and analyzed by qRT-PCR. Gene expression was normalized to 18 S rRNA. Values are represented as mean ± S.D.; untreated control is set to 1, and treated probes are referred as fold change to control. *, $p \leq 0.05$; ***, $p \leq 0.001$; $n = 3$.

after 6 days (1.8-fold, $p \leq 0.05$) and after 14 days (2.1-fold, $p \leq 0.05$) of treatment with Hcys; although the difference in Hcys-mediated CpG methylation between 6 and 14 days was not significantly different.

To prove the role of DNA methylation in Hcys-dependent down-regulation of *Lox* expression, MC3T3-E1 cells were cultured for 6 days with or without 3.6 mM Hcys in the presence or absence of 50 μM zebularine, an inhibitor of DNA CpG methylation. As shown in Fig. 11*c*, Hcys again attenuated expression of *Lox* mRNA expression significantly. Zebularine when added to the Hcys-treated cells significantly increased *Lox* expression, even above the expression level of untreated cells, thus indicating a prevalent basal CpG methylation.

To test whether the IL-6-JAK2-FLI1 pathway was a prerequisite for *Lox* suppression, MC3T3-E1 cells were treated for 6 days with or without Hcys and for the last 3 culture days in the absence or presence of the JAK2 inhibitor AG490. As shown in Fig. 12*a*, Hcys down-regulated the mRNA expression of *Lox*, whereas AG490, having no effect on basal expression, abolished the Hcys-dependent repression of *Lox*. Very similar effects were observed on the protein level by immunoblot analysis (Fig. 12, *b* and *c*). At the protein level, again, Hcys down-regulated LOX protein expression, whereas AG490 treatment induced *Lox* expressions when compared with control; however, only the difference between Hcys and Hcys + AG490 was statistically significant.

DISCUSSION

Genome-wide mRNA expression analysis of Hcys-treated MC3T3-E1 cells revealed a strong up-regulation of IL-6 and of several genes involved in IL-6/JAK2-dependent signal transduction pathways. The up-regulation of IL-6 by Hcys was confirmed at the protein level by measurements with an ELISA. The IL-6 concentrations were in the range expected to permit the stimulation of *Fli1* and *Dnmt1* via JAK2.

The stimulation of IL-6 expression by Hcys in the pre-osteoblastic MC3T3-E1 cell line *per se* was an unexpected finding of these experiments; it suggests that Hcys affects via IL-6 both osteoblasts, the bone-forming cells, and osteoclasts, the bone-resorbing cells (24).

The published reports concerning the effects of IL-6 on bone cells are conflicting (24–26). IL-6-deficient mice have no obvious bone phenotype, but they are protected from bone loss caused by estrogen depletion (27). In bone marrow cultures from ovariectomized mice, the increased osteoclast formation could be prevented by 17β-estradiol or by a neutralizing IL-6-antibody (28, 29). It was also reported that IL-6 stimulates RANKL expression in osteoblasts (30), which induces osteoclastogenesis. On the other hand, it was shown that IL-6 inhibits RANKL-induced osteoclast formation and bone resorption (31). These contradictory effects of IL-6 might be attributed to the ambivalent character of this cytokine. IL-6 activates via *Jak1/2* several intracellular pathways. Activation of STAT protein pathways induces expression of genes implicated in growth inhibition, apoptosis, and differentiation, whereas activation of MAPK, protein-kinase B (*Akt*), or PKCδ counterbalances these signals (24, 26). As we have shown previously, Hcys weakly down-regulates cell multiplication, triggers cell differentiation (9), and favors the expression of the pro-apoptotic gene *Fas* (data not shown). The

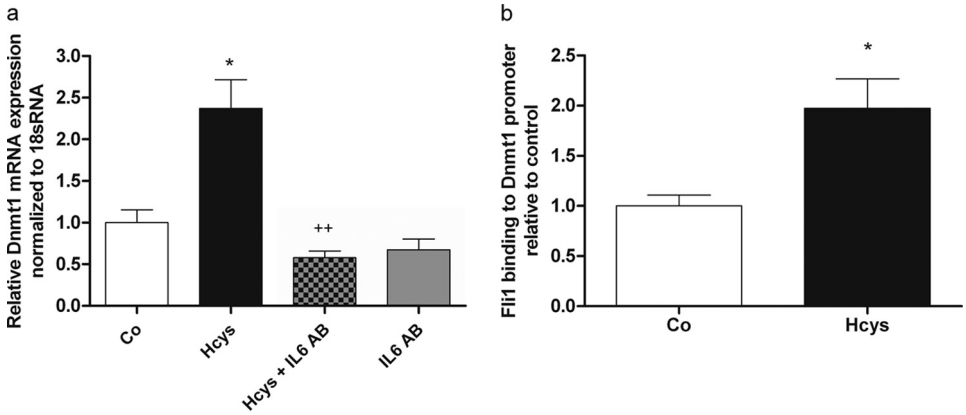

FIGURE 10. **Hcys-mediated up-regulation of *Dnmt1* is IL-6- and *Fli1*-dependent.** After 1 week of Hcys treatment, IL-6 Ab significantly abrogated the effect of Hcys on *Dnmt1* expression while leaving *Dnmt1* mRNA expression in Hcys-untreated cells unaffected (*a*). Involvement of FLI1 transcription factor in Hcys-driven *Dnmt1* up-regulation was shown by chromatin immunoprecipitation analysis (ChIP) (*b*). After 1 week, Hcys-treated cells showed a significant increase of FLI1 binding affinity to the selected *Dnmt1* promoter sequence. mRNA expressions as well as ChIP-DNA were analyzed by qRT-PCR. Gene expression was normalized to 18 S rRNA. For ChIP quantitation, DNA signals of the FLI1-precipitated chromatin were normalized to the unprecipitated chromatin fraction (1% of the total chromatin). Values are represented as mean ± S.D.; untreated control (*Co*) is set to 1, and treated probes are referred as fold change to control. *, $p \leq 0.05$; ++, $p \leq 0.01$ refers to significance to Hcys-treated probes; for all graphs $n = 3$.

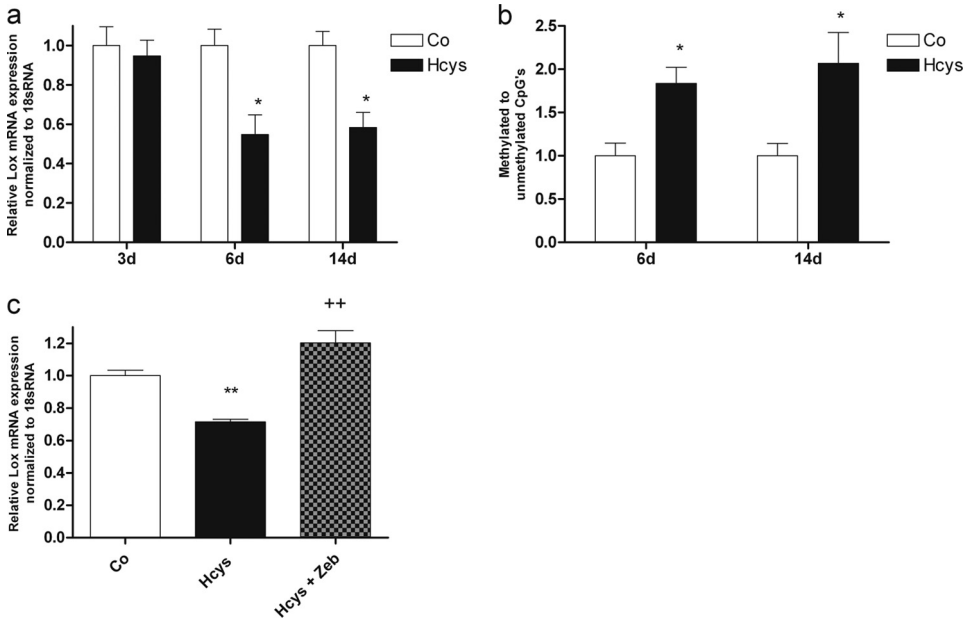

FIGURE 11. **Hcys affects *Lox* mRNA expression by promoter methylation in pre-osteoblastic MC3T3-E1 cells.** After 6 and 14 days of treatment with 3.6 mM Hcys in the culture medium, a significant ($p \leq 0.05$) decrease of *Lox* mRNA expression was observed when compared with control (*Co*) (*a*). To the contrary, CpG methylation of *Lox* promoter and the first untranslated exon was significantly ($p \leq 0.05$) increased after 6 and 14 days of treatment with 3.6 mM Hcys (*b*). Addition of the CpG methylation inhibitor zebularine (50 μM) to Hcys-treated MC3T3-E1 cells (3.6 mM) abrogated the repressive effect of Hcys on *Lox* mRNA expression (*c*). To analyze mRNA expression of *Lox* (*a* and *c*), RNA was isolated and analyzed by qRT-PCR. Gene expression was normalized to 18 S rRNA. For promoter methylation (*b*), DNA was isolated, and the ratio of methylated to unmethylated CpGs was analyzed by MECP2 binding. Values are represented as mean ± S.D.; untreated controls (*Co*) are set to 1, and treated probes are referred as fold change to controls for *, $p \leq 0.05$; **, $p \leq 0.01$; ++, $p \leq 0.01$ refers to significance to Hcys-treated probes. For all graphs $n = 3$.

stimulation of *Fli1* expression by IL-6, as described in this work, was shown to be STAT3-dependent but MAPK-independent in erythroleukemia cells (23), suggesting that Hcys-dependent up-regulation of *Fli1* and *Dnmt1* in MC3T3-E1 cells depends on the STAT pathway.

Analysis of the mouse *Dnmt1* promoter revealed three putative binding sites for FLI1 with identical sequence and a structure comparable with the human promoter (19). Truncation of the promoter as well as mutation of the putative FLI1-binding sites demonstrated that all three binding sites were necessary for full expression. As already mentioned, IL-6 activates several intracellular signaling pathways, which can stimulate transcription of *DNMT1*. In colon cancer cells, IL-6 was also shown to mediate gene silencing via epigenetic DNA methylation by *DNMT1* involving STAT signaling (32). In malignant T-lymphocytes, *DNMT1* was stimulated by STAT3, which binds to the promoter of *DNMT1* (33). Similarly to human erythroleukemia cells (19), in MC3T3-E1 cells we clearly show that IL-6 stimulates *Dnmt1* via FLI1. Nevertheless, we cannot fully exclude STAT3-binding sites upstream of the used *Dnmt1* promoter fragment, which may regulate *Dnmt1* directly. All those data support our finding of an IL-6-induced expression of *Dnmt1* by Hcys, which in turn mediates *Lox* down-regulation (Fig. 13).

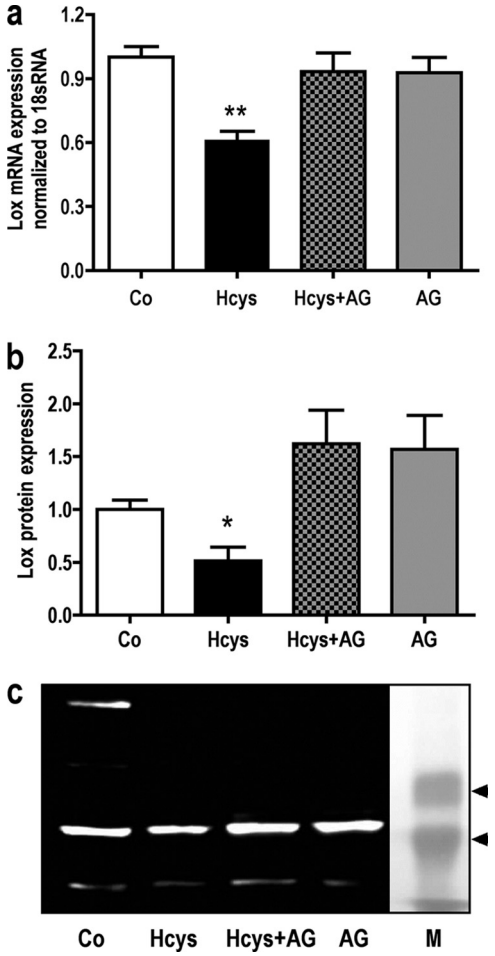

FIGURE 12. **Hcys-attenuated *Lox* mRNA expression is abrogated by the JAK2 inhibitor AG490.** Co-treatment of MC3T3-E1 cells with Hcys (3.6 mM) and the JAK2 inhibitor AG490 (*AG*) (30 μM) erased the suppressive effect of Hcys (3.6 mM) on *Lox* mRNA expression. Treatment of AG490 alone did not influence Lox mRNA expression in the pre-osteoblasts (*a*). A similar effect was observed when protein expression was analyzed (*b* and *c*). RNA was isolated and analyzed by qRT-PCR. Gene expression was normalized to 18 S rRNA. 30 μg of protein of each sample were fractionated by SDS-gel electrophoresis and immunoblotted. Values are represented as mean $\pm$ S.D., untreated controls (*Co*) are set to 1, and treated probes are referred to as fold change to controls for *, $p \leq 0.05$; **, $p \leq 0.01$; +, $p \leq 0.05$; ++, $p \leq 0.01$ refers to significance to Hcys-treated probes. For all graphs $n = 3$. One representative immunoblot is shown. *Lane M* refers to protein molecular weight standards.

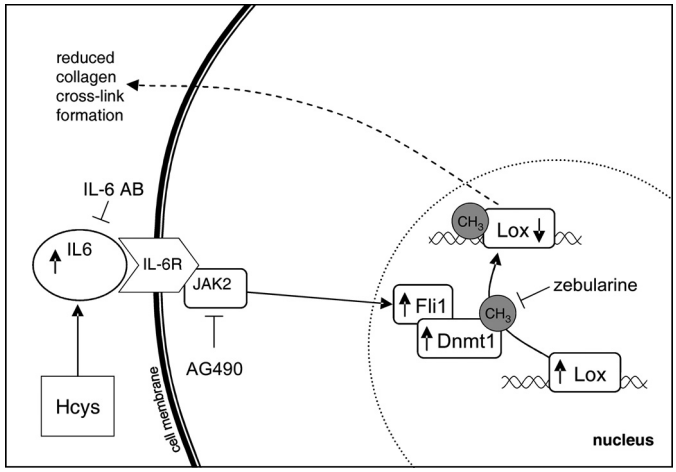

FIGURE 13. **Schematic representation of the suggested pathway for the down-regulation of *Lox* by Hcys.** Hcys stimulates IL-6 expression, which in turn activates JAK2 kinase (IL-6 as well as JAK2 kinase can be blocked by an IL-6 Ab as well as by the inhibitor AG490, respectively), leading to an up-regulation of the *Dnmt1* transcription factor Fli1. This increases *Dnmt1* expression, which provokes promoter methylation of Lox and thus its transcriptional depletion (co-treatment of the cells with the DNA (cytosine-5)-methyltransferase (*Dnmt*) inhibitor zebularine abrogates Hcys *Lox* promoter methylation). Consequently, the post-translational collagen cross-link formation is reduced. Abbreviations used are as follows: *Hcys*, homocysteine; *IL-6*, interleukin 6; *IL-6 Ab*, interleukin 6 antibody; *IL-6R*, interleukin 6 receptor; *Fli1*, Friend leukemia virus integration 1; *Dnmt1*, DNA methyltransferase 1; *Lox*, lysyl oxidase; *CH3*, methyl group.

Epigenetic DNA methylation controls important cellular events like apoptosis (17, 34) or cell differentiation (35). The influence of Hcys on epigenetic CpG methylation is mainly discussed in light of the role of Hcys as metabolite in the DNA methylation cycle (16). As presented in this study, in pre-osteoblastic MC3T3-E1 cells Hcys increases the expression of genes involved in DNA methylation, namely *Dnmt1*, *Dnmt3b*, and *Hells*, but no regulation was found for the gene *Dnmt3a*. *Hells* was suggested to play an important role in bone cells as *Hells*-depleted mice develop osteopenia and osteoporosis (36). These are interesting aspects as *Hells* was shown to play a crucial role for a proper CpG methylation by recruiting *Dnmt1* and *Dnmt3b* to promoters (37).

According to the literature, *Dnmt1* is mainly related to maintenance of DNA global methylation, whereas *Dnmt3a* and *Dnmt3b* are described as *de novo* DNA methyltransferases (38). However, it was shown that for efficient CpG island methylation of the gene *HOXB13*, a transcription factor indispensable for vertebrate embryonic development, cooperation of *DNMT1* with *DNMT3b* is essential (39). As we have shown here, inhibition of JAK2 eliminates Hcys-dependent *Fli1* and thus *Dnmt1* stimulation and abolishes Hcys-mediated *Lox* down-regulation. These results underline the necessity of both JAK2 and *Dnmt1* for Hcys-dependent *Lox* methylation. Therefore, we hypothesize that besides the role of *Dnmt1* as keeper of global DNA methylation, under certain circumstances specific DNA methylation involves *Dnmt1*.

As already mentioned, Hcys inhibits LOX (7) enzymatic activity similarly to lathyrogens like β-aminopropionitrile and affects bone quality because of disturbed cross-linking (14). As shown previously (9, 10) and as demonstrated here, the effect of Hcys on collagen cross-link formation does not exclusively rely on Hcys enzymatic inhibition of LOX. Besides its function in collagen cross-linking, the N-terminal peptide of Lox acts as a tumor suppressor. In tumors, *Lox* expression is prevented by CpG methylation of the promoter as shown in humans (40–42) and mice (34). Treatment of MC3T3-E1 cells with zebularine, an inhibitor of DNA methyltransferases, prevented attenuation of *Lox* by Hcys. Methylation analysis of the Lox promoter revealed that treatment of MC3T3-E1 cells with Hcys increased promoter methylation of a CpG-rich region around the transcription start, which represents a common epigenetic mechanism involved in silencing of gene expression (17, 34).

In conclusion, we demonstrate that Hcys stimulates IL-6 synthesis, which could modulate osteoclast development and differentiation via a general inflammatory response or by direct activation resulting in increased bone resorption.

Moreover, Hcys inhibits proper collagen cross-linking biochemically by inhibiting LOX enzymatic activity, and as demonstrated here, it attenuates *Lox* expression epigenetically via IL-6, JAK2, *Fli*, and *Dnmt1* leading to decreased bone matrix quality (14). All these findings, including accelerated differentiation of osteoblasts by Hcys (9, 10), could explain high bone turnover in some patients with elevated Hcys serum levels (43). This also has significant implications for other cells and tissues. Silencing of *Lox* in skin and blood vessels, for example, could reduce tissue strength. Finally, this gene acts as a tumor suppressor in several tissues. Our findings add new mechanistic insights to the role of Hcys as a risk factor for bone health.

REFERENCES

1. Iannucci, C. V., Capoccia, D., Calabria, M., and Leonetti, F. (2007) *Curr. Pharm. Des.* **13,** 2148–2168
2. Audelin, M. C., and Genest, J., Jr. (2001) *Atherosclerosis* **159,** 497–511
3. Raisz, L. G. (2004) *N. Engl. J. Med.* **350,** 2089–2090
4. McLean, R. R., Jacques, P. F., Selhub, J., Tucker, K. L., Samelson, E. J., Broe, K. E., Hannan, M. T., Cupples, L. A., and Kiel, D. P. (2004) *N. Engl. J. Med.* **350,** 2042–2049
5. van Meurs, J. B., Dhonukshe-Rutten, R. A., Pluijm, S. M., van der Klift, M., de Jonge, R., Lindemans, J., de Groot, L. C., Hofman, A., Witteman, J. C., van Leeuwen, J. P., Breteler, M. M., Lips, P., Pols, H. A., and Uitterlinden, A. G. (2004) *N. Engl. J. Med.* **350,** 2033–2041
6. Gjesdal, C. G., Vollset, S. E., Ueland, P. M., Refsum, H., Meyer, H. E., and Tell, G. S. (2007) *J. Bone Miner. Res.* **22,** 747–756
7. Liu, G., Nellaiappan, K., and Kagan, H. M. (1997) *J. Biol. Chem.* **272,** 32370–32377
8. Raposo, B., Rodríguez, C., Martínez-González, J., and Badimon, L. (2004) *Atherosclerosis* **177,** 1–8
9. Thaler, R., Spitzer, S., Rumpler, M., Fratzl-Zelman, N., Klaushofer, K., Paschalis, E. P., and Varga, F. (2010) *Bone* **46,** 703–709
10. Turecek, C., Fratzl-Zelman, N., Rumpler, M., Buchinger, B., Spitzer, S., Zoehrer, R., Durchschlag, E., Klaushofer, K., Paschalis, E. P., and Varga, F. (2008) *Calcif. Tissue Int.* **82,** 392–400
11. Claes, L., Schmalenbach, J., Herrmann, M., Olkü, I., Garcia, P., Histing, T., Obeid, R., Schorr, H., Herrmann, W., Pohlemann, T., Menger, M. D., and Holstein, J. H. (2009) *Calcif. Tissue Int.* **85,** 17–21
12. Leboff, M. S., Narweker, R., LaCroix, A., Wu, L., Jackson, R., Lee, J., Bauer, D. C., Cauley, J., Kooperberg, C., Lewis, C., Thomas, A. M., and Cummings, S. (2009) *J. Clin. Endocrinol. Metab.* **94,** 1207–1213
13. Zhu, K., Beilby, J., Dick, I. M., Devine, A., Soós, M., and Prince, R. L. (2009) *Osteoporos Int.* **20,** 1183–1191
14. Blouin, S., Thaler, H. W., Korninger, C., Schmid, R., Hofstaetter, J. G., Zoehrer, R., Phipps, R., Klaushofer, K., Roschger, P., and Paschalis, E. P. (2009) *Bone* **44,** 959–964
15. Esteller, M., and Herman, J. G. (2002) *J. Pathol.* **196,** 1–7
16. Yi, P., Melnyk, S., Pogribna, M., Pogribny, I. P., Hine, R. J., and James, S. J. (2000) *J. Biol. Chem.* **275,** 29318–29323
17. Thaler, R., Karlic, H., Spitzer, S., Klaushofer, K., and Varga, F. (2010) *Apoptosis* **15,** 728–737
18. Pfaffl, M. W. (2001) *Nucleic Acids Res.* **29,** e45
19. Hodge, D. R., Xiao, W., Clausen, P. A., Heidecker, G., Szyf, M., and Farrar, W. L. (2001) *J. Biol. Chem.* **276,** 39508–39511
20. Kishikawa, S., Murata, T., Kimura, H., Shiota, K., and Yokoyama, K. K. (2002) *Eur. J. Biochem.* **269,** 2961–2970
21. Kanehisa, M., Araki, M., Goto, S., Hattori, M., Hirakawa, M., Itoh, M., Katayama, T., Kawashima, S., Okuda, S., Tokimatsu, T., and Yamanishi, Y. (2008) *Nucleic Acids Res.* **36,** D480–D484
22. Kanehisa, M., and Goto, S. (2000) *Nucleic Acids Res.* **28,** 27–30
23. Hodge, D. R., Li, D., Qi, S. M., and Farrar, W. L. (2002) *Biochem. Biophys. Res. Commun.* **292,** 287–291
24. Blanchard, F., Duplomb, L., Baud'huin, M., and Brounais, B. (2009) *Cytokine Growth Factor Rev.* **20,** 19–28
25. Wong, P. K., Campbell, I. K., Egan, P. J., Ernst, M., and Wicks, I. P. (2003) *Arthritis Rheum.* **48,** 1177–1189
26. Franchimont, N., Wertz, S., and Malaise, M. (2005) *Bone* **37,** 601–606
27. Poli, V., Balena, R., Fattori, E., Markatos, A., Yamamoto, M., Tanaka, H., Ciliberto, G., Rodan, G. A., and Costantini, F. (1994) *EMBO J.* **13,** 1189–1196
28. Jilka, R. L., Hangoc, G., Girasole, G., Passeri, G., Williams, D. C., Abrams, J. S., Boyce, B., Broxmeyer, H., and Manolagas, S. C. (1992) *Science* **257,** 88–91
29. Schiller, C., Gruber, R., Redlich, K., Ho, G. M., Katzgraber, F., Willheim, M., Pietschmann, P., and Peterlik, M. (1997) *Endocrinology* **138,** 4567–4571
30. Karmakar, S., Kay, J., and Gravallese, E. M. (2010) *Rheum. Dis. Clin. North Am.* **36,** 385–404
31. Duplomb, L., Baud'huin, M., Charrier, C., Berreur, M., Trichet, V., Blanchard, F., and Heymann, D. (2008) *Endocrinology* **149,** 3688–3697
32. Foran, E., Garrity-Park, M. M., Mureau, C., Newell, J., Smyrk, T. C., Limburg, P. J., and Egan, L. J. (2010) *Mol. Cancer Res.* **8,** 471–481
33. Zhang, Q., Wang, H. Y., Woetmann, A., Raghunath, P. N., Odum, N., and Wasik, M. A. (2006) *Blood* **108,** 1058–1064
34. Gazin, C., Wajapeyee, N., Gobeil, S., Virbasius, C. M., and Green, M. R. (2007) *Nature* **449,** 1073–1077
35. Dean, W., Santos, F., and Reik, W. (2003) *Semin. Cell Dev. Biol.* **14,** 93–100
36. Sun, L. Q., Lee, D. W., Zhang, Q., Xiao, W., Raabe, E. H., Meeker, A., Miao, D., Huso, D. L., and Arceci, R. J. (2004) *Genes Dev.* **18,** 1035–1046
37. Myant, K., and Stancheva, I. (2008) *Mol. Cell. Biol.* **28,** 215–226
38. Bestor, T. H. (2000) *Hum. Mol. Genet.* **9,** 2395–2402
39. Ghoshal, K., Motiwala, T., Claus, R., Yan, P., Kutay, H., Datta, J., Majumder, S., Bai, S., Majumder, A., Huang, T., Plass, C., and Jacob, S. T. (2010) *PLoS One* **5,** e10338
40. Kaneda, A., Wakazono, K., Tsukamoto, T., Watanabe, N., Yagi, Y., Tatematsu, M., Kaminishi, M., Sugimura, T., and Ushijima, T. (2004) *Cancer Res.* **64,** 6410–6415
41. So, K., Tamura, G., Honda, T., Homma, N., Waki, T., Togawa, N., Nishizuka, S., and Motoyama, T. (2006) *Cancer Sci.* **97,** 1155–1158
42. Tamura, G., So, K., Miyoshi, H., Honda, T., Nishizuka, S., and Motoyama, T. (2009) *Pathol. Int.* **59,** 895–899
43. Gerdhem, P., Ivaska, K. K., Isaksson, A., Pettersson, K., Väänänen, H. K., Obrant, K. J., and Akesson, K. (2007) *J. Bone Miner. Res.* **22,** 127–134

Apoptosis
DOI 10.1007/s10495-010-0462-3

ORIGINAL PAPER

Extra-celluar matrix suppresses expression of the apoptosis mediator Fas by epigenetic DNA methylation

Roman Thaler · Heidrun Karlic · Silvia Spitzer · Klaus Klaushofer · Franz Varga

Abstract The extracellular matrix (ECM) of bone consists mainly of collagen type I, which induces osteoblastic differentiation and prevents apoptosis. Fas induces apoptosis in cells improperly adhering to ECM. Recently, it was described that Fas expression is modulated by epigenetic DNA methylation. Mouse MC3T3-E1 pre-osteoblastic cells were cultured either on collagen coated or on uncoated culture dishes for control. mRNA was isolated and gene expression was analyzed by quantitative RT–PCR. Furthermore, we measured global and specific DNA methylation. Compared to controls, cells cultured on collagen-coated dishes increased the expression of Runx2 and OCN indicating differentiation of pre-osteoblastic cells. Additionally, collagen up-regulated cyclin-A2 and down-regulated Fas expression suggesting increased cell multiplication. Furthermore, the expression of Dnmt1 and Hells, key mediators of the DNA-methylation process, was increased. As a consequence, we demonstrate that global DNA methylation and specific methylation of the Fas promoter was higher in MC3T3-E1 cells cultured on collagen when compared to controls. Investigation of signal transduction pathways by mean of inhibitors suggests that focal adhesion kinase, MAP- and Jun-kinases and AP-1 are involved in this process. In summary, we demonstrate that ECM prevents activation of Fas by epigenetic DNA-methylation.

Keywords Fas expression · Extracellular matrix · DNA methylation · Osteoblasts · Differentiation

R. Thaler · S. Spitzer · K. Klaushofer · F. Varga (✉)
Ludwig Boltzmann Institute of Osteology at the Hanusch Hospital of WGKK and AUVA Trauma Center Meidling, 4th Medical Department, Hanusch Hospital, Heinrich Collin-Str. 30, 1140 Vienna, Austria
e-mail: franz.varga@osteologie.at

H. Karlic
Ludwig Boltzmann Institute for Leukemia Research and Hematology, Hanusch Hospital, and Ludwig Boltzmann Cluster Oncology, Vienna, Austria

Introduction

Bone development and homeostasis are regulated by signals that balance continuous differentiation of bone matrix-producing cells against apoptosis and matrix removal [1]. It is well known that cell adhesion to extracellular matrix (ECM) mediates structural anchorage and primary survival signals to the cell. Osteoblasts, the bone forming cells synthesize and deposit their own ECM, which promotes differentiation by enhancing the expression of cell type specific genes [2, 3]. Integrins, which represent cellular ECM anchorage proteins, in coordination with growth- and differentiation factors, induce signal transduction cascades important in the determination of cell proliferation, differentiation and apoptosis [4, 5]. Cells interaction with an adequate ECM prevents from anoikis (homelessness), a specific form of apoptosis [6]. Among many described pathways, Fas mediated apoptosis signaling pathway was demonstrated to play a considerable role in this process [7].

In K-ras transformed NIH-3T3 mouse fibroblasts, apoptosis is inhibited by epigenetic silencing of Fas mRNA expression through DNA methyltransferase 1 (Dnmt1). This methylation process implies 28 genes (including MAPK1) and knockdown of any of these genes results in failure to recruit Dnmt1 to Fas promoter preventing so CpG methylation and allowing Fas expression [8].

In mammals, Dnmt's mediated epigenetic DNA methylation is characterized by deoxycytidine methylation at

Published online: 29 April 2010

position 5′ of the base, whereas neighboring deoxyguanosines are essential resulting in specific methylation at CG sites (CpG). Additionally, Hells (PASG, LSH), a protein involved in chromatin remodeling, was recently shown to associate with Dnmt1 enhancing DNA methylation [9]. DNA methylation dependent changes of chromatin status lead to modulation of gene expressions and chromatin stability determining differentiation, pathogenesis and senescence of a cell. In somatic cells, Dnmt1 expression is regulated in a cell cycle dependent manner by the transcription factors Sp1 and Sp3 [10]. Furthermore, a regulation of the gene by the Ras-AP1 signaling pathway was reported for the mouse P19 teratocarcinoma cell line [11, 12].

MC3T3-E1 cells represent a pre-osteoblastic cell line, which differentiates from a pre-osteoblastic phenotype into mature osteoblasts. During the differentiation process expression of osteocalcin (OCN) and its regulator Runx2, two well-known markers of osteoblastic differentiation, increase. Those features make this cell line an excellent model system to study osteoblastic growth, differentiation and apoptosis [2, 13] [14, 15].

In this study we investigated the consequences of osteoblastic adherence on collagen type I, the major organic component of bone ECM, on mRNA expression of the pro apoptotic gene Fas, the proliferation associated gene cyclin A2 and the differentiation related genes Runx2 and OCN. Furthermore, we investigated by which mechanism collagen regulates Fas expression. Our results demonstrate that collagen type I repress Fas expression by promoter CpG methylation showing that epigenetic mechanisms are involved in ECM mediated signaling in osteoblasts.

Experimental procedures

Cell culture and collagen coating

MC3T3-E1 cells, a clonal preosteoblastic cell line derived from newborn mouse calvaria (kindly donated by Dr. Kumegawa, Meikai University, Department of Oral Anatomy, Sakado, Japan), were cultured in humidified air under 5% CO_2 at 37°C in alpha-minimum essential medium (α-MEM; Biochrom, Berlin, Germany) supplemented with 5% fetal calf serum (Biochrom), 50 µg/ml ascorbic acid (Sigma), and 10 µg/ml gentamycin (Sigma). For propagation, cells were sub-cultured twice a week using 0.001% pronase E (Roche) and 0.02% EDTA in Ca^{2+}- and Mg^{2+}- free phosphate-buffered saline (PBS) before achieving confluence. To prevent a potential phenotypic drift during repeated sub-cultures the cells were not used more than 4 weeks after thawing.

For experiments the cells were seeded in culture dishes coated with or without rat-tail collagen at a density of 2,000/cm^2 and cultured for the indicated time with medium changes twice a week. For collagen coating, cell culture dishes were coated at a concentration of 5 µg/cm^2 as suggested by the supplier (BD Biosciences). Cells cultured on collagen-coated dishes were confluent after 4–5 days while control cells needed 6–7 days of culture for confluence. However, seeding at 2,000 compared to 20,000 cells/cm^2 did not influence Dnmt1 expression significantly (R. Thaler, unpublished observations).

Treatment with inhibitors of signal transduction was performed with the focal adhesion kinase inhibitor (FAK) genistein [16] (10 µM, Sigma), the selective MAP-/ER-kinase inhibitor PD98059 [17] (10 µM, Promega) and the AP1 inhibitor resveratrol [18] (40 µM, Sigma). In these experiments, inhibitors were added to the cells 30 min before seeding. Genistein and PD98059 were solved in DMSO as 1,000-fold stock-solution to prevent influence on gene expression (Thaler, R et al. in preparation) and resveratrol was dissolved in ethanol.

Isolation of nucleic acids and expression analysis by QRT-PCR

DNA and RNA were extracted using a DNA/RNA Isolation Kit (Qiagen). cDNA was synthesized from about 0.5 µg RNA using the 1st Strand cDNA Synthesis Kit as described by the supplier (Roche). The obtained cDNA was subjected to PCR amplification with a real-time cycler using FastStart SYBR Master Mix (Roche) for the genes Dnmt1, Hells, c-Fos, c-Jun, Fas and Cycline A2. SYBR-Green PCR was started with 10 min of an initial denaturation step at 95°C and then continued with 45 cycles consisting of 30 s denaturation at 95°C, 30 s annealing at primer specific temperatures and extension at 72°C. For amplification of Runx2 and OCN (Bglap2) we used TaqMan gene expression probes (Mm00501578_m1 and X04142-EX2, respectively, Applied Biosystems) and for normalization we used the 18S RNA TaqMan probe (4319413E, Applied Biosystems). All reactions were performend in TaqMan Gene Expression Master Mix (Applied Biosystems) with an initial denaturation at 95°C for 10 min followed by 45 cycles alternating 60°C for 30 s and 95°C for 10 s. All PCRs were performed in triplicate. Expression was evaluated using the comparative quantization method [19].

Global methylation

MC3T3-E1 cells seeded at a density of 2,000/cm^2 and cultured for 4 days on collagen type I coated dishes or uncoated control dishes, were washed twice with PBS,

detached with 0.02% Pronase in PBS and then collected by centrifugation (1,400 rpm). Thereafter, DNA and RNA were isolated from about 5×10^5 cells with a DNA/RNA isolation Kit (Quiagen). Global methylation was addressed [20] from 100 ng DNA digested in multi core buffer (Promega) with 5 U MspI or HpaII or incubated without enzyme (background) for 3 h at 37°C in a total volume of 30 µl. The restriction of the DNA was followed by an end-fill reaction where to the restriction digest 20 µl of a mixture containing 0.1 µM Biotin-11-dCTP and 0.1 µM Biotin-11-dGTP (Perkin Elmer, Boston, MA) and 0.5 U Klenow-fragment of DNA-polymerase III (Promega) in 500 mM Tris–HCl, pH 7.2, 100 mM $MgSO_4$ and 1 mM dithiothreitol have been added and incubated at room temperature for half an hour. Thereafter, the reaction was transferred into multi-well plates (Optiplate, Beckman) and 100 µl of Reacti-Bind™ DNA Coating Solution (Pierce, Rockford, IL) was added to each well and incubated over night at room temperature. On the next day, the wells were washed once with TBS (10 mM Tris–HCl pH 8.0, 150 mM NaCl). After a blocking step with 1% blocking solution (Roche) in TBS for 1 h, a solution of 50 ng/µl streptavidin-horse radish peroxidase conjugate (Promega) in TBS was added and incubated for one further hour at room temperature. Thereafter, the wells were washed three times with TBS containing 0.5% Tween 20 and two times with water. 100 µl of the chemo-luminescence substrate was added to each well and the light emission was measured in a top-counter (Packard Instruments).

Specific promoter methylation

To analyze Fas promoter methylation, two appropriate fragments of the targeted Fas region were generated by digestion of 1 µg of genomic DNA with 40 U of the CpG-methylation insensitive restriction enzyme MboII (New England Biolabs) for 20 min from cells cultured for 4 days on collagen type I coated dishes or uncoated control dishes. Subsequently, the enzyme was heat inactivated at 65°C for 20 min. The two regions were selected according to literature [8]. As shown in Fig. 1, fragment 1 had 627 bp and contains 25 CpG-sites. It includes 130 bp of the proximal promoter region of Fas, the short first exon (79 bp) with the coding region for the first 10 amino acids (30 bp), and 455 bp of the first intron, which is 16,380 bp long. The second fragment (fragment 2) with 863 bp includes 15 CpGs and starts at −2,800 bp, counted from the transcription start. Although both fragments contain an accumulation of CpG sites, it does not meet the criteria of a CpG-island (Fig. 1). After MboII digestion, DNA was purified using a commercially available PCR clean-up Kit following the supplier's instructions. In the next step methylated DNA fragments were captured with the "MetylMiner Methylated DNA Enrichment Kit" (Invitrogen) following the supplier's instructions. In brief, methylated DNA was captured by methyl blinding protein 2 (MBD2) coupled to magnetic beads and subsequently separated from the unmethylated DNA fraction. Methylated DNA was eluted from the MBD2-beads with 200 µl of 2 M NaCl solution as single fraction independent from the CpG methylation density and concentrated by ethanol precipitation. Finally, the mean methylation status of the fragments was determined by amplifying the fragments by quantitative real-time PCR. Amplification ratios of the bound (methylated) DNA fraction to unbound (unmethylated) DNA fraction were calculated (for primer design see Table 1).

Statistical analysis

Statistical analyses were performed using either ANOVA or Student's *t*-test using Prism 4.03 (GraphPad Software, San Diego, CA). $P \leq 0.05$ was considered as significant. For each experiment, the triplicate results of the RT–qPCR were averaged and this mean value was treated as a single statistical unit. The data of the triplicate experiments are presented as means ± standard deviation (SD).

Results

Extracellular collagen influences expression of genes related to osteoblastic differentiation, proliferation, and apoptosis of MC3T3-E1 pre-osteoblasts

MC3T3-E1 cells were seeded either on rat-tail collagen or on normal culture dishes (control) and cultured for 1 and 4 days. On day 1 there was a low expression of the mRNA of both Runx2 and OCN and no significant difference between control and collagen seeded cultures was observed. On day 4 however, there was a significant stimulation of Runx2 (1.39 ± 0.10-fold, Fig. 2a) as well as OCN (1.63 ± 0.03-fold, Fig. 2b). To address whether collagen influences cell multiplication, mRNA expression of cyclin A2 as proliferation marker and expression of the apoptosis related Fas was measured. In collagen seeded cells, Cyclin A2 was up regulated on day 1 and day 4 (4.8 ± 0.28-fold, Fig. 2c) and as Fig. 2d shows Fas was down regulated on both, day 1 (3.03 ± 0.02-fold) and day 4 (2.70 ± 0.01-fold) suggesting reduced apoptosis on collagen covered culture dishes.

Down regulation of the apoptosis related gene Fas by collagen is due to DNA methylation

As demonstrated above, seeding of osteoblasts on collagen inhibits the expression of the apoptosis related gene Fas.

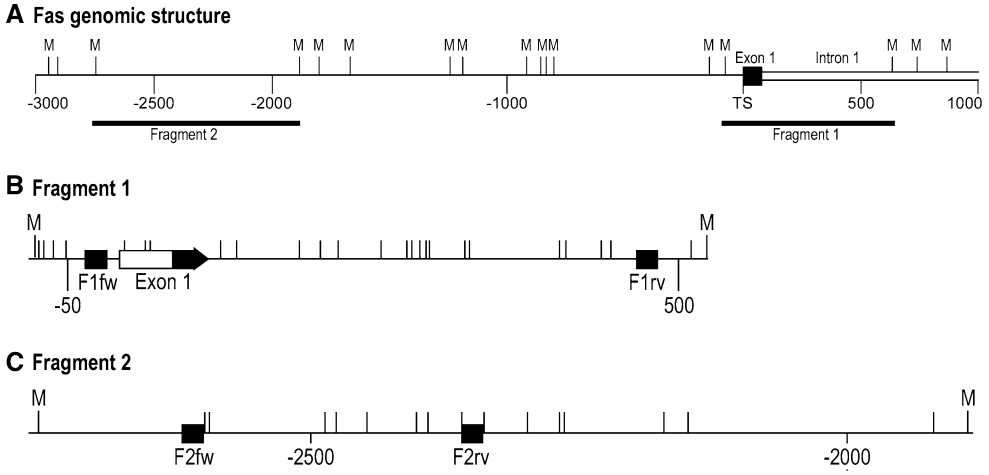

Fig. 1 Fas genomic structure with the first exon (79 bp) and a small part of the first intron (921 of 16,380 bp). **a** Schematic diagram depicting the exon 1, the part of intron 1 and the location of the two fragments used for methylation analysis. **b** Schematic diagram of fragment 1 depicting the location of the Exon 1 with the untranslated region (*open box*) and the coding region (*black arrow*). Indicated as *black boxes* are the forward (F1fw) and the reverse (F1rv) primers used for amplification of the DNA after the "MetylMiner" assay. The *vertical bars* above the *horizontal line* of the gene indicate the 25 CpGs of the region. **c** Fragment 2 with the location of the forward (F1fw) and the reverse (F1rv) primers as *black boxes*. Again, the *vertical bars* indicate the 14 CpGs of this region. The Mbo II restriction sites are indicated with M and the numbers below the gene-line denote the distance to the transcription start (TS)

Table 1 QRT-PCR primer for mRNA expression and Fas CpG methylation with Sybr Green

Gene	Forward primer (5′–3′)	Reverse primer (5′–3′)	Tm (°C)
Dnmt1	ACCGCTTCTACTTCCTCGAGGCCTA	GTTGCAGTCCTCTGTGAACACTGTGG	62
Hells	TGAGGATGAAAGCTCTTCCACT	ACATTTCCGAACTGGGTCAAAA	62
Fas	TATCAAGGAGGCCCATTTTGC	TGTTTCCACTTCTAAACCATGCT	64
Ccna2	ACATTCACACGTACCTTAGGGA	CATAGCAGCCGTGCCTACA	62
c-Fos	CGGGTTTCAACGCCGACTA	TTGGCACTAGAGACGGACAGA	63
c-Jun	CCTTCTACGACGATGCCCTC	GGTTCAAGGTCATGCTCTGTTT	63
Primer for Fas CpG methylation analysis			
Fragment 1	CATACCCACAGGCAGTCTAGA	CAGCCCAGAGTAACTCACTTC	62
Fragment 2	GAAGTAGAAACAGAAGCTGAG	TTGCTACATCCCAACTGTAAC	62

Fas mRNA expression was demonstrated before to be regulated by CpG methylation of its promoter by Dnmt1 [8]. Therefore, two regions in the Fas promoter were studied (Fig. 1); one starting at −2,800 bp and the other located near the transcription start [8]. In the region near the transcription start (Fig. 1b, 25 CpGs) CpG methylation was significantly increased (6.53 ± 1.03-fold, Fig. 3a) after 4 days of culture in collagen-seeded osteoblasts when compared to control cultures. A similar situation was found with the second fragment (Fig. 1c, 14 CpGs) where the stimulation of methylation was 2.20 ± 0.09 (Fig. 3b) when compared to control cultures.

Collagen up regulates Dnmt1 and Hells expression in MC3T3-E1 osteoblastic cells

As we found that the collagen dependent inhibition of Fas expression is due to Fas promoter hypermethylation, mRNA expression of Dnmt1 was analyzed. After seeding of MC3T3-E1 cells in control cultures and on rat-tail collagen, RNA was isolated at different times (2, 4, 6 h, 1, 2, 4 and 8 days). During the first 6 h of culture, expression of Dnmt1 changed neither in control- nor in collagen-seeded cultures. After 1 day of culture, in both, control cultures as well as in cultures seeded on collagen, a significant increase in Dnmt1 expression could be observed (Fig. 4). However, in collagen-seeded cells the increase was 2.18 ± 0.02-fold stronger than in control cultures. Moreover, the up regulation of Dnmt1 disappeared in control cultures after 2 days whereby in collagen-seeded cells the effect was highest at day 2 (5.88 ± 0.13-fold) and still observable after 8 days. At days 2, 4 and 8 the differences were statistically highly significant (Fig. 4). To show that ECM produced by MC3T3-E1 cells also has the potential to regulate expression of Dnmt1, we prepared ECM by growing MC3T3-E1 cells for 8 days and removed living

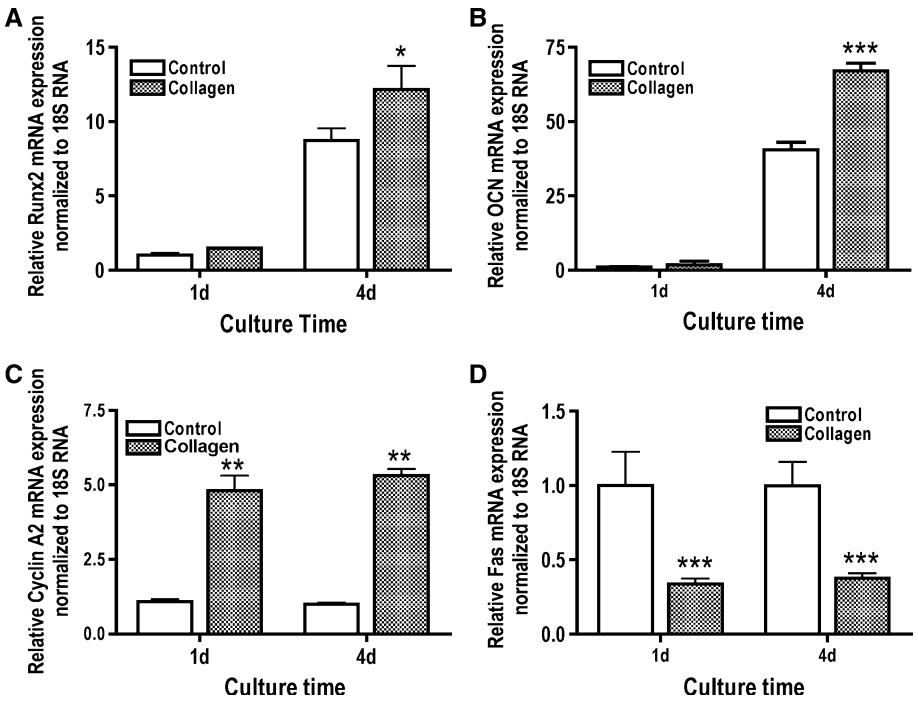

Fig. 2 Extracellular collagen influences expression of genes related to osteoblastic differentiation, proliferation, and apoptosis of MC3T3-E1 pre-osteoblasts. After 4 days of culture MC3T3-E1 cells cultured on collagen express higher levels of Runx2 (**a**) and OCN (**b**) mRNA compared to control cultures indicating progress in differentiation. MC3T3-E1 cells cultured on collagen, express higher levels of mRNA for cyclin A2 (**c**), a marker for proliferation, and lower levels of Fas (**d**), a marker of apoptosis. MC3T3-E1 were either seeded on rat-tail coated (Collagen) or on uncoated (Control) culture dishes and cultured for 1 and 4 days. RNA was isolated and analyzed by QRT–PCR. The specific gene expression was normalized to 18S rRNA. *The bars* represent the mean ± SD. * $P \leq 0.05$; ** $P \leq 0.01$; $N = 3$; *** $P \leq 0.001$; $N = 3$

cells by detergent [21]. Figure 5 demonstrates that MC3T3-E1 cells seeded and cultured on native ECM, which means ECM produced by MC3T3-E1 at previous cultures, increased the Dnmt1 mRNA levels as well.

Hells was recently described to be involved in DNA methylation as enhancer of the DNA methylation process [9]. Different to Dmnt1 (Fig. 4), Hells was not up regulated after 1 day of culture on collagen but on day 4 there was a significant up-regulation of Hells mRNA expression compared to control as well to control and collagen on day one (3.5-fold, Fig. 6).

Effect of collagen on global DNA methylation

The up regulation of Dnmt1 by collagen suggested a general effect on DNA methylation. To this end we used a recently published assay based on the sensitivity of the HpaII restriction enzyme to methylated CpGs compared to the insensitivity of MspI to cut such restriction sites. Figure 7 clearly demonstrates, that after 4 days of culture DNA global methylation was significantly lower in control cultures compared to collagen seeded cultures (2.38 ± 0.32-fold).

Collagen stimulation of Dnmt1 expression involves FAK/MAP-kinase/AP1-pathway

Using genistein a naturally occurring inhibitor of FAK phosphorylation [22] the expression of Dnmt1 was down regulated in collagen-seeded cultures compared to control (Fig 8, Gen labeled bar). A similar behavior was found when cells were treated with PD98059 a potent and selective inhibitor of the MAP-/ER-kinase. Figure 8 (PD labeled bar) clearly shows that at the used concentration, Dnmt1 mRNA expression was similarly attenuated as with genistein. Signals of the MAP-kinase pathway usually regulates AP1 activity that could be inhibited by resveratrol as described before [23]. While in control cultures Dnmt1 mRNA expression was not affected by resveratrol treatment, this inhibitor clearly abolished the up regulation of Dnmt1 in collagen-seeded cultures (Fig. 9). mRNA down regulation of c-Jun as well as of c-Fos, the genes coding for the proteins of AP-1, could be observed in dependence of resveratrol in collagen seeded as well as in control cultures (Fig. 10). Attenuation of collagen-induced Dnmt1 treatment of the cells with CHX, an inhibitor of protein-synthesis suggests

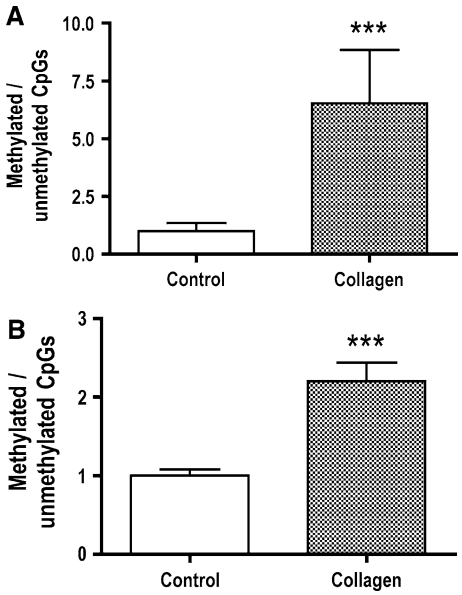

Fig. 3 Down-regulation of the apoptosis related gene Fas by collagen is due to DNA methylation. Methylation status of two CpG rich region of the Fas-promoter depended whether MC3T3-E1 cells are cultured on collagen-coated or on uncoated culture plates. MC3T3-E1 were either seeded on rat-tail coated or on uncoated (Control) culture dishes and cultured for 4 days. Thereafter, DNA was isolated and the ratio of methylated to unmethylated CpGs at the promoter positions −30 bp (**a**) or −2,600 bp (**b**) from the transcription start were calculated. *The bars* represent the mean ± SD. ***$P \leq 0.001$; $N = 3$

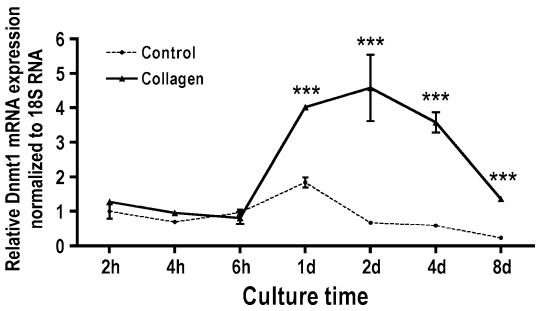

Fig. 4 Collagen up-regulates Dnmt1 expression in MC3T3-E1 osteoblastic cells. Time course of Dnmt1 expression of MC3T3-E1 cells cultured either on collagen covered or normal culture dishes. MC3T3-E1 were either seeded on rat-tail coated (Collagen) or on uncoated (Control) culture dishes and cultured for the indicated time. Thereafter, RNA was isolated and analyzed by QRT–PCR. The specific gene expression was normalized to 18S rRNA. *The symbols* represent the mean ± SD. *** $P \leq 0.001$; $N = 3$

that de-novo protein synthesis is involved in collagen-mediated up regulation of Dnmt1 (Fig. 11).

Discussion

Adhesion to an appropriate ECM prevents cells from apoptosis. This well established process involves several biochemical signal transduction pathways [24, 25]. ECM

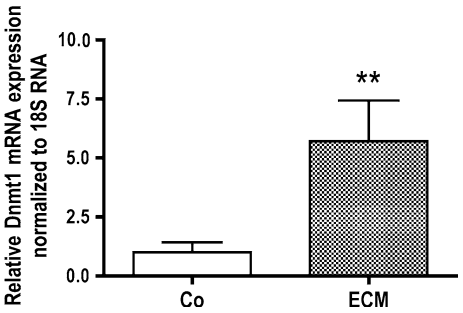

Fig. 5 ECM synthesized by MC3T3-E1 cells increased Dnmt1 expression of MC3T3-E1 cells compared to cells cultured on normal culture dishes. MC3T3-E1 cultures were cultured 1 week to produce ECM. After removing living cell, fresh MC3T3-E1 were seeded onto this matrix and cultured for another week. Thereafter, RNA was isolated and analyzed by QRT-PCR. The specific gene expression was normalized to 18S rRNA. MC3T3-E1 cells grown on uncoated culture dishes served as controls (Co). *The symbols* represent the mean ± SD. **$P \leq 0.01$; $N = 3$

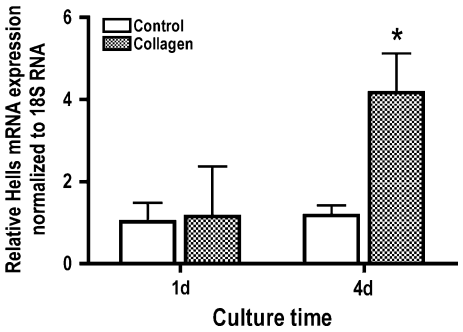

Fig. 6 Collagen up-regulates Hells expression in MC3T3-E1 osteoblastic cells on day 4. MC3T3-E1 were either seeded on rat-tail coated (Collagen) or on uncoated (Control) culture dishes and cultured for the indicated time. Thereafter, RNA was isolated and analyzed by QRT–PCR. The specific gene expression was normalized to 18S rRNA. *The symbols* represent the mean ± SD. * $P \leq 0.05$; $N = 3$

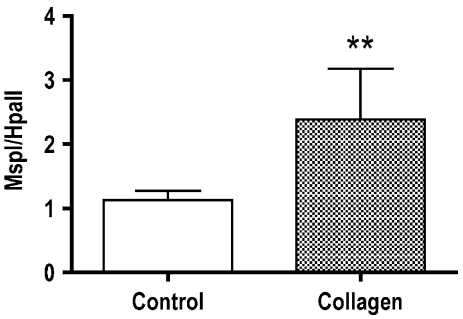

Fig. 7 MC3T3-E1 cells cultured on collagen had increased global CpG-methylation of DNA compared to cells cultured on uncoated culture plates. MC3T3-E1 cells were either seeded on rat-tail coated or on uncoated culture dishes and cultured for 4 days. Thereafter, DNA was isolated and the ratio of methylated to unmethylated CpGs was compared. *The bars* represent the mean ± SD. ** $P \leq 0.01$; $N = 3$

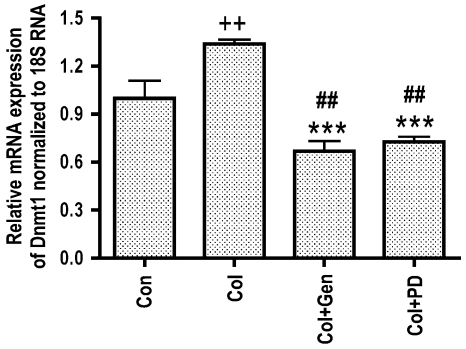

Fig. 8 Specific inhibitors of the MAP-kinase-pathway inhibited Dnmt1 expression of MC3T3-E1 cells cultured on collagen compared to control cultures. MC3T3-E1 were either seeded on rat-tail coated (Col) or on uncoated (Con) culture dishes and cultured for 1 day with either 10 μM Genistein (Gen) or 10 μM PD98059 (PD). Both inhibitors down regulated the expression of Dnmt1 in MC3T3-E1 cells, when cultured on collagen. RNA was isolated and analyzed by QRT-PCR. The specific gene expression was normalized to 18S rRNA. The bars represent the mean ± SD. $^{++}$ $P \leq 0.01$ Col versus Con; $^{\#\#}$ $P \leq 0.01$ Col+Gen, Col+PD versus Con; *** $P \leq 0.001$ Col+Gen, Col+PD versus Col; Gen versus PD n.s.; N = 3

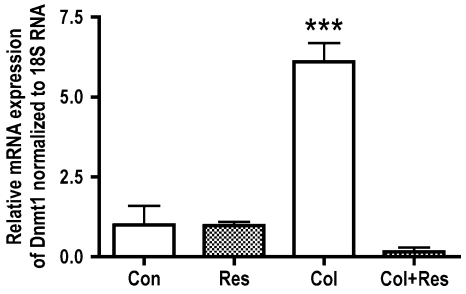

Fig. 9 Resveratrol inhibited Dnmt1 expression of MC3T3-E1 cells cultured on collagen compared to control cultures. MC3T3-E1 were either seeded on rat-tail (Col) coated or on uncoated (Con) culture dishes and cultured for 1 day. While resveratrol (Res) did not influence basal expression of Dnmt1 it strongly inhibited the collagen-induced expression. RNA was isolated and analyzed by QRT-PCR. The specific gene expression was normalized to 18S rRNA. *The bars* represent the mean ± SD. *** $P \leq 0.001$ collagen-grown versus the other cultures; $N = 3$

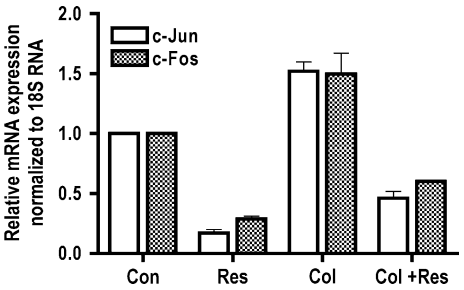

Fig. 10 MC3T3-E1 cells cultured on collagen-coated culture dishes express higher levels of the genes of the AP1 complex compared to cells cultured on normal dishes. Both basal as well as collagen stimulated expression was down regulated by resveratrol MC3T3-E1 were either seeded on rat-tail coated or on uncoated culture dishes and cultured for 1 day and treated without or with 40 μM resveratrol (Res). RNA was isolated and analyzed by QRT-PCR. The specific gene expression was normalized to 18S rRNA. *The bars* represent the mean ± SD. All differences were highly significant ($P \leq 0.001$) different, except Res versus Res+Col where it was $P \leq 0.05$. $N = 3$

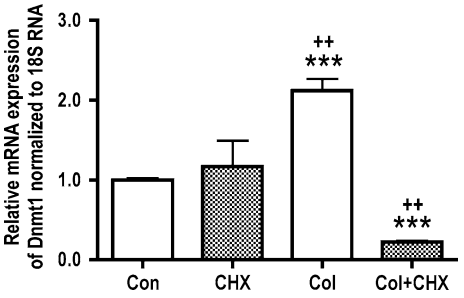

Fig. 11 Cycloheximid (CHX) inhibited Dnmt1 expression of MC3T3-E1 cells cultured on collagen compared to control cultures. MC3T3-E1 were either seeded on rat-tail (Col) coated or on uncoated (Col) culture dishes and cultured for 1 day without or with 10 μg/ml CHX. While CHX did not influence basal expression of Dnmt1, it strongly inhibited the collagen-induced expression. RNA was isolated and analyzed by QRT-PCR. The specific gene expression was normalized to 18S rRNA. The bars represent the mean ± SD. *** $P \leq 0.001$ Col versus Con and Col+CHX; $^{++}$ $P \leq 0.01$ Col+CHX versus Con and Col versus CHX. $N = 3$

sends signals to proceed through cell cycle checkpoints, to either proliferate, differentiate or to go into anoikis. These signals protrude from growth factor receptors and ECM receptors, the integrins; thus, a coordinate action of both determine cells fate [26].

Fas is a member of the TNF-receptor super family and play a central role in the physiological regulation of programmed cell death. The involvement of Fas in anoikis is well documented, however, the mechanism is still unclear [7]. Physiologically, during development and maintenance of tissue homeostasis, Fas up regulation occurs in case of detachment of cells from their ECM. Pathologically, as for metastatic tumor cells, down regulation of genes like Fas enable these cells to circumvent anoikis and so to adhere to an un-physiological substrate [27]. In such metastatic processes, Ras was shown to play an important role in Dnmt1 mediated Fas silencing by promoter methylation [8]. In the present work we demonstrate that seeding of pre-osteoblastic MC3T3-E1 cells on collagen type I coated dishes, compared to uncoated, repressed Fas expression and increased Dnmt1 expression; this suggested a similar mechanism in Fas regulation.

Analysis of the methylation status of two CpG rich regions located around the transcription start that are hypermethylated in K-ras transformed NIH 3T3 cells [8] revealed a higher methylation status in collagen-seeded cells. These data suggests that collagen either increased methylation of that CpGs or prevented it from demethylation, at least. The latter consideration is supported by

findings that global methylation had been decreased during culture on uncoated culture dishes for 2 weeks and correlates with Fas mRNA expression (Thaler et al. in preparation). Although the 5′-region as well as the first exon (79 bp) and the first intron (16,380 bp) are CpG rich, they do not contain CpG-islands when recent published criteria are applied [28]. An unmethylated core region of about 1,000 bp centered at the transcriptional start site was recently reported to be requisite for active transcription [29]; this mean that methylation of this region will diminish transcription as found in our experiments. As already mentioned the large first intron (16,380 bp) is also rich in CpG. In is feasible that methylated CpG in this intron could also contribute to gene silencing as recently demonstrated for the integrin collagen receptor locus [30] and the zeta-chain (TCR) associated protein kinase ZAP70 gene [31].

The presented finding can be considered as an epigenetic physiological process, which avoids anoikis of cells. Moreover, the presented results show DNA methylation as a collagen regulated cellular process. Therefore, as collagen adhesion of osteoblasts is known to trigger cell multiplication and as mRNA expression of the proliferation marker cyclin A2, which promotes cell cycle at G1-S and G2-M stage, was described to be enhanced by CpG methylation at two repressor binding sites in its promoter [32], expression and CpG methylation of this gene was analyzed. Although we found a stimulation of cyclin A2 mRNA expression, no changes of the methylation patterns in the promoter were found (data not shown). Further, up regulation of cyclin D1 (data not shown) and down regulation of the cell cycle inhibitor p19-INK4D (data not shown) underline the role of collagen for cell fate decisions in osteoblasts. A further aspect of ECM mediated cell surveillance includes regulation of cell differentiation. Extra cellular collagen type I differentiates mesenchymal stem cells [5] and the results presented in this paper confirm the collagen mediated differentiation of pre-osteoblasts [33] as demonstrated by stimulated expression of Runx2 and OCN, both well described proteins of the differentiated osteoblastic phenotype [34, 35].

Starting from the globally low methylated stem cell, ongoing cell differentiation implies epigenetic reprogramming [36, 37]. The delicate organization of DNA methylation and chromatin status regulates the normal cellular homeostasis of gene expression patterns and confers stability to the genome [38, 39]. Collagen dependent maintenance of global DNA-methylation may additionally contribute to chromatin organization and stability, consolidating the adopted phenotype during the differentiation process. To what extend collagen's influence on DNA methylation affects differentiation of osteoblasts cannot be answered yet.

Using inhibitors of signal transduction pathways and following KEGG PATHWAY database [40] we draw a scheme how ECM could signal to Dnmt1 effecting DNA methylation (Fig. 12). Resveratrol, an inhibitor of AP1 activity [23] attenuated the mRNA expression of Dnmt1 in collagen seeded cells suggesting the involvement of this protein-complex. This is in line with recent reports describing a stimulation of Dnmt1 mRNA transcription by over expressing cJun, a component of the AP1 complex. This effect was abrogated by a deletion of the AP1 response elements in the Dnmt1 promoter demonstrating that Dnmt1 is regulated via a Ras/Jun signaling pathway [11, 12]. In addition, for the collagen dependent maintenance of DNA methylation in osteoblasts, our experiments suggest the involvement of the focal adhesion kinase and of the MAP-kinase pathway, as demonstrated for Dnmt1 dependent Fas methylation in Ras transformed fibroblasts [8]. Interestingly, for fibroblasts only the ECM component fibronectin but not collagen sends a survival signal via focal adhesion kinase to cJun amino-terminal kinase (JNK) even under serum free conditions. However, the involvement of JNK in survivals signaling is discussed controversial and seems to be cell type specific, especially because FAK engages multiple pathways for survival of fibroblasts and endothelial cells [41]. Our results suggest that in osteoblasts both pathways are needed to stimulate Dnmt1 expression for epigenetic silencing of the pro-apoptotic gene Fas triggering cell survival, although, the precise mechanism has still to be clarified.

Attenuation of the collagen effect on Dnmt1 expression by genistein and resveratrol, which represent the main flavonoid present in soy and a phytoalexin present in red grapes, respectively, may imply consequences in vivo. For genistein and for other nutritional factors as well as for

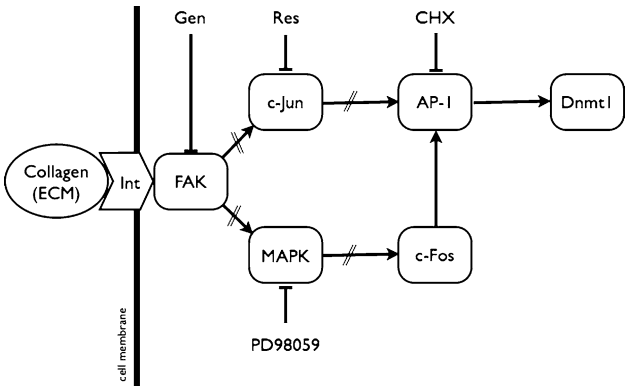

Fig. 12 Schematic representation of the suggested pathway for regulation of Dnmt1 by the ECM. The ECM activates via integrins the focal adhesion kinase, which itself activates both pathways the Jun-Kinase and the MAP-Kinase pathway leading to increased AP-1 transcription. The indicated block by CHX means that translation is a prerequisite for activation of Dnmt1 transcription by AP1. Abbreviations: Int, integrins; FAK, focal adhesion kinase; MAPK, mitogen activated protein kinase; Gen, genistein; Res, resveratrol; CHX, cycloheximid

nutritional habits interference with epigenetic regulation of gene expression was demonstrated [42–44]. Therefore, we speculate that nutritional factors may influence bone development and homeostasis by the involvement of epigenetic mechanisms.

Signaling by integrins gain much attraction in bone research as they are discussed as transducer of mechanical forces, which is fairly important in the bone remodeling process, where the osteoblasts construct a matrix in line with the applied forces to the bone. Cyclic loading on bone cells will result in both increased proliferation but also in enhanced differentiation. It is exciting to speculate that integrins, which also control cell-division axis at mitosis, may regulate CpG-methylation of DNA during DNA synthesis in the S phase of the cell cycle. Attachment sites of interphase cells connect the cytoskeleton via integrins to the ECM. During mitosis when the cell rounds up the cell remains attached to the substratum through retraction fibers; thus the ECM controls the cells during the whole cell cycle [26]. This is especially important for bone cells because external forces will direct via ECM the orientation of the daughter cells [45]; not properly oriented cells will not gain the methylation signal for silencing Fas and will, therefore, apoptose. Therefore, we assume that integrins play a role in initiating the pathway leading from collagen to DNA methylation. However, if and at which extent and under which circumstances this may occur remains to be clarified.

In summary, we demonstrate that adhered osteoblasts on collagen type I repress mRNA expression of the pro-apoptotic gene Fas by preservation of CpG methylation of its promoter. This relies on a collagen dependent up regulation of Dnmt1 and may play an important role for osteoblasts in avoiding anoikis by adhesion to an adequate ECM. Furthermore, increase in expression of proliferation and differentiation markers underline cell fate decisions directed by collagen. Finally, maintenance of DNA global methylation by collagen may stabilize chromatin and homeostasis of the differentiated phenotype. In conclusion, we demonstrate epigenetic imprinting of survival signals coming from ECM leading to increased tissue formation and differentiation.

Acknowledgments This study was supported by the Fonds zur Foerderung der wissenschaftlichen Forschung (FWF; The Austrian Science Fund) Project P20646-B11, the WGKK (Social Health Insurance Vienna), and the AUVA (Austrian Social Insurance for Occupational Risks). The authors thank to Dr. E. Paschalis for critical review of the manuscript and valuable comments.

References

1. Blair HC, Zaidi M, Schlesinger PH (2002) Mechanisms balancing skeletal matrix synthesis and degradation. Biochem J 364:329–341
2. Franceschi RT (1999) The developmental control of osteoblast-specific gene expression: role of specific transcription factors and the extracellular matrix environment. Crit Rev Oral Biol Med 10:40–57
3. Lian JB, Stein GS, Javed A et al (2006) Networks and hubs for the transcriptional control of osteoblastogenesis. Rev Endocr Metab Disord 7:1–16
4. Guan JL (1997) Focal adhesion kinase in integrin signaling. Matrix Biol 16:195–200
5. Salasznyk RM, Klees RF, Williams WA, Boskey A, Plopper GE (2007) Focal adhesion kinase signaling pathways regulate the osteogenic differentiation of human mesenchymal stem cells. Exp Cell Res 313:22–37
6. Frisch SM, Screaton RA (2001) Anoikis mechanisms. Curr Opin Cell Biol 13:555–562
7. Grossmann J (2002) Molecular mechanisms of "detachment-induced apoptosis–Anoikis". Apoptosis 7:247–260
8. Gazin C, Wajapeyee N, Gobeil S, Virbasius CM, Green MR (2007) An elaborate pathway required for Ras-mediated epigenetic silencing. Nature 449:1073–1077
9. Myant K, Stancheva I (2008) LSH cooperates with DNA methyltransferases to repress transcription. Mol Cell Biol 28:215–226
10. Kishikawa S, Murata T, Kimura H, Shiota K, Yokoyama KK (2002) Regulation of transcription of the Dnmt1 gene by Sp1 and Sp3 zinc finger proteins. Eur J Biochem 269:2961–2970
11. Rouleau J, MacLeod AR, Szyf M (1995) Regulation of the DNA methyltransferase by the Ras-AP-1 signaling pathway. J Biol Chem 270:1595–1601
12. Bigey P, Ramchandani S, Theberge J, Araujo FD, Szyf M (2000) Transcriptional regulation of the human DNA Methyltransferase (dnmt1) gene. Gene 242:407–418
13. Franceschi RT, Iyer BS, Cui Y (1994) Effects of ascorbic acid on collagen matrix formation and osteoblast differentiation in murine MC3T3–E1 cells. J Bone Miner Res 9:843–854
14. Varga F, Luegmayr E, Fratzl-Zelman N et al (1999) Tri-iodothyronine inhibits multilayer formation of the osteoblastic cell line, MC3T3–E1, by promoting apoptosis. J Endocrinol 160:57–65
15. Fratzl-Zelman N, Horandner H, Luegmayr E et al (1997) Effects of triiodothyronine on the morphology of cells and matrix, the localization of alkaline phosphatase, and the frequency of apoptosis in long-term cultures of MC3T3–E1 cells. Bone 20:225–236
16. Liao QC, Xiao ZS, Qin YF, Zhou HH (2007) Genistein stimulates osteoblastic differentiation via p38 MAPK-Cbfa1 pathway in bone marrow culture. Acta Pharmacol Sin 28:1597–1602
17. Chen TH, Chen WM, Hsu KH, Kuo CD, Hung SC (2007) Sodium butyrate activates ERK to regulate differentiation of mesenchymal stem cells. Biochem Biophys Res Commun 355:913–918
18. Backesjo CM, Li Y, Lindgren U, Haldosen LA (2006) Activation of Sirt1 decreases adipocyte formation during osteoblast differentiation of mesenchymal stem cells. J Bone Miner Res 21:993–1002
19. Pfaffl MW (2001) A new mathematical model for relative quantification in real-time RT-PCR. Nucleic Acids Res 29:e45
20. Anisowicz A, Huang H, Braunschweiger KI et al (2008) A high-throughput and sensitive method to measure global DNA methylation: application in lung cancer. BMC Cancer 8:222
21. Turecek C, Fratzl-Zelman N, Rumpler M et al (2008) Collagen cross-linking influences osteoblastic differentiation. Calcif Tissue Int 82:392–400
22. Sawai H, Okada Y, Funahashi H et al (2005) Activation of focal adhesion kinase enhances the adhesion and invasion of pancreatic cancer cells via extracellular signal-regulated kinase-1/2 signaling pathway activation. Mol Cancer 4:37
23. Gao Z, Ye J (2008) Inhibition of transcriptional activity of c-JUN by SIRT1. Biochem Biophys Res Commun 376:793–796
24. Cordes N (2006) Integrin-mediated cell-matrix interactions for prosurvival and antiapoptotic signaling after genotoxic injury. Cancer Lett 242:11–19

25. Keeble JA, Gilmore AP (2007) Apoptosis commitment–translating survival signals into decisions on mitochondria. Cell Res 17:976–984
26. Streuli CH (2009) Integrins and cell-fate determination. J Cell Sci 122:171–177
27. Nguyen DX, Bos PD, Massague J (2009) Metastasis: from dissemination to organ-specific colonization. Nat Rev Cancer 9:274–284
28. Takai D, Jones PA (2002) Comprehensive analysis of CpG islands in human chromosomes 21 and 22. Proc Natl Acad Sci USA 99:3740–3745
29. Eckhardt F, Lewin J, Cortese R et al (2006) DNA methylation profiling of human chromosomes 6, 20 and 22. Nat Genet 38:1378–1385
30. Cheli Y, Kanaji S, Jacquelin B, Chang M, Nugent DJ, Kunicki TJ (2007) Transcriptional and epigenetic regulation of the integrin collagen receptor locus ITGA1-PELO-ITGA2. Biochim Biophys Acta 1769:546–558
31. Chantepie SP, Vaur D, Grunau C, et al. (2010) ZAP-70 intron1 DNA methylation status: determination by pyrosequencing in B chronic lymphocytic leukemia. Leuk Res 34(6):800–808
32. Jamaluddin MD, Chen I, Yang F et al (2007) Homocysteine inhibits endothelial cell growth via DNA hypomethylation of the cyclin A gene. Blood 110:3648–3655
33. Tamura Y, Takeuchi Y, Suzawa M et al (2001) Focal adhesion kinase activity is required for bone morphogenetic protein–Smad1 signaling and osteoblastic differentiation in murine MC3T3–E1 cells. J Bone Miner Res 16:1772–1779
34. Komori T, Yagi H, Nomura S et al (1997) Targeted disruption of Cbfa1 results in a complete lack of bone formation owing to maturational arrest of osteoblasts. Cell 89:755–764
35. Ducy P, Zhang R, Geoffroy V, Ridall AL, Karsenty G (1997) Osf2/Cbfa1: a transcriptional activator of osteoblast differentiation. Cell 89:747–754
36. de Magalhaes JP (2004) From cells to ageing: a review of models and mechanisms of cellular senescence and their impact on human ageing. Exp Cell Res 300:1–10
37. Dean W, Santos F, Reik W (2003) Epigenetic reprogramming in early mammalian development and following somatic nuclear transfer. Semin Cell Dev Biol 14:93–100
38. Esteller M, Herman JG (2002) Cancer as an epigenetic disease: DNA methylation and chromatin alterations in human tumours. J Pathol 196:1–7
39. Rizwana R, Hahn PJ (1999) CpG methylation reduces genomic instability. J Cell Sci 112(Pt 24):4513–4519
40. Kanehisa M, Araki M, Goto S et al (2008) KEGG for linking genomes to life and the environment. Nucleic Acids Res 36:D480–D484
41. Zouq NK, Keeble JA, Lindsay J et al (2009) FAK engages multiple pathways to maintain survival of fibroblasts and epithelia: differential roles for paxillin and p130Cas. J Cell Sci 122:357–367
42. Ingrosso D, Perna AF (2008) Epigenetics in hyperhomocysteinemic states. A special focus on uremia. Biochim Biophys Acta 1790:892–899
43. Dolinoy DC. (2008) The agouti mouse model: an epigenetic biosensor for nutritional and environmental alterations on the fetal epigenome. Nutr Rev 66 Suppl 1:S7-11
44. Thaler R, Karlic H, Rust P, Haslberger AG (2009) Epigenetic regulation of human buccal mucosa mitochondrial superoxide dismutase gene expression by diet. Br J Nutr 101:743–749
45. Young SR, Gerard-O'Riley R, Kim JB, Pavalko FM (2009) Focal adhesion kinase is important for fluid shear stress-induced mechanotransduction in osteoblasts. J Bone Miner Res 24: 411–424

6. Discussion

Lathyrogens like bAPN and the metabolite hcys affect cross-linking of collagen and with it the quality of bone in animal models. Aim of the studies was to get insights into molecular mechanisms of the lathyrogens actions. The data demonstrate that both compounds influence osteoblastic proliferation and differentiation and hinder a stable bone matrix formation via inhibition of the collagen cross-linker LOX on the enzymatic level as well as by down-regulation of its mRNA expression. Investigating the mechanisms, we could elucidate the pathway by which hcys down-regulates LOX expression and demonstrate that beside the discussed function of hcys as methyl carrier in DNA methylation, it also influences the expression of *Dnmts* itself leading to epigenetic methylation of *Lox* promoter in osteoblasts. Furthermore, we revealed a new mechanism contributing to osteoblast proliferation and differentiation on collagen type I containing ECM. Here, collagen type I suppresses via *Dnmt1* dependent promoter methylation the expression of the pro-apoptotic gene *Fas* thus guaranteeing osteoblastic survival and proliferation on an adequate ECM.

The lathyrogenic effect of bAPN was extensively described in the past (1-4, 6), however, the role of hcys as lathyrogen is not as clear as for bAPN. Thus, the one purpose was to directly compare the effect of bAPN and hcys on collagen cross-links and additionally on mRNA expression level of genes involved in post-translational modification of collagen cross-linking in pre-osteoblasts (105) thus expanding previous studies (6). Pyr/divalent cross-link ratio analysis by FTIR showed that both bAPN and hcys provoked a dose-dependent increase of the ratio indicating a reduction of LOX activity. Furthermore, similar results were observed in a human study which found an association between plasma hcys levels and collagen cross-link ratio (72). Thus, it can be concluded that regarding the lathyrogenic activity of hcys and bAPN, both compounds act in a comparable manner. Interestingly, both compounds regulate mRNA expression of important osteoblastic genes. Thus, the central osteoblastic transcription factor *Runx2* was up regulated and as shown by qPCR, genes involved in collagen cross-linking like *Plod2* and *Lox* were down regulated by both compounds after 1 week at a concentration of 4 mM in medium. This indicates that both lathyrogens disrupt the formation of a physiological ECM in bone but concomitantly induce osteoblastic differentiation and bone matrix mineralization as shown by the increased ALP levels. This may be a further patho-

physiological effect induced by the two lathyrogens. However, if the effect of both compounds is compared at the level of mRNA expression of modulators of *Runx2* activity or further genes related to the osteoblastic phenotype, two different effects are observed. Thus, as seen by gene array analysis, the mRNA expressions of several genes interacting with *Runx2* activity (*Aes*, *Myst3*, *Myst4*, *Stat1*, *Tle2* and others) (119) were up-regulated by hcys but not by bAPN suggesting a distinct and environmental dependent effect of hcys on osteoblastic differentiation. Furthermore, a general evaluation of genome wide gene expression revealed that only a small part of genes is co-regulated by both compounds; 5.5-fold more genes are down- and 3.8-fold more genes are up regulated by hcys compared to bAPN. This demonstrates the divergent genome wide effects on mRNA expression between hcys and bAPN.

As mentioned above, both compounds not only inhibited enzymatically collagen cross-link formation, but also down-regulated the mRNA expression of *Lox* and of other genes involved in post-translational collagen cross-link formation such as *Plod1*, *Plod2*, *P4ha1* and *P4ha2* (120). However, generally a stronger effect was seen by hcys treatment.

Lathyrogens are defined by their enzymatic inhibition of the enzyme LOX (5). The attenuation of LOX via down-regulation of its expression by hcys in osteoblasts represents a new aspect; furthermore compared to bAPN, hcys plays clinically a more relevant role. Thus, we started to investigate the cellular mechanisms directing down regulation of *Lox* expression by hcys. In this context first suggestions were given by analysis of genome wide mRNA expression of MC3T3-E1 cells treated one week with hcys with Affymetrix GeneChip technique. This method allows the observation of an effect of a substance on the expression of selected genes involved in different pathways and therefore permits first deductions of possible signaling pathways activated by the specific compound analyzed. Intense gene array analysis revealed a strong hcys dependent up-regulation of IL-6 and of several genes involved in IL-6/JAK2 dependent signal transduction pathways. The stimulation of IL-6 expression by hcys in the pre-osteoblastic MC3T3-E1 cell-line per se was an unexpected and intriguing finding of these experiments: it suggests that hcys affects via IL-6 both, osteoblasts the bone forming cells as well as osteoclasts, the bone resorbing cells. Osteoclasts are large multinucleate, macrophage derived cells and in various cell cultures it was shown that IL-6 enhances osteoclast formation (121). For osteoclast maturation the production of soluble factors by osteoblasts as well as tight

cell-cell interactions with osteoblastic or stromal cells are needed (122). Concerning cell-cell contacts between osteoblasts and osteoclasts, the interaction between the tumor necrosis factor (ligand) superfamily, member 11 (TNFSF11, RANKL) and the osteoclastic tumor necrosis factor receptor superfamily, member 11a, (TNFRSF11A, RANK) was found to be the major mechanism implicated in osteoclast differentiation and maturation (122). IL-6 dependent stimulation of *RANKL* expression was shown in osteoblasts (123) thus inducing osteoclastogenesis. In addition, treatment of bone marrow cells from ovariectomized mice with IL-6 antibody prevented enhanced osteoclast formation (124, 125). However, recent publications suggested that IL-6 has an inhibitory effect on RANKL induced osteoclast formation and bone resorption (121, 125). Furthermore, IL-6 knockout mice do not show an obvious bone phenotype (126), showing that the published reports concerning the effects of IL-6 on bone cells are conflicting. These contradictory effects of IL-6 might be due to the ambivalent character of this cytokine and attributed to the environmental influences which result in activation via *Jak1/2* of several different intracellular pathways (121). As mentioned above, we suggest that hcys dependent stimulation of IL-6 expression activates via *Jak2* the STAT signaling pathways which induce the expression of genes involved in growth inhibition, apoptosis and differentiation as we have observed that hcys affects cell multiplication and cell differentiation and favors the expression of the pro-apoptotic gene *Fas*. Thus, in cases of chronically elevated hcys serum levels, besides the inhibitory effect of hcys on the generation of a stable bone matrix formation by enzymatic and transcriptional inhibition of LOX, hcys may further affect bone homeostasis by modulation of bone mineralization, osteoblastic differentiation and activation of osteoclasts. This would go in line with recently published reports that showed a correlation between diet dependent plasma hcys levels and bone mineral density (82), with the correlation found between plasma hcys levels and collagen cross-link ratio in forming trabecular surfaces in humans (72) and with recently published clinical and epidemiological articles which demonstrated a correlation between blood hcys levels and bone fracture risk (72-74). The results and mechanisms presented in this thesis and the here mentioned publications emphasize the complex role of hcys for bone health and metabolism. Thereby the long-term effect of this metabolic compound on bone homeostasis may depend on several factors like the local environment, nutrition, genetic predisposition, serum concentrations and others. Thus, targeted dietary approaches designed to counteract

high hcys serum levels may be useful to alleviate or minimize the negative effects of hcys on bone. However, in order to understand the implications and the effects of such approaches, further large-scale studies are needed. Nevertheless, first small scale studies showed that nutritional habits influence epigenetic DNA methylation thus modulating specific gene promoter methylation. Thus, it was published that compared to omnivores, consumers of a vegetarian diet express higher levels of the enzyme super oxide dismutase 2 (*SOD2*) which acts as radical scavenger in mitochondria. This difference was linked to a higher *SOD2* promoter methylation in omnivores when compared to consumers of a vegetarian diet. The results were suggested to rely on the different vitamin B12 intake between the two groups (127).

In regard to *Lox* promoter methylation by hcys, we show for the first time that beside the role of hcys in DNA methylation cycle, via a complex signaling pathway this compound directly modulates the expression of the genes involved in DNA methylation. Interestingly, hcys up-regulated the expression of *Dnmt1*, *Dnmt3b* and of *Hells* leaving the expression of *Dnmt3a* unaffected. HELLS was recently reported to act as DNA methylation supporter by recruiting DNMT1 and DNMT3B to the promoter (85). Furthermore, *Hells* was shown to play an essential role in bone development as *Hells* knock down mice show a clear, pathological bone phenotype including osteoporosis, osteopenia, delay in bone development, decreased bone mineral density and smaller epiphyses (128). Recently we observed that DMSO down regulates the expression of *Dnmt1*, *Dnmt3b* and *Hells*. However, as demonstrated here, DMSO also failed to regulate *Dnmt3a* (personal observations). Therefore, in addition to the synchronized activity of DNMT1, DNMT3B and HELLS at the protein level, we suggest a common mechanism regulating the mRNA expressions of these three genes, which may exclude regulation of *Dnmt3a* mRNA expression.

In contrast to other cells and tissues, to date little research has been performed concerning epigenetic gene regulation in bone development and pathogenesis. *Lox* expression was shown to be regulated by epigenetic DNA methylation in humans (129-131) and mice (110). Besides LOX role in collagen cross-linking, the N-terminal peptide of this enzyme acts as tumor-suppressor. In tumors, *Lox* expression is prevented by CpG-methylation of the promoter. Thus, our findings add new mechanistic insights to hcys' role as a risk factor for bone health.

In the experiments described in this thesis, we decided to treat the pre-osteoblastic MC3T3-E1 cells with pharmacological hcys doses which are even abundantly higher than mean pathological serum levels in humans. It is well known that pathologies related to high hcys serum levels rely on chronically high serum levels of this compound. Therefore, to increase the possibility to detect effects, to reduce treatment time and thus making experiments suitable for cell culture conditions we selected the hcys concentrations showed in the results. Furthermore, *in vivo* on tissue or even on cellular level, it cannot be excluded that local hcys accumulations/concentrations are much higher than the measured hcys serum concentrations.

As we have shown here, lathyrogens like bAPN and hcys modulate ECM formation hindering collagen cross-link formation. Furthermore, by gene array analysis we have shown that hcys down-regulates the mRNA expression of several genes implicated in intra and extracellular post-translational collagen folding and assembling. Very recent works provide first insights in the role of collagen folding for ECM to cell signaling. Aberrant collagen triple helix assembling which results in a partially denatured collagen triple-helix, exposes specific binding sites which are hypothesized via specific cell adhesion receptors to regulate cellular behavior during tissue repair and regeneration (11). It was shown that osteoblasts adhering to partially denatured type I collagen behave differently as osteoblasts seeded on plates coated with correctly folded type I collagen. Thus, the mRNA expression of osteoblastic genes like *Runx2* or bone sialo-protein as well as the extracellular calcium deposition was significantly higher in cells attaching on native collagen then on partially denatured collagen (21). The here described effects of hcys on the mRNA expression of collagen-folding enzymes let presume that beside the attenuated collagen cross-link formation, efficient collagen triple helix folding is also hindered under elevated hcys concentrations. However, interpreting the literature regarding this issue (21), this would be in contrast with the observed effect of enhancement of osteoblastic differentiation by hcys. As described above, hcys affects several cellular pathways (as for example the IL-6/JAK2/Stat pathway) and mechanisms. Thus, the feedback signals rising from a hcys-marred ECM may be decoupled and/or subordinate to the hcys activated Il-6/JAK2/STAT signaling pathway which is known to trigger cell differentiation. This aspect may represent a further pathological aspect for bone in regard to high hcys levels: triggering of osteoblastic differentiation with concomitant

degeneration/malformation of bone ECM. However, effects of hcys on fibrillogenesis during ECM formation as well as the specific osteoblastic response on the diverse pathological bone matrix are still open issues.

ECM to cell interactions control important cellular events. Adhesion of osteoblasts to ECM not only guarantees structural anchorage of the cells but also mediates primary signals to the cells (6, 11, 21, 22). It is well known that interaction of cells with an adequate ECM prevents from anoikis (homelessness, a specific form of apoptosis) and triggers cell differentiation. The involvement of the pro-apoptotic gene *Fas* in anoikis is well documented (132); however, until recently the mechanism behind was still unclear. *Fas*, a member of the TNF-receptor super family, plays an essential role in the initiation of programmed cell death (110, 132). In this work we demonstrated for the first time that the main organic bone ECM-component, namely collagen type I, up-regulates the expression of genes involved in differentiation and cell cycle regulation and down regulates *Fas* in MC3T3-E1 mouse osteoblasts (107). Recently, *Dnmt1* was shown to play central role in maintenance of *Fas* promoter methylation (110) and findings presented in this thesis concerning ECM up regulation of Dnmt1, suggested an epigenetic mechanism for attenuation of *Fas* expression. This was confirmed by methylation analysis of the *Fas*-promoter, where it could be demonstrated increased methylation of a CpG rich region (107).

Additionally to repression of *Fas*, collagen type I dependent up-regulation of Cyclin A2 mRNA expression was found as well. Increase of Cyclin A2 expression was recently demonstrated to be epigenetically regulated via CpG methylation. Unlike the common repressive effect of promoter CpG methylation on gene expression, in the case of Cyclin A2 it was shown that methylation of two specific CpG sites located at two repressor binding sites on Cyclin A2 promoter hinder binding of the repressor factors thus increasing Cyclin A2 expression (89). Therefore, assuming epigenetic methylation for collagen mediated up-regulation of Cyclin A2 expression, we compared Cyclin A2 promoter methylation in collagen seeded to plastic seeded MC3T3-E1 cells. However, in this case there was no associated methylation of those CpG sites which should repress Cyclin A2 mRNA expression (data not shown).

We found that the collagen mediated methylation of *Fas* promoter by *Dnmt1* was FAK, MAPK and AP-1 transcription factor dependent. Depletion of the collagen effects in cell culture was achieved by using natural food compounds like genistein and resveratrol, which represent the main flavonoid present in soy and a phytoalexin

present in red grapes, respectively. For genistein, resveratrol and other nutritional factors as well as for nutritional habits, interference with epigenetic regulation of gene expression was demonstrated before (127, 133-135). For example, it was shown that maternal genistein protects agouti mice offspring from obesity by modifying the promoter CpG methylation status of the agouti gene (134). Further, it was shown that vegetarians show a higher *SOD2* expression in buccal swab cells when compared to omnivores due to a lower CpG promoter methylation of this gene (127).

The influence of environmental factors including nutrition habits and food compounds on epigenetic regulation of gene expression, become more and more important topics in medical research. The elucidation of possible associations between the environment and modulation of gene expressions as well as of the development of diseases like cancer, diabetes, adipositas and others, is a main target of the actual research efforts. The presented data on epigenetic effects of natural food compounds on collagen mediated osteoblastic cell multiplication, differentiation and function allow speculations that nutritional factors may influence bone development and homeostasis by the involvement of epigenetic mechanisms. Furthermore, an adequate environment for osteoblasts, which guarantees correct ECM synthesis and assembly, may be of particular importance for a physiological bone development.

In summary, results presented in this thesis revealed a new epigenetic mechanism which may play an important role for osteoblasts in avoiding anoikis by adhesion to an adequate ECM. Furthermore, the stimulation of the expression of markers of osteoblastic proliferation and differentiation underlines cell fate decisions directed by collagen. Furthermore, hcys influences not only collagen cross-linking by inhibition LOX enzymatic activity, it itself down regulates *Lox* expression by epigenetic DNA CpG methylation. This increased methylation is mediated by increased expression of *Dnmt1*, which is regulated by *Fli1* that is stimulated via JAK2 by IL-6. IL-6 itself is a pleiotropic factor, which also influences osteoclastic development and function.

In conclusion, the work presented in this thesis add important information on the action of nutritional components and endogenous metabolites on bone metabolism and how these components can influence bone quality and with it the quality of life.

7. References

1. Ponseti IV. 50 years ago in CORR : skeletal lesions produced by aminonitriles by Ignacio V. Ponseti MD CORR 1957;9:131-144. Clin Orthop Relat Res. 2008 Jan;466(1):255-6.

2. Spencer PS, Schaumburg HH. Lathyrism: a neurotoxic disease. Neurobehav Toxicol Teratol. 1983 Nov-Dec;5(6):625-9.

3. Gardner AF, Dasler W, Weinmann JP. Masticatory apparatus of albino rats in experimental lathyrism. J Dent Res. 1958 Jun;37(3):492-515.

4. Gardner AF. Experimental lathyrism: review of the literature. Am J Clin Nutr. 1959 Mar-Apr;7(2):213-23.

5. Levene CI, Carrington MJ. The inhibition of protein-lysine 6-oxidase by various lathyrogens. Evidence for two different mechanisms. Biochem J. 1985 Nov 15;232(1):293-6.

6. Turecek C, Fratzl-Zelman N, Rumpler M, Buchinger B, Spitzer S, Zoehrer R, et al. Collagen cross-linking influences osteoblastic differentiation. Calcif Tissue Int. 2008 May;82(5):392-400.

7. Levene CI, Heale G, Robins SP. Collagen cross-link synthesis in cultured vascular endothelium. Br J Exp Pathol. 1989 Dec;70(6):621-6.

8. Dawson DA, Rinaldi AC, Poch G. Biochemical and toxicological evaluation of agent-cofactor reactivity as a mechanism of action for osteolathyrism. Toxicology. 2002 Aug 15;177(2-3):267-84.

9. Vernon-Roberts B. Morphological and functional interrelationships of bone cells and matrix. Aust N Z J Med. 1979 Feb;9(1):1-8.

10. Takeuchi Y, Nakayama K, Matsumoto T. Differentiation and cell surface expression of transforming growth factor-beta receptors are regulated by interaction with matrix collagen in murine osteoblastic cells. J Biol Chem. 1996 Feb 16;271(7):3938-44.

11. Taubenberger AV, Woodruff MA, Bai H, Muller DJ, Hutmacher DW. The effect of unlocking RGD-motifs in collagen I on pre-osteoblast adhesion and differentiation. Biomaterials. Apr;31(10):2827-35.

12. Chen XD, Dusevich V, Feng JQ, Manolagas SC, Jilka RL. Extracellular matrix made by bone marrow cells facilitates expansion of marrow-derived mesenchymal progenitor cells and prevents their differentiation into osteoblasts. J Bone Miner Res. 2007 Dec;22(12):1943-56.

13. Senturk N, Keles GC, Kaymaz FF, Yildiz L, Acikgoz G, Turanli AY. The role of ascorbic acid on collagen structure and levels of serum interleukin-6 and tumour

necrosis factor-alpha in experimental lathyrism. Clin Exp Dermatol. 2004 Mar;29(2):168-75.
14. Viguet-Carrin S, Garnero P, Delmas PD. The role of collagen in bone strength. Osteoporos Int. 2006;17(3):319-36.

15. Prockop DJ, Sieron AL, Li SW. Procollagen N-proteinase and procollagen C-proteinase. Two unusual metalloproteinases that are essential for procollagen processing probably have important roles in development and cell signaling. Matrix Biol. 1998 Feb;16(7):399-408.

16. Knott L, Bailey AJ. Collagen cross-links in mineralizing tissues: a review of their chemistry, function, and clinical relevance. Bone. 1998 Mar;22(3):181-7.

17. Leblond CP. Synthesis and secretion of collagen by cells of connective tissue, bone, and dentin. Anat Rec. 1989 Jun;224(2):123-38.

18. Gallop PM, Paz MA. Posttranslational protein modifications, with special attention to collagen and elastin. Physiol Rev. 1975 Jul;55(3):418-87.

19. Bailey AJ, Paul RG, Knott L. Mechanisms of maturation and ageing of collagen. Mech Ageing Dev. 1998 Dec 1;106(1-2):1-56.

20. Saito M, Marumo K. Collagen cross-links as a determinant of bone quality: a possible explanation for bone fragility in aging, osteoporosis, and diabetes mellitus. Osteoporos Int. 2010 Feb;21(2):195-214.

21. Mauney J, Volloch V. Collagen I matrix contributes to determination of adult human stem cell lineage via differential, structural conformation-specific elicitation of cellular stress response. Matrix Biol. 2009 Jun;28(5):251-62.

22. Mauney J, Olsen BR, Volloch V. Matrix remodeling as stem cell recruitment event: a novel in vitro model for homing of human bone marrow stromal cells to the site of injury shows crucial role of extracellular collagen matrix. Matrix Biol. 2010 Oct;29(8):657-63.

23. Xu L, Anderson AL, Lu Q, Wang J. Role of fibrillar structure of collagenous carrier in bone sialoprotein-mediated matrix mineralization and osteoblast differentiation. Biomaterials. 2007 Feb;28(4):750-61.

24. Bonnet D. Biology of human bone marrow stem cells. Clin Exp Med. 2003 Nov;3(3):140-9.

25. Mauney J, Volloch V. Progression of human bone marrow stromal cells into both osteogenic and adipogenic lineages is differentially regulated by structural conformation of collagen I matrix via distinct signaling pathways. Matrix Biol. 2009 Jun;28(5):239-50.

26. Perez-Ruiz A, Ono Y, Gnocchi VF, Zammit PS. beta-Catenin promotes self-renewal of skeletal-muscle satellite cells. J Cell Sci. 2008 May 1;121(Pt 9):1373-82.

27. Abiola M, Favier M, Christodoulou-Vafeiadou E, Pichard AL, Martelly I, Guillet-Deniau I. Activation of Wnt/beta-catenin signaling increases insulin sensitivity through a reciprocal regulation of Wnt10b and SREBP-1c in skeletal muscle cells. PLoS One. 2009;4(12):e8509.

28. Pope FM, Nicholls AC, Dorling J, Webb J. Molecular abnormalities of collagen: a review. J R Soc Med. 1983 Dec;76(12):1050-62.

29. Kocher MS, Shapiro F. Osteogenesis imperfecta. J Am Acad Orthop Surg. 1998 Jul-Aug;6(4):225-36.

30. Hasegawa K. [Genetic basis for skeletal disease. Osteogenesis imperfecta and genetic abnormalities]. Clin Calcium. Aug;20(8):1190-5.

31. Pittenger MF, Mackay AM, Beck SC, Jaiswal RK, Douglas R, Mosca JD, et al. Multilineage potential of adult human mesenchymal stem cells. Science. 1999 Apr 2;284(5411):143-7.

32. Franceschi RT. The developmental control of osteoblast-specific gene expression: role of specific transcription factors and the extracellular matrix environment. Crit Rev Oral Biol Med. 1999;10(1):40-57.

33. Lian JB, Stein GS. Development of the osteoblast phenotype: molecular mechanisms mediating osteoblast growth and differentiation. Iowa Orthop J. 1995;15:118-40.

34. Stein GS, Lian JB, Stein JL, Van Wijnen AJ, Montecino M. Transcriptional control of osteoblast growth and differentiation. Physiol Rev. 1996 Apr;76(2):593-629.

35. Lian JB, Stein GS, Stein JL, van Wijnen AJ. Transcriptional control of osteoblast differentiation. Biochem Soc Trans. 1998 Feb;26(1):14-21.

36. Sudo H, Kodama HA, Amagai Y, Yamamoto S, Kasai S. In vitro differentiation and calcification in a new clonal osteogenic cell line derived from newborn mouse calvaria. J Cell Biol. 1983 Jan;96(1):191-8.

37. Lanyon LE. Osteocytes, strain detection, bone modeling and remodeling. Calcif Tissue Int. 1993;53 Suppl 1:S102-6; discussion S6-7.

38. Parfitt AM. Plasma calcium control at quiescent bone surfaces: a new approach to the homeostatic function of bone lining cells. Bone. 1989;10(2):87-8.

39. Rodan GA, Heath JK, Yoon K, Noda M, Rodan SB. Diversity of the osteoblastic phenotype. Ciba Found Symp. 1988;136:78-91.

40. Leis HJ, Hulla W, Gruber R, Huber E, Zach D, Gleispach H, et al. Phenotypic heterogeneity of osteoblast-like MC3T3-E1 cells: changes of bradykinin-induced prostaglandin E2 production during osteoblast maturation. J Bone Miner Res. 1997 Apr;12(4):541-51.

41. Watabe T, Miyazono K. Roles of TGF-beta family signaling in stem cell renewal and differentiation. Cell Res. 2009 Jan;19(1):103-15.

42. Sammons J, Ahmed N, El-Sheemy M, Hassan HT. The role of BMP-6, IL-6, and BMP-4 in mesenchymal stem cell-dependent bone development: effects on osteoblastic differentiation induced by parathyroid hormone and vitamin D(3). Stem Cells Dev. 2004 Jun;13(3):273-80.

43. Hoffmann A, Gross G. BMP signaling pathways in cartilage and bone formation. Crit Rev Eukaryot Gene Expr. 2001;11(1-3):23-45.

44. Yamaguchi A. Regulation of differentiation pathway of skeletal mesenchymal cells in cell lines by transforming growth factor-beta superfamily. Semin Cell Biol. 1995 Jun;6(3):165-73.

45. Ryoo HM, Lee MH, Kim YJ. Critical molecular switches involved in BMP-2-induced osteogenic differentiation of mesenchymal cells. Gene. 2006 Jan 17;366(1):51-7.

46. Prince M, Banerjee C, Javed A, Green J, Lian JB, Stein GS, et al. Expression and regulation of Runx2/Cbfa1 and osteoblast phenotypic markers during the growth and differentiation of human osteoblasts. J Cell Biochem. 2001;80(3):424-40.

47. Lian JB, Stein GS, Javed A, van Wijnen AJ, Stein JL, Montecino M, et al. Networks and hubs for the transcriptional control of osteoblastogenesis. Rev Endocr Metab Disord. 2006 Jun;7(1-2):1-16.

48. Ducy P, Zhang R, Geoffroy V, Ridall AL, Karsenty G. Osf2/Cbfa1: a transcriptional activator of osteoblast differentiation. Cell. 1997 May 30;89(5):747-54.

49. Komori T, Yagi H, Nomura S, Yamaguchi A, Sasaki K, Deguchi K, et al. Targeted disruption of Cbfa1 results in a complete lack of bone formation owing to maturational arrest of osteoblasts. Cell. 1997 May 30;89(5):755-64.

50. Thomas DM, Johnson SA, Sims NA, Trivett MK, Slavin JL, Rubin BP, et al. Terminal osteoblast differentiation, mediated by runx2 and p27KIP1, is disrupted in osteosarcoma. J Cell Biol. 2004 Dec 6;167(5):925-34.

51. Westendorf JJ, Zaidi SK, Cascino JE, Kahler R, van Wijnen AJ, Lian JB, et al. Runx2 (Cbfa1, AML-3) interacts with histone deacetylase 6 and represses the p21(CIP1/WAF1) promoter. Mol Cell Biol. 2002 Nov;22(22):7982-92.

52. Lengner CJ, Steinman HA, Gagnon J, Smith TW, Henderson JE, Kream BE, et al. Osteoblast differentiation and skeletal development are regulated by Mdm2-p53 signaling. J Cell Biol. 2006 Mar 13;172(6):909-21.

53. Lee KS, Kim HJ, Li QL, Chi XZ, Ueta C, Komori T, et al. Runx2 is a common target of transforming growth factor beta1 and bone morphogenetic protein 2, and cooperation between Runx2 and Smad5 induces osteoblast-specific gene expression in the pluripotent mesenchymal precursor cell line C2C12. Mol Cell Biol. 2000 Dec;20(23):8783-92.

54. Ducy P, Karsenty G. Two distinct osteoblast-specific cis-acting elements control expression of a mouse osteocalcin gene. Mol Cell Biol. 1995 Apr;15(4):1858-69.

55. Hesse E, Saito H, Kiviranta R, Correa D, Yamana K, Neff L, et al. Zfp521 controls bone mass by HDAC3-dependent attenuation of Runx2 activity. J Cell Biol. 2010 Dec 27;191(7):1271-83.

56. Correa D, Hesse E, Seriwatanachai D, Kiviranta R, Saito H, Yamana K, et al. Zfp521 is a target gene and key effector of parathyroid hormone-related peptide signaling in growth plate chondrocytes. Dev Cell. 2010 Oct 19;19(4):533-46.

57. Hesse E, Kiviranta R, Wu M, Saito H, Yamana K, Correa D, et al. Zinc finger protein 521, a new player in bone formation. Ann N Y Acad Sci. 2010 Mar;1192:32-7.

58. Wu M, Hesse E, Morvan F, Zhang JP, Correa D, Rowe GC, et al. Zfp521 antagonizes Runx2, delays osteoblast differentiation in vitro, and promotes bone formation in vivo. Bone. 2009 Apr;44(4):528-36.

59. Cheng SL, Shao JS, Charlton-Kachigian N, Loewy AP, Towler DA. MSX2 promotes osteogenesis and suppresses adipogenic differentiation of multipotent mesenchymal progenitors. J Biol Chem. 2003 Nov 14;278(46):45969-77.

60. Hassan MQ, Javed A, Morasso MI, Karlin J, Montecino M, van Wijnen AJ, et al. Dlx3 transcriptional regulation of osteoblast differentiation: temporal recruitment of Msx2, Dlx3, and Dlx5 homeodomain proteins to chromatin of the osteocalcin gene. Mol Cell Biol. 2004 Oct;24(20):9248-61.

61. Ichida F, Nishimura R, Hata K, Matsubara T, Ikeda F, Hisada K, et al. Reciprocal roles of MSX2 in regulation of osteoblast and adipocyte differentiation. J Biol Chem. 2004 Aug 6;279(32):34015-22.

62. Yoshizawa T, Takizawa F, Iizawa F, Ishibashi O, Kawashima H, Matsuda A, et al. Homeobox protein MSX2 acts as a molecular defense mechanism for preventing ossification in ligament fibroblasts. Mol Cell Biol. 2004 Apr;24(8):3460-72.

63. Kim YJ, Kim HN, Park EK, Lee BH, Ryoo HM, Kim SY, et al. The bone-related Zn finger transcription factor Osterix promotes proliferation of mesenchymal cells. Gene. 2006 Jan 17;366(1):145-51.

64. Pratap J, Galindo M, Zaidi SK, Vradii D, Bhat BM, Robinson JA, et al. Cell growth regulatory role of Runx2 during proliferative expansion of preosteoblasts. Cancer Res. 2003 Sep 1;63(17):5357-62.

65. Wagner EF. Functions of AP1 (Fos/Jun) in bone development. Ann Rheum Dis. 2002 Nov;61 Suppl 2:ii40-2.

66. Grigoriadis AE, Schellander K, Wang ZQ, Wagner EF. Osteoblasts are target cells for transformation in c-fos transgenic mice. J Cell Biol. 1993 Aug;122(3):685-701.

67. Sandberg M, Vuorio T, Hirvonen H, Alitalo K, Vuorio E. Enhanced expression of TGF-beta and c-fos mRNAs in the growth plates of developing human long bones. Development. 1988 Mar;102(3):461-70.

68. Kim YI. Nutritional epigenetics: impact of folate deficiency on DNA methylation and colon cancer susceptibility. J Nutr. 2005 Nov;135(11):2703-9.

69. Liu G, Nellaiappan K, Kagan HM. Irreversible inhibition of lysyl oxidase by homocysteine thiolactone and its selenium and oxygen analogues. Implications for homocystinuria. J Biol Chem. 1997 Dec 19;272(51):32370-7.

70. Audelin MC, Genest J, Jr. Homocysteine and cardiovascular disease in diabetes mellitus. Atherosclerosis. 2001 Dec;159(2):497-511.

71. Iannucci CV, Capoccia D, Calabria M, Leonetti F. Metabolic syndrome and adipose tissue: new clinical aspects and therapeutic targets. Curr Pharm Des. 2007;13(21):2148-68.

72. Blouin S, Thaler HW, Korninger C, Schmid R, Hofstaetter JG, Zoehrer R, et al. Bone matrix quality and plasma homocysteine levels. Bone. 2009 May;44(5):959-64.

73. Gjesdal CG, Vollset SE, Ueland PM, Refsum H, Meyer HE, Tell GS. Plasma homocysteine, folate, and vitamin B 12 and the risk of hip fracture: the hordaland homocysteine study. J Bone Miner Res. 2007 May;22(5):747-56.

74. McLean RR, Jacques PF, Selhub J, Tucker KL, Samelson EJ, Broe KE, et al. Homocysteine as a predictive factor for hip fracture in older persons. N Engl J Med. 2004 May 13;350(20):2042-9.

75. Raiszadeh F, Hoover DR, Lee I, Shi Q, Anastos K, Gao W, et al. Plasma homocysteine is not associated with HIV serostatus or antiretroviral therapy in women. J Acquir Immune Defic Syndr. 2009 Jun 1;51(2):175-8.

76. van Meurs JB, Dhonukshe-Rutten RA, Pluijm SM, van der Klift M, de Jonge R, Lindemans J, et al. Homocysteine levels and the risk of osteoporotic fracture. N Engl J Med. 2004 May 13;350(20):2033-41.

77. Bezold G, Lange M, Peter RU. Homozygous methylenetetrahydrofolate reductase C677T mutation and male infertility. N Engl J Med. 2001 Apr 12;344(15):1172-3.

78. Stabler SP. Vitamins, homocysteine, and cognition. Am J Clin Nutr. 2003 Sep;78(3):359-60.

79. Papandreou D, Rousso I, Malindretos P, Makedou A, Arvanitidou M. Effects of oral folate supplementation on serum total homocysteine and cholesterol levels in hyperhomocysteinemic children. Nutr Clin Pract. Aug;25(4):390-3.

80. Waskiewicz A, Sygnowska E, Broda G. Dietary intake of vitamins B6, B12 and folate in relation to homocysteine serum concentration in the adult Polish population - WOBASZ Project. Kardiol Pol. Mar;68(3):275-82.

81. Yang Q, Cogswell ME, Hamner HC, Carriquiry A, Bailey LB, Pfeiffer CM, et al. Folic acid source, usual intake, and folate and vitamin B-12 status in US adults: National Health and Nutrition Examination Survey (NHANES) 2003-2006. Am J Clin Nutr. Jan;91(1):64-72.

82. Krivosikova Z, Krajcovicova-Kudlackova M, Spustova V, Stefikova K, Valachovicova M, Blazicek P, et al. The association between high plasma homocysteine levels and lower bone mineral density in Slovak women: the impact of vegetarian diet. Eur J Nutr. Apr;49(3):147-53.

83. Bestor TH. The DNA methyltransferases of mammals. Hum Mol Genet. 2000 Oct;9(16):2395-402.

84. Ghoshal K, Motiwala T, Claus R, Yan P, Kutay H, Datta J, et al. HOXB13, a target of DNMT3B, is methylated at an upstream CpG island, and functions as a tumor suppressor in primary colorectal tumors. PLoS One. 2010;5(4):e10338.

85. Myant K, Stancheva I. LSH cooperates with DNA methyltransferases to repress transcription. Mol Cell Biol. 2008 Jan;28(1):215-26.

86. Schermelleh L, Haemmer A, Spada F, Rosing N, Meilinger D, Rothbauer U, et al. Dynamics of Dnmt1 interaction with the replication machinery and its role in postreplicative maintenance of DNA methylation. Nucleic Acids Res. 2007;35(13):4301-12.

87. Li E. Chromatin modification and epigenetic reprogramming in mammalian development. Nat Rev Genet. 2002 Sep;3(9):662-73.

88. Wade PA. Methyl CpG binding proteins: coupling chromatin architecture to gene regulation. Oncogene. 2001 May 28;20(24):3166-73.

89. Jamaluddin MD, Chen I, Yang F, Jiang X, Jan M, Liu X, et al. Homocysteine inhibits endothelial cell growth via DNA hypomethylation of the cyclin A gene. Blood. 2007 Nov 15;110(10):3648-55.

90. Mathers JC. Nutritional modulation of ageing: genomic and epigenetic approaches. Mech Ageing Dev. 2006 Jun;127(6):584-9.

91. Mandrioli M, Borsatti F. DNA methylation of fly genes and transposons. Cell Mol Life Sci. 2006 Sep;63(17):1933-6.

92. Ramirez MA, Pericuesta E, Fernandez-Gonzalez R, Moreira P, Pintado B, Gutierrez-Adan A. Transcriptional and post-transcriptional regulation of retrotransposons IAP and MuERV-L affect pluripotency of mice ES cells. Reprod Biol Endocrinol. 2006;4:55.

93. Christophersen NS, Helin K. Epigenetic control of embryonic stem cell fate. J Exp Med. 2010 Oct 25;207(11):2287-95.

94. Gonzalo S. Epigenetic alterations in aging. J Appl Physiol. 2010 Aug;109(2):586-97.

95. Portela A, Esteller M. Epigenetic modifications and human disease. Nat Biotechnol. 2010 Oct;28(10):1057-68.

96. Ikeda S, Namekawa T, Sugimoto M, Kume S. Expression of methylation pathway enzymes in bovine oocytes and preimplantation embryos. J Exp Zool A Ecol Genet Physiol. Mar 1;313(3):129-36.

97. Fryer AA, Emes RD, Ismail KM, Haworth KE, Mein C, Carroll WD, et al. Quantitative, high-resolution epigenetic profiling of CpG loci identifies associations with cord blood plasma homocysteine and birth weight in humans. Epigenetics. Jan 1;6(1):86-94.

98. Waterland RA, Jirtle RL. Transposable elements: targets for early nutritional effects on epigenetic gene regulation. Mol Cell Biol. 2003 Aug;23(15):5293-300.

99. Pogribny IP, Tryndyak VP, Boureiko A, Melnyk S, Bagnyukova TV, Montgomery B, et al. Mechanisms of peroxisome proliferator-induced DNA hypomethylation in rat liver. Mutat Res. 2008 Sep 26;644(1-2):17-23.

100. Pogribny IP, Tryndyak VP, Ross SA, Beland FA. Differential expression of microRNAs during hepatocarcinogenesis induced by methyl deficiency in rats. Nutr Rev. 2008 Aug;66 Suppl 1:S33-5.

101. Hodge DR, Cho E, Copeland TD, Guszczynski T, Yang E, Seth AK, et al. IL-6 enhances the nuclear translocation of DNA cytosine-5-methyltransferase 1 (DNMT1) via phosphorylation of the nuclear localization sequence by the AKT kinase. Cancer Genomics Proteomics. 2007 Nov-Dec;4(6):387-98.

102. Gasche JA, Hoffmann J, Boland CR, Goel A. Interleukin-6 promotes tumorigenesis by altering DNA methylation in oral cancer cells. Int J Cancer. 2010 Nov 12.

103. Kishikawa S, Murata T, Kimura H, Shiota K, Yokoyama KK. Regulation of transcription of the Dnmt1 gene by Sp1 and Sp3 zinc finger proteins. Eur J Biochem. 2002 Jun;269(12):2961-70.

104. Kishikawa S, Murata T, Ugai H, Yamazaki T, Yokoyama KK. Control elements of Dnmt1 gene are regulated in cell-cycle dependent manner. Nucleic Acids Res Suppl. 2003(3):307-8.

105. Thaler R, Spitzer S, Rumpler M, Fratzl-Zelman N, Klaushofer K, Paschalis EP, et al. Differential effects of homocysteine and beta aminopropionitrile on preosteoblastic MC3T3-E1 cells. Bone. 2010 Mar;46(3):703-9.

106. Thaler R, Agsten M, Spitzer S, Paschalis EP, Karlic H, Klaushofer K, et al. Homocysteine Suppresses the Expression of the Collagen Cross-linker Lysyl Oxidase Involving IL-6, Fli1, and Epigenetic DNA Methylation. J Biol Chem. 2011 Feb 18;286(7):5578-88.

107. Thaler R, Karlic H, Spitzer S, Klaushofer K, Varga F. Extra-cellular matrix suppresses expression of the apoptosis mediator Fas by epigenetic DNA methylation. Apoptosis. 2010 Jun;15(6):728-37.

108. Fratzl-Zelman N, Horandner H, Luegmayr E, Varga F, Ellinger A, Erlee MP, et al. Effects of triiodothyronine on the morphology of cells and matrix, the localization of alkaline phosphatase, and the frequency of apoptosis in long-term cultures of MC3T3-E1 cells. Bone. 1997 Mar;20(3):225-36.

109. Luegmayr E, Varga F, Frank T, Roschger P, Klaushofer K. Effects of triiodothyronine on morphology, growth behavior, and the actin cytoskeleton in mouse osteoblastic cells (MC3T3-E1). Bone. 1996 Jun;18(6):591-9.

110. Gazin C, Wajapeyee N, Gobeil S, Virbasius CM, Green MR. An elaborate pathway required for Ras-mediated epigenetic silencing. Nature. 2007 Oct 25;449(7165):1073-7.

111. Liao QC, Xiao ZS, Qin YF, Zhou HH. Genistein stimulates osteoblastic differentiation via p38 MAPK-Cbfa1 pathway in bone marrow culture. Acta Pharmacol Sin. 2007 Oct;28(10):1597-602.

112. Chen TH, Chen WM, Hsu KH, Kuo CD, Hung SC. Sodium butyrate activates ERK to regulate differentiation of mesenchymal stem cells. Biochem Biophys Res Commun. 2007 Apr 20;355(4):913-8.

113. Backesjo CM, Li Y, Lindgren U, Haldosen LA. Activation of Sirt1 decreases adipocyte formation during osteoblast differentiation of mesenchymal stem cells. J Bone Miner Res. 2006 Jul;21(7):993-1002.

114. Kurihara N, Ikeda K, Hakeda Y, Tsunoi M, Maeda N, Kumegawa M. Effect of 1,25-dihydroxyvitamin D3 on alkaline phosphatase activity and collagen synthesis in osteoblastic cells, clone MC3T3-E1. Biochem Biophys Res Commun. 1984 Mar 15;119(2):767-71.

115. Rodan GA, Noda M. Gene expression in osteoblastic cells. Crit Rev Eukaryot Gene Expr. 1991;1(2):85-98.

116. Pfaffl MW. A new mathematical model for relative quantification in real-time RT-PCR. Nucleic Acids Res. 2001 May 1;29(9):e45.

117. Paschalis EP, Verdelis K, Doty SB, Boskey AL, Mendelsohn R, Yamauchi M. Spectroscopic characterization of collagen cross-links in bone. J Bone Miner Res. 2001 Oct;16(10):1821-8.

118. Hodge DR, Xiao W, Clausen PA, Heidecker G, Szyf M, Farrar WL. Interleukin-6 regulation of the human DNA methyltransferase (HDNMT) gene in human erythroleukemia cells. J Biol Chem. 2001 Oct 26;276(43):39508-11.

119. Huang W, Yang S, Shao J, Li YP. Signaling and transcriptional regulation in osteoblast commitment and differentiation. Front Biosci. 2007;12:3068-92.

120. Hofbauer KH, Gess B, Lohaus C, Meyer HE, Katschinski D, Kurtz A. Oxygen tension regulates the expression of a group of procollagen hydroxylases. Eur J Biochem. 2003 Nov;270(22):4515-22.

121. Blanchard F, Duplomb L, Baud'huin M, Brounais B. The dual role of IL-6-type cytokines on bone remodeling and bone tumors. Cytokine Growth Factor Rev. 2009 Feb;20(1):19-28.

122. Theoleyre S, Wittrant Y, Tat SK, Fortun Y, Redini F, Heymann D. The molecular triad OPG/RANK/RANKL: involvement in the orchestration of pathophysiological bone remodeling. Cytokine Growth Factor Rev. 2004 Dec;15(6):457-75.

123. Kim S, Yamazaki M, Shevde NK, Pike JW. Transcriptional control of receptor activator of nuclear factor-kappaB ligand by the protein kinase A activator forskolin and the transmembrane glycoprotein 130-activating cytokine, oncostatin M, is exerted through multiple distal enhancers. Mol Endocrinol. 2007 Jan;21(1):197-214.

124. Jilka RL, Hangoc G, Girasole G, Passeri G, Williams DC, Abrams JS, et al. Increased osteoclast development after estrogen loss: mediation by interleukin-6. Science. 1992 Jul 3;257(5066):88-91.

125. Schiller C, Gruber R, Redlich K, Ho GM, Katzgraber F, Willheim M, et al. 17Beta-estradiol antagonizes effects of 1alpha,25-dihydroxyvitamin D3 on interleukin-6 production and osteoclast-like cell formation in mouse bone marrow primary cultures. Endocrinology. 1997 Nov;138(11):4567-71.

126. Poli V, Balena R, Fattori E, Markatos A, Yamamoto M, Tanaka H, et al. Interleukin-6 deficient mice are protected from bone loss caused by estrogen depletion. EMBO J. 1994 Mar 1;13(5):1189-96.

127. Thaler R, Karlic H, Rust P, Haslberger AG. Epigenetic regulation of human buccal mucosa mitochondrial superoxide dismutase gene expression by diet. Br J Nutr. 2009 Mar;101(5):743-9.

128. Sun LQ, Lee DW, Zhang Q, Xiao W, Raabe EH, Meeker A, et al. Growth retardation and premature aging phenotypes in mice with disruption of the SNF2-like gene, PASG. Genes Dev. 2004 May 1;18(9):1035-46.

129. Kaneda A, Wakazono K, Tsukamoto T, Watanabe N, Yagi Y, Tatematsu M, et al. Lysyl oxidase is a tumor suppressor gene inactivated by methylation and loss of heterozygosity in human gastric cancers. Cancer Res. 2004 Sep 15;64(18):6410-5.

130. So K, Tamura G, Honda T, Homma N, Waki T, Togawa N, et al. Multiple tumor suppressor genes are increasingly methylated with age in non-neoplastic gastric epithelia. Cancer Sci. 2006 Nov;97(11):1155-8.

131. Tamura G, So K, Miyoshi H, Honda T, Nishizuka S, Motoyama T. Quantitative assessment of gene methylation in neoplastic and non-neoplastic gastric epithelia using methylation-specific DNA microarray. Pathol Int. 2009 Dec;59(12):895-9.

132. Frisch SM, Screaton RA. Anoikis mechanisms. Curr Opin Cell Biol. 2001 Oct;13(5):555-62.

133. Ingrosso D, Perna AF. Epigenetics in hyperhomocysteinemic states. A special focus on uremia. Biochim Biophys Acta. 2009 Sep;1790(9):892-9.

134. Dolinoy DC. The agouti mouse model: an epigenetic biosensor for nutritional and environmental alterations on the fetal epigenome. Nutr Rev. 2008 Aug;66 Suppl 1:S7-11.

135. Wakeling LA, Ions LJ, Ford D. Could Sirt1-mediated epigenetic effects contribute to the longevity response to dietary restriction and be mimicked by other dietary interventions? Age (Dordr). 2009 Jul 1.

8. Curriculum Vitae

Name	Mag. Roman Thaler
Date and place of Birth	05.08.1981 in Brixen, South Tyrol, Italy
Nationality	Italian
Family status	Unwed
Residence	Rokitanskygasse 10-1, 1170 Vienna, Austria
Mother tongue	Ladinish
Language skills	Italian, German, English fluently in written and spoken language, France and Portuguese basically in written and spoken language
Education	
Since July 2008	Ph.D. thesis at the Ludwig Boltzmann Institute of Osteology in Vienna
April 2008	Graduation in Nutritional Sciences at the University of Vienna
2006/ 2007	Diploma thesis “Influence of Diets, Age and the V16A SNP on the Expression of the MnSOD Gene” at the Department of Nutritional Sciences at the University of Vienna
July 2000	General qualification for university entrance

Awards

Research price 2011 of the Austrian Society for Endocrinology and Metabolism for the submitted work “*Is Serum Amyloid A3 (Saa3) a Link Between Hyperhomocysteinemia and the Development of Degenerative Skeletal Pathologies?”* at the 16th annual meeting of the Austrian Society for Endocrinology and Metabolism, 12–13 May 2011 in Vienna.

Travel award of the European Calcified Tissue Society and the International Bone and Mineral society based on the submitted abstract “*Homocysteine disrupted extracellular matrix up-regulates the acute phase protein SAA3 which in turn*

stimulates MMP13" at the 38th European Symposium on Calcified Tissues, 3rd joint ECTS/IBMS meeting, 7-11 May 2011 in Athens.

Travel award of the Austrian Society for Endocrinology and Metabolism for the oral presentation *"Homocystein reguliert die Expression von Genen des Cholesterin- und Fettstoffwechsels sowie der Osteoblastendifferenzierung"* at the 15th annual meeting of the Austrian Society for Endocrinology and Metabolism, 7–8 May 2010 in Vienna.

Number of scientific publications in peer reviewed journals:	8
Number of abstracts/proceedings:	13
Number of scientific oral presentations:	4

Publications

Thaler R, Agsten M, Spitzer S, Paschalis EP, Karlic H, Klaushofer K, Varga F. *Homocysteine suppresses the expression of the collagen cross-linker lysyl oxidase involving IL-6, Fli1 and epigenetic DNA methylation.* J Biol Chem. 2010 Dec 9. [Epub], IF= 5.328, Q1 (Impact factor)

Thaler R, Rumpler M, Spitzer S, Klaushofer K, Varga F. *Mospd1, a new player in mesenchymal versus epidermal cell differentiation.* J Cell Physiol. 2010 Dec 9. [Epub], IF= 4.586, Q1

Thaler R, Karlic H, Spitzer S, Klaushofer K, Varga F. *Extra-cellular matrix suppresses expression of the apoptosis mediator Fas by epigenetic DNA methylation*. Apoptosis. 2010 Jun;15(6):728-37. IF= 4.066

Thaler R, Spitzer S, Rumpler M, Fratzl-Zelman N, Klaushofer K, Paschalis EP, Varga F. *Differential effects of homocysteine and beta aminopropionitrile on preosteoblastic MC3T3-E1 cells*. Bone. 2010 Mar;46(3):703-9. Epub 2009 Nov 4. IF= 4.089

Thaler R, Karlic H, Rust P, Haslberger AG. *Epigenetic regulation of human buccal mucosa mitochondrial superoxide dismutase gene expression by diet*. Br J Nutr. 2009 Mar;101(5):743-9. Epub 2008 Aug 7. IF= 3.446, Q1

Thaler R, Aumüller E, Berner C, Haslberger AG. *Interaction of Hereditary and Epigenetic Mechanisms in the Regulation of Gene Expression*. *Book chapter in* "Epigenetics and Human Health, Linking Hereditary, Environmental and Nutritional Aspects" pages 13-34, 2010 Wiley-VCH Verlag GmbH & Co.

Karlic H, Varga J, **Thaler R,** Berger C, Spitzer S, Pfeilstöcker M, Klaushofer K, Varga F. *Effects of Epigenetic Drugs (Vorinostat, Decitabine) on Metabolism-Related Pathway Factors in Leukemic Cells*. The Open Leukemia Journal, 2010, 3, 34-42.

Varga F, Rumpler M, Zoehrer R, Turecek C, Spitzer S, **Thaler R,** Paschalis EP, Klaushofer K. *T3 affects expression of collagen I and collagen cross-linking in bone cell cultures*. Biochem Biophys Res Commun. 2010 Nov 12;402(2):180-5, Epub 2010 Aug 11. IF= 2.548

Liszt K, Zwielehner J, Handschur M, Hippe B, **Thaler R,** Haslberger AG. *Characterization of bacteria, clostridia and Bacteroides in faeces of vegetarians using qPCR and PCR-DGGE fingerprinting.* Ann Nutr Metab. 2009;54(4):253-7. Epub 2009 Jul 27. IF= 1.970

Posters and oral presentations:

Thaler R., Spitzer S., Rumpler M., Hassler N., Paschalis E., Klaushofer K., Varga F. *Homocysteine disrupted extracellular matrix up-regulates the acute phase protein SAA3 which in turn stimulates MMP13.* 38th European Symposium on Calcified Tissues, Athens, Greece 7-11 May 2011, accepted poster.

Thaler R., Agsten M., Spitzer S., Paschalis E.P., Karlic H., Klaushofer K., Varga F. *Homocysteins doppelte Rolle in der Behinderung der Bildung einer stabilen Knochenmatrix. Wissenschaftliche Herbsttagung der Österreichischen Gesellschaft für Knochen und Mineralstoffewechsel*, Vienna, Austria 26-27 November 2010, oral presentation.

Thaler R., Karlic H., Spitzer S., Klaushofer K, Varga F. *The effect of DMSO on MC3T3-E1 mouse osteoblast like cells focusing in DNA methylation and markers of differentiation and senescence*. 37th European Symposium on Calcified Tissues, Glasgow, Scotland 26-30 June 2010, Bone 47, suppl 1:S135, abstract P167 and poster.

Thaler R., Agsten M., Spitzer S., Klaushofer K, Paschalis P., Varga F. *Effects of Homocysteine on the expression of osteoblastic genes and on genes related to cholesterol and fat metabolism*. 37th European Symposium on Calcified Tissues, Glasgow, Scotland 26-30 June 2010, Bone 47, suppl 1:S135, abstract P166 and poster.

Hassler N., **Thaler R.**, Rumpler M., Klaushofer K., Paschalis E. *Investigation of extracellular matrix (ECM) by attenuated total reflection (ATR) spectroscopy*. SPEC 2010 Manchester, United Kingdom June 2010.

Thaler R., Hassler N., Spitzer S., Klaushofer K., Paschalis E., Varga F. *Homocystein reguliert die Expression von Genen des Cholesterin- und Fettstoffwechsels sowie der Osteoblasten-differenzierung.* 15. Jahrestagung der Österreichischen Gesellschaft für Endokrinologie und Stoffwechsel, Vienna, 7-8 May 2010, oral presentation

Thaler R., Spitzer S., Rumpler M., Fratzl-Zelman N, Klaushofer K., Paschalis E., Varga F. *Störungen der Kollagenquervernetzung durch Homocystein beeinflusst die Differenzierung von Osteoblasten*. 15. Jahrestagung der Österreichischen Gesellschaft für Endokrinologie und Stoffwechsel, Vienna 7-8 May 2010, oral presentation

Thaler R., Paschalis EP, Spitzer S, Rumpler M, Fratzl-Zelman N, Klaushofer K, Varga F. *Differential effects of Homocysteine and beta-aminopropionitrile on osteoblastic gene expression*. 36th European Symposium on Calcified Tissues, Vienna, Austria 23-27 May 2009, Bone 44, suppl 1:S317-S318, abstract P172 and poster

Thaler R., Paschalis EP, Spitzer S, Rumpler M, Fratzl-Zelman N, Klaushofer K, Varga F. *Effects of disturbed extracellular matrix on osteoblastic gene expression*. 36th European Symposium on Calcified Tissues, Vienna, Austria 23-27 May 2009, Bone 44, suppl 1:S349, abstract P251 and poster

Thaler R., Klaushofer K, Varga F. *Effects of collagen on DNA methyl transferase expression in osteoblasts.* 36th European Symposium on Calcified Tissues, Vienna, Austria 23-27 May 2009, Bone 44, suppl 1:S317-S318, abstract P171 and poster

Buchinger B., **Thaler R.**, Varga F., Spitzer S., Klaushofer K. *The effects of valproate and 5`-aza-2`-deoxycytidine (5-AZAC) on the expression of osteoblast-specific genes in human metastatic prostate cancer cells.* 36th European Symposium on Calcified Tissues, Vienna, Austria 23-27 May 2009

Hassler N., **Thaler R.**, Varga F., Klaushofer K., Paschalis E. *FTIR attenuated total reflection (ATR) spectroscopy as a tool to investigate extracellular matrix.* 36th European Symposium on Calcified Tissues, Vienna, Austria 23-27 May 2009

Varga F., Spitzer S., Karlic H., **Thaler R.**, Klaushofer K. *Cell-contacts are a prerequisite for basal and T3 regulated osteocalcin expression in MC3T3-E1 osteoblast like cells*. 36th European Symposium on Calcified Tissues, Vienna, Austria 23-27 May 2009

Thaler R., Kubala K, Sagl V, Karlic H, Elmadfa I, Haslberger AG. *Natural food compounds affect DNA methyltransferases, promoter methylation and gene expression of selected genes in the $CACO_2$ cell-line.* XX International Congress of Genetics, Berlin, Germany, July 12-17, 2008

Karlic H, Varga F, Spitzer S, **Thaler R.**, Pfeilstöcker M, Pittermann E. *RTQPCR shows close Association of gene demethylation with transcriptional activation of tumor suppressor genes in cells treated with chromatin- or tyrosine kinase - targeting drugs*. Onkologie 2008; Vienna 31 (S4) VIII+260, 133 (Abstract No 379)

Thaler R., Veronika S, Haslberger AG. *Characterization of environmental and nutritional influences on DNA methylation and epigenetic regulation of gene*

expression. Vienna Research Platform of Nutrition and Food Sciences (VRPNFS), first meeting; New Aspects in Quality and Biofunctionality of Foods, Vienna, April 25, 2008. Oral presentation

Thaler R., Schuster D, Karlic H, Haslberger AG. *Expression of MnSOD is epigenetically regulated by diets in human buccal mucosa.* DMMC International Workshop – Epigenetics: From Mechanisms to Medicines, University College Dublin, Ireland, June 24-26, 2007